Theor Chem Acc (2004) 112: 349–393
DOI 10.1007/s00214-004-0567-2

Theoretical
Chemistry Accounts

Feature article

Method of moments of coupled-cluster equations: a new formalism for designing accurate electronic structure methods for ground and excited states

P. Piecuch[1,2], **K. Kowalski**[1], **I. S. O. Pimienta**[1], **P.-D. Fan**[1], **M. Lodriguito**[1], **M. J. McGuire**[1], **S. A. Kucharski**[1,3], **T. Kuś**[1,3], **M. Musiał**[1,3]

[1]Department of Chemistry, Michigan State University, East Lansing, MI 48824, USA
[2]Department of Physics and Astronomy, Michigan State University, East Lansing, MI 48824, USA
[3]Institute of Chemistry, University of Silesia, Szkolna 9, 40-006 Katowice, Poland

Received: 8 July 2003 / Accepted: 14 December 2003 / Published online: 1 July 2004

Abstract. The method of moments of coupled-cluster equations (MMCC), which provides a systematic way of improving the results of the standard coupled-cluster (CC) and equation-of-motion CC (EOMCC) calculations for the ground- and excited-state energies of atomic and molecular systems, is described. The MMCC theory and its generalized MMCC (GMMCC) extension that enables one to use the cluster operators resulting from the standard as well as nonstandard CC calculations, including those obtained with the extended CC (ECC) approaches, are based on rigorous mathematical relationships that define the many-body structure of the differences between the full configuration interaction (CI) and CC or EOMCC energies. These relationships can be used to design the noniterative corrections to the CC/EOMCC energies that work for chemical bond breaking and potential energy surfaces of excited electronic states, including excited states dominated by double excitations, where the standard single-reference CC/EOMCC methods fail. Several MMCC and GMMCC approximations are discussed, including the renormalized and completely renormalized CC/EOMCC methods for closed- and open-shell states, the quadratic MMCC approaches, the CI-corrected MMCC methods, and the GMMCC approaches for multiple bond breaking based on the ECC cluster amplitudes.

Keywords: Coupled-cluster theory – Method of moments of coupled-cluster equations – Renormalized coupled-cluster methods – Extended coupled-cluster theory – Potential energy surfaces

1 Introduction

The single-reference coupled-cluster (CC) theory [1, 2, 3, 4, 5] has become the de facto standard for high-accuracy calculations for atomic and molecular systems (see Refs. [6, 7, 8, 9, 10, 11, 12] and references therein). The basic single-reference CC methods, such as the CC approach with singles and doubles (CCSD) [13] and the noniterative CCSD + T(CCSD) = CCSD[T] [14] and CCSD(T) [15] approaches that account for the effect of triexcited clusters using arguments based on the many-body perturbation theory (MBPT), in either the spin-orbital [13, 14, 15] and spin-free [16, 17, 18] or the orthogonally spin-adapted [19, 20, 21] forms, are particularly attractive, since they offer an excellent compromise between the high accuracy in describing the many-electron correlation effects and the relatively low computer cost, as has been demonstrated in numerous molecular applications [7, 8, 9, 10, 11, 12]. Similar remarks apply to the response CC methods [22, 23, 24, 25, 26, 27] and the closely related equation-of-motion CC (EOMCC) approaches [28, 29, 30, 31] and their symmetry-adapted cluster configuration interaction (CI) analog [32, 33, 34, 35, 36], which provide excellent results for excited electronic states dominated by one-electron transitions at the basic singles and doubles level with the ease of the single-reference calculation [12, 28, 29, 30, 37, 38, 39, 40, 41, 42, 43].

Several problems arise when the standard single-reference CC methods are applied to potential energy surfaces (PESs) involving bond breaking and, in the case of the EOMCC or response CC methods, to excited states dominated by two-electron and other many-electron transitions. The ground-state CCSD method fails to describe bond breaking, since it neglects the important triply and quadruply excited clusters, T_3 and T_4, respectively. The noniterative triples or triples and quadruples corrections of the CCSD[T], CCSD(T), and CCSD(TQ$_\mathrm{f}$) [44] approaches fail too, since the standard

---

Correspondence to: P. Piecuch
e-mail: piecuch@cem.msu.edu

MBPT arguments, on which these approximations are based no longer apply owing to the divergent behavior of the MBPT series at larger internuclear separations. The iterative [20, 45, 46, 47, 48] and higher-order noniterative [44, 49] analogs of the CCSD[T], CCSD(T), and CCSD(TQ$_f$) approximations, in which arguments originating from MBPT are used to select the dominant contributions due to T_3 and T_4 clusters, work somewhat better, but the overall performance of all of the previously mentioned CC approximations in the bond breaking region is poor. As a result, the ground-state PESs obtained with the CCSD(T), CCSD(TQ$_f$), and similar noniterative or iterative approximations are inaccurate and display unphysical features at larger internuclear distances, particularly when the spin-adapted restricted Hartree–Fock (RHF) configuration is used as a reference (Refs. [9, 12, 50, 51, 52, 53, 54, 55, 56, 57, 58, 59, 60, 61, 62, 63, 64, 65, 66] and references therein). Similar remarks apply to PESs of excited states. The standard response CC and EOMCC approximations, including EOMCCSD [28, 29, 30], and their iterative [37, 38, 40, 41, 42, 43] and noniterative [37, 38, 42, 43] extensions, in which the effects of triply excited configurations are estimated using the arguments originating from MBPT, fail to describe excited states having large contributions due to doubly excited configurations and excited-state PESs along bond breaking coordinates [12, 30, 37, 38, 39, 40, 41, 42, 43, 61, 67, 68, 69, 70, 71, 72, 73, 74, 75].

The most natural solution to all of these problems is obtained by abandoning the single-reference description and by switching to the multireference CC (MRCC) formalisms, which introduce concepts of a multidimensional reference or model space and active orbitals and which are specifically designed to handle general open-shell and quasidegenerate electronic states, including, at least in principle, various cases of bond breaking and all kinds of excited states (see Refs. [9, 76] for recent reviews and developments). However, it is much easier to apply the standard single-reference CC methods of the CCSD or CCSD(T) type, which do not require defining active orbitals and which do not suffer from intruder states and multiple, singular, or unphysical solutions that plague the genuine MRCC theories [77, 78, 79, 80, 81, 82, 83, 84]. The recently developed state-specific MRCC approaches [85, 86, 87, 88, 89, 90, 91, 92, 93, 94], the active-space CC or state-selective MRCC methods combining the idea of using active orbitals with the single-reference CC theory [51, 53, 54, 58, 69, 70, 71, 95, 96, 97, 98, 99, 100, 101, 102, 103, 104, 105, 106, 107], the reduced multi-reference CCSD approach [9, 108, 109, 110, 111, 112, 113], and the MRCC method combining the genuine multi-reference MBPT and MRCC concepts [76, 114] may change this situation, but none of the existing MRCC methods are simple or general enough to be as widely applicable as the standard CCSD/EOMCCSD or CCSD(T) approaches.

The failures of the standard single-reference CC and response CC/EOMCC approximations in the bond breaking region and for excited states dominated by two- and other many-electron transitions can also be remedied by using the high-end single-reference CC approximations, such as full CC singles, doubles, and triples (CCSDT) [115, 116], full CC singles, doubles, triples, and quadruples (CCSDTQ) [99, 117, 118, 119], and full CC singles, doubles, triples, quadruples, and pentuples (CCSDTQP) [120], and their excited-state or response extensions, such as the recently implemented full EOMCCSDT approach [70, 71, 121]. In these methods, the T_3, T_4, and other higher-order clusters and the corresponding higher–than–two-body components of the EOMCC excitation operator are determined in an iterative fashion without making additional approximations employing MBPT. Unfortunately, the prohibitive costs of the CCSDT/EOMCCSDT, CCSDTQ, and other such methods limit their applicability to very small systems, consisting of at most a few light atoms described by relatively small basis sets. For example, the full CCSDTQ method requires iterative steps that scale as $n_o^4 n_u^6$ [n_o (n_u) is the number of occupied (unoccupied) orbitals in the molecular orbital basis]. This $\mathcal{N}^{10}$ scaling with the system size $\mathcal{N}$ should be contrasted with the iterative $n_o^2 n_u^4$ (or $\mathcal{N}^6$) and noniterative $n_o^3 n_u^4$ (or $\mathcal{N}^7$) steps of the CCSD and CCSD(T) methods, which can nowadays be routinely applied to systems containing 10–20 light atoms and a few heavy atoms (approximately 100 light atoms, hundreds of correlated electrons, and more than 1000 basis functions when the local correlation formalism of Pulay and Saebø [122, 123, 124] is employed [125, 126, 127]) without a significant loss of accuracy when compared, for example, with the full CCSDT method. The CCSD(TQ$_f$) method [44], with its relatively inexpensive $n_o^2 n_u^5$ ($\mathcal{N}^7$) steps in the noniterative part related to the calculation of the connected quadruples (Q$_f$) correction, should become increasingly more popular in the future, particularly when there is a need to include the combined effect of T_3 and T_4 clusters in the calculations. In analogy to the ground-state CCSD and CCSD(T) methods, the EOMCCSD approach and its similarity-transformed EOMCC extension [128, 129] can be used to calculate the excited states of systems as big as free-base porphin [128, 129, 130] (the recently formulated local EOMCCSD approaches [131, 132] will enable calculations for even larger systems). All of this indicates that in searching for new methods that would eliminate the failures of the standard CC/EOMCC approaches, such as CCSD, CCSD(T), or EOMCCSD, in the bond breaking region, one should focus on improving the results of the low-order CC/EOMCC calculations, such as CCSD or EOMCCSD, using the noniterative corrections of the CCSD(T) or CCSD(TQ$_f$) type, or the reference configurations of the non-RHF type. It seems to us that only such methods have a chance to be applied to a wide range of molecular problems in the not-too-distant future.

A few new classes of the single-reference CC/EOMCC approaches have been proposed in recent years with the intention of removing the pervasive failing of the standard RHF-based CC/EOMCC approximations at larger internuclear separations and for excited states dominated by two-electron transitions. The most notable examples include the renormalized (R) and completely renormalized (CR) CCSD(T) and CCSD(TQ) methods [12, 55, 56, 57, 58, 59, 60, 61, 63, 64, 74] and other noniterative CC approaches [12, 55, 62, 64, 65, 66, 72, 73] based on the general formalism of the method of moments of CC equations (MMCC) introduced by Piecuch and Kowalski [55, 56, 57, 72, 73, 133], the noniterative CC approaches based on the partitioning of the similarity-transformed Hamiltonian pursued by Gwaltney, Head-Gordon, and coworkers [134, 135, 136, 137, 138] (see, also, Ref. [139]), the spin-flip CC methods developed by Krylov and coworkers [140, 141, 142], and the CCSD-like methods [64, 65, 137, 138, 143, 144] based on the extended CC (ECC) theories of Arponen, Bishop and coworkers [145, 146, 147, 148, 149, 150, 151, 152, 153, 154] and Piecuch and Bartlett [31]. The underlying philosophy of all of these methods is to improve the performance of the single-reference CC methods in the bond breaking region, while avoiding the complexity of the genuine multireference theory and astronomical costs of the CCSDTQ, CCSDTQP, and similar calculations, although the applicability of the MMCC formalism of Piecuch and Kowalski goes way beyond the bond breaking problem in chemistry (e.g., the MMCC theory applies to single-reference as well as multireference formalisms [133] and it can deal with the ground as well as excited electronic [12, 72, 73, 74] and other many-fermion [155] states). The noniterative CC approaches developed by Gwaltney, Head-Gordon, and coworkers, which are based on the partitioning of the similarity-transformed Hamiltonian [134, 135, 136, 137, 138], the R-CC, CR-CC, and other MMCC approaches developed by Piecuch and coworkers [12, 55, 56, 57, 58, 59, 60, 61, 62, 63, 64, 65, 66, 72, 73, 74], and the ECC singles and doubles (ECCSD) or ECC doubles (ECCD) theories tested by Piecuch and coworkers [64, 65] and Head-Gordon and coworkers [137, 138, 143, 144] provide substantial improvements in the bond breaking region, including multiple bond dissociation, in spite of using the spin-adapted reference configurations of the RHF type. The spin-flip CC methods of Krylov and coworkers [140, 141, 142] achieve similar improvements for singly bonded molecules by using the restricted but "spin-flipped" reference configurations and by generating the desired diradical ground state as a formal excitation from the approximate triplet state obtained in the spin-orbital CCSD calculations with the high-spin, "spin-flipped", reference. All these methods have their specific strengths. The major advantages of the CR-CC and other MMCC approaches developed by Piecuch and coworkers [12, 55, 56, 57, 58, 59, 60, 61, 62, 63, 64, 65, 66, 72, 73, 74] are the excellent control of accuracy by directly addressing the quantity of interest, which is the difference between the full CI and CC or EOMCC energies (this is very useful in designing new MMCC approximations in a systematic manner), the uniform and approximately variational treatment of ground and excited states (the CR-CC and MMCC energies are usually above the corresponding full CI energies, in spite of the nonvariational collapse of the underlying standard CC approaches in the bond breaking region), and the ease with which various higher-order effects, necessary to describe more complicated types of quasidegenerate electronic states and multiple bond breaking, can be incorporated into the formalism at a relatively low cost (as indicated, for example, by the recent development of the quasivariational and quadratic MMCC (QMMCC) approaches [64, 65, 66]).

In this article, we overview the renormalized and completely renormalized CCSD(T) and CCSD(TQ) methods and their newest QMMCC and excited-state extensions [12, 55, 56, 57, 58, 59, 60, 61, 62, 63, 64, 65, 66, 72, 73, 74]. We also review the underlying MMCC formalism [55, 56, 57, 72, 73, 133], on which all of these approaches are based, including its generalization to nonstandard choices of cluster operators. Finally, we discuss the recently discovered (P. Piecuch, K. Kowalski, P.-D. Fan, M. Lodriguito, unpublished results) new possibilities offered by combining the MMCC and ECC theories. Formal considerations are accompanied by a few examples of applications of the R-CC, CR-CC, and MMCC methods to ground- and excited-state PESs, including the preliminary results for bond breaking on nonsinglet PESs (T. Kuś, P. Piecuch, S. A. Kucharski, M. J. McGuire, K. Kowalski, unpublished results). A list of the acronyms representing all quantum-chemical methods discussed or referred to in this article is provided in the Appendix.

2 The method of moments of coupled-cluster equations: basic concepts

The main idea of the MMCC formalism of Refs. [55, 56, 57, 72, 73, 133] is that of the state-selective and noniterative energy corrections

$$\delta_K^{(\mathrm{A})} \equiv E_K - E_K^{(\mathrm{A})}, \tag{1}$$

which, when added to the energies of ground ($K = 0$) and excited ($K > 0$) states, $E_K^{(\mathrm{A})}$, obtained in the standard CC/EOMCC calculations, such as CCSD/EOMCCSD and CCSDT/EOMCCSDT (commonly termed as method A), recover the corresponding exact, i.e. full CI, energies E_K. The main objective of all approximate MMCC calculations, including the renormalized and completely renormalized CCSD(T) and CCSD(TQ) methods [12, 55, 56, 57, 58, 59, 60, 61, 63, 64, 65] and their newest QMMCC extensions [12, 64, 65, 66], the CI-corrected MMCC approaches [12, 55, 62, 72, 73] (adopted recently by others [156, 157, 158]), and the excited-state MMCC and renormalized CC methods [12, 72, 73, 74], is to approximate corrections $\delta_K^{(\mathrm{A})}$, such that the resulting MMCC energies, defined as

$$E_K^{(\mathrm{MMCC})} = E_K^{(\mathrm{A})} + \delta_K^{(\mathrm{A})}, \tag{2}$$

are close to the corresponding exact energies E_K. All MMCC approximations are obtained from the rigorous formulas for the exact corrections $\delta_K^{(\mathrm{A})}$ in terms of the generalized moments of the CC/EOMCC equations, derived by Piecuch and Kowalski in Refs. [55, 56, 72, 73] (see, also, Ref. [12]) and discussed later. Similar formulas for the noniterative corrections $\delta_K^{(\mathrm{A})}$ to the ground- and excited-state energies obtained in the genuine MRCC calculations that are based on the generalized moments of the MRCC equations and that recover full CI energies E_K (obtained in this case by diagonalizing the effective

Hamiltonian in the multidimensional reference space) have been described in Ref. [133]. In this article, we focus on the MMCC corrections to single-reference CC/EOMCC energies.

The MMCC formalism and the renormalized and completely renormalized CC approaches and other approximations that originate from it preserve the conceptual and computational simplicity of the noniterative CC methods, such as CCSD(T), which are based on adding noniterative a posteriori energy corrections due to higher-order clusters to lower-order CC or EOMCC (e.g., CCSD/EOMCCSD) results, while offering us a new way of controlling the quality of CC or EOMCC results by directly focusing on the quantity of interest, which is the difference between the full CI and CC or EOMCC energies. In other words, in MMCC calculations, we are not just interested in improving the Hartree–Fock or some other independent-particle-model (IPM) description by adding corrections due to correlation, as we normally do in standard quantum-chemical approaches, with the hope that the more high-order terms we add the better the results (which may not always be the case). We are rather dealing with the remanent errors that occur in the standard CC or EOMCC calculations, which we are trying to estimate by using the explicit relationships between the CC or EOMCC and full CI energies defining the MMCC theory. As we will see in a few numerical examples provided later, this new level of controlling the accuracy of CC calculations is particularly advantageous in situations where the conventional arguments originating from MBPT, which are used to design the standard CC/EOMCC approximations, fail owing to divergent behavior of the MBPT series (as is, for example, the case in studies of quasidegenerate and excited states, and bond breaking).

We begin our description of the MMCC methods with the exact MMCC formalism. The approximate MMCC methods are discussed in the next section. For a detailed description of the multireference extension of the MMCC formalism, which we do not discuss in this article, we refer the reader to the original work [133].

2.1 The exact ground-state MMCC theory

In the ground-state MMCC theory, we use corrections $\delta_0^{(\mathrm{A})}$ to improve the results of the standard CC calculations. By the standard CC calculation, referred here and elsewhere to as method A, we mean any single-reference calculation in which the many-body expansion for the cluster operator T, defining the CC ground-state wave function

$$|\Psi_0\rangle = \mathrm{e}^{T}|\Phi\rangle \ , \tag{3}$$

where $|\Phi\rangle$ is the IPM reference configuration (e.g., the Hartree–Fock determinant), is truncated at some excitation level $m_{\mathrm{A}} < N$ (N is the number of electrons in a system). An example of the standard CC approximation is the CCSD method. In this case, $m_{\mathrm{A}} = 2$ and the cluster operator T is approximated by

$$T^{(\mathrm{CCSD})} = T_1 + T_2 \ , \tag{4}$$

where

$$T_1 = \sum_{\substack{i_1\\a_1}} t_{a_1}^{i_1} E_{i_1}^{a_1} \tag{5}$$

and

$$T_2 = \sum_{\substack{i_1<i_2\\a_1<a_2}} t_{a_1a_2}^{i_1i_2} E_{i_1i_2}^{a_1a_2} \tag{6}$$

are the singly and doubly excited cluster components and $E_{i_1}^{a_1}$ and $E_{i_1i_2}^{a_1a_2}$ are the corresponding excitation operators, generating the singly and doubly excited configurations, $|\Phi_{i_1}^{a_1}\rangle$ and $|\Phi_{i_1i_2}^{a_1a_2}\rangle$, respectively, when acting on reference $|\Phi\rangle$. As usual, letters i and a designate the occupied and unoccupied spin–orbitals, respectively, and $t_{a_1}^{i_1}$ and $t_{a_1a_2}^{i_1i_2}$ are the singly and doubly excited cluster amplitudes. Other examples of the standard CC approximations are provided by the full CCSDT, CCSDTQ, and CCSDTQP approaches mentioned in the Introduction, in which $m_{\mathrm{A}} = 3 - 5$, respectively. The general form of the truncated cluster operator defining a standard approximation A, characterized by the excitation level m_{A}, is

$$T^{(\mathrm{A})} = \sum_{n=1}^{m_{\mathrm{A}}} T_n \ , \tag{7}$$

where

$$T_n = \sum_{\substack{i_1<\cdots<i_n\\a_1<\cdots<a_n}} t_{a_1\ldots a_n}^{i_1\ldots i_n} E_{i_1\ldots i_n}^{a_1\ldots a_n} \ , \tag{8}$$

$n = 1, \ldots, m_{\mathrm{A}}$, are the many-body components of $T^{(\mathrm{A})}$ and $E_{i_1\ldots i_n}^{a_1\ldots a_n}$ and $t_{a_1\ldots a_n}^{i_1\ldots i_n}$ are the corresponding excitation operators and cluster amplitudes. The system of equations for the cluster amplitudes $t_{a_1\ldots a_n}^{i_1\ldots i_n}$ defining the T_n components of $T^{(\mathrm{A})}$ has the following general form:

$$\langle\Phi_{i_1\ldots i_n}^{a_1\ldots a_n}|\bar{H}^{(\mathrm{A})}|\Phi\rangle = 0, \ i_1 < \cdots < i_n, \ a_1 < \cdots < a_n \ , \tag{9}$$

where $n = 1, \ldots, m_{\mathrm{A}}$,

$$\bar{H}^{(\mathrm{A})} = \mathrm{e}^{-T^{(\mathrm{A})}} H \mathrm{e}^{T^{(\mathrm{A})}} = (H\mathrm{e}^{T^{(\mathrm{A})}})_{\mathrm{C}} \tag{10}$$

is the similarity-transformed Hamiltonian of the CC theory, subscript C designates the connected part of the corresponding operator expression, and $|\Phi_{i_1\ldots i_n}^{a_1\ldots a_n}\rangle = E_{i_1\ldots i_n}^{a_1\ldots a_n}|\Phi\rangle$ are the n-tuply excited configurations. In particular, the standard CCSD equations for the singly and doubly excited cluster amplitudes $t_{a_1}^{i_1}$ and $t_{a_1a_2}^{i_1i_2}$ defining operators T_1 and T_2, respectively, are

$$\langle\Phi_{i_1}^{a_1}|\bar{H}^{(\mathrm{CCSD})}|\Phi\rangle = 0, \tag{11}$$

$$\langle\Phi_{i_1i_2}^{a_1a_2}|\bar{H}^{(\mathrm{CCSD})}|\Phi\rangle = 0, \ i_1 < i_2, \ a_1 < a_2 \ , \tag{12}$$

where

$$\bar{H}^{(\mathrm{CCSD})} = \mathrm{e}^{-(T_1+T_2)} H \mathrm{e}^{T_1+T_2} = (H\mathrm{e}^{T_1+T_2})_{\mathrm{C}} \tag{13}$$

is the similarity-transformed Hamiltonian of the CCSD approach. Once the system of equations, Eq. (9), is solved for $T^{(\mathrm{A})}$ (or Eqs. 11, 12 are solved for T_1 and T_2), the CC energy corresponding to the standard method A is calculated using the equation

$$E_0^{(\mathrm{A})} = \langle\Phi|\bar{H}^{(\mathrm{A})}|\Phi\rangle \ . \tag{14}$$

For Hamiltonians used in quantum chemistry, which do not contain higher–than–two-body interactions, $E_0^{(\mathrm{A})}$ depends on the T_1 and T_2 clusters only, independent of the excitation level m_A defining method A (assuming that $m_\mathrm{A} \geq 2$). We have,

$$E_0^{(\mathrm{A})} = \langle\Phi|H|\Phi\rangle + \langle\Phi|[H_\mathrm{N}(T_1 + T_2 + \frac{1}{2}T_1^2)]_\mathrm{C}|\Phi\rangle \ , \tag{15}$$

where $H_\mathrm{N} = H - \langle\Phi|H|\Phi\rangle$ is the Hamiltonian in the normal-ordered form.

The MMCC theory is based on the idea of recovering the exact, full CI, energies from the results of approximate CC calculations. In order to explain what quantities provided by the CC theory may be needed to recover the full CI ground-state energy from the results of approximate CC calculations, such as CCSD, we should mention that the single-reference CC equations, Eq. (9), are formally obtained by inserting the CC wave function $|\Psi_0\rangle$, Eq. (3), into the electronic Schrödinger equation,

$$H|\Psi_0\rangle = E_0|\Psi_0\rangle \ , \tag{16}$$

premultiplying both sides of Eq. (16) on the left by e^{-T} to obtain the connected cluster form of the Schrödinger equation [3, 4, 6, 9, 55],

$$\bar{H}|\Phi\rangle = E_0|\Phi\rangle \ , \tag{17}$$

with

$$\bar{H} = \mathrm{e}^{-T}H\mathrm{e}^{T} = (H\mathrm{e}^{T})_\mathrm{C} \ , \tag{18}$$

and projecting Eq. (17), in which $T = T^{(\mathrm{A})}$, onto the excited configurations $|\Phi_{i_1\ldots i_n}^{a_1\ldots a_n}\rangle$ generated by this $T^{(\mathrm{A})}$. This general prescription how to derive the equations for all standard CC methods, which is used until today and which was introduced by Čížek [3, 4], implies that projections of the connected cluster form of the Schrödinger equation, Eq. (17), on all excited configurations $|\Phi_{i_1\ldots i_k}^{a_1\ldots a_k}\rangle$, i.e.,

$$\mathscr{M}_{a_1\ldots a_k}^{i_1\ldots i_k}(m_\mathrm{A}) = \langle\Phi_{i_1\ldots i_k}^{a_1\ldots a_k}|\bar{H}^{(\mathrm{A})}|\Phi\rangle \ , \tag{19}$$

represent the most fundamental quantities for the CC theory. These projections define the generalized moments of CC equations (for a discussion of the relationship between the method of moments of Krylov [159], used in various areas of mathematical physics, and the single-reference CC theory, see Ref. [160]). In the language of the method of moments of Krylov [159], we might say that the standard CC equations, Eq. (9), are obtained by requiring that all $\mathscr{M}_{a_1\ldots a_k}^{i_1\ldots i_k}(m_\mathrm{A})$ moments with $k = 1, \ldots, m_\mathrm{A}$ vanish. However, the use of the generalized moments of CC equations, Eq. (19), does not end there. Once the cluster operator $T^{(\mathrm{A})}$, Eq. (7), is determined by zeroing moments $\mathscr{M}_{a_1\ldots a_k}^{i_1\ldots i_k}(m_\mathrm{A})$ with $k = 1, \ldots, m_\mathrm{A}$, we can calculate the remaining moments $\mathscr{M}_{a_1\ldots a_k}^{i_1\ldots i_k}(m_\mathrm{A})$ with $k > m_\mathrm{A}$. As shown by Piecuch and Kowalski in Refs. [55, 56] (see, also, Ref. [12]), the $\mathscr{M}_{a_1\ldots a_k}^{i_1\ldots i_k}(m_\mathrm{A})$ moments with $k > m_\mathrm{A}$ allow us to determine the desired noniterative correction $\delta_0^{(\mathrm{A})}$, Eq. (1), and, thus, the exact ground-state energy E_0. For example, if we want to recover the full CI energy E_0 by adding the correction $\delta_0^{(\mathrm{A})}$ to the CCSD energy (the $m_\mathrm{A} = 2$ case), we must calculate the generalized moments of the CCSD equations, i.e., the projections of these equations on triply, quadruply, pentuply, and hextuply excited configurations or

$$\mathscr{M}_{a_1\ldots a_k}^{i_1\ldots i_k}(2) = \langle\Phi_{i_1\ldots i_k}^{a_1\ldots a_k}|\bar{H}^{(\mathrm{CCSD})}|\Phi\rangle, \ \ k = 3 - 6 \ . \tag{20}$$

The projections of the CCSD equations on higher–than–hextuply excited configurations do not have to be calculated, since for Hamiltonians containing up to two-body interactions the generalized moments $\mathscr{M}_{a_1\ldots a_k}^{i_1\ldots i_k}(2)$ with $k > 6$ vanish.

The fundamental formula given by Piecuch and Kowalski in Refs. [55, 56], which relates the noniterative correction $\delta_0^{(\mathrm{A})}$, Eq. (1), with the generalized moments of the single-reference CC equations and which defines the ground-state MMCC theory, has the following form:

$$\begin{aligned}\delta_0^{(\mathrm{A})} &\equiv E_0 - E_0^{(\mathrm{A})} \\ &= \sum_{n=m_\mathrm{A}+1}^{N} \sum_{k=m_\mathrm{A}+1}^{n} \langle\Psi_0|C_{n-k}(m_\mathrm{A})M_k(m_\mathrm{A})|\Phi\rangle / \\ &\qquad \langle\Psi_0|\mathrm{e}^{T^{(\mathrm{A})}}|\Phi\rangle \ .\end{aligned} \tag{21}$$

Here,

$$C_{n-k}(m_\mathrm{A}) = (\mathrm{e}^{T^{(\mathrm{A})}})_{n-k} \tag{22}$$

are the $(n-k)$-body components of the exponential wave operator $\mathrm{e}^{T^{(\mathrm{A})}}$, defining the CC method A, $|\Psi_0\rangle$ is the full CI ground state, and

$$M_k(m_\mathrm{A})|\Phi\rangle = \sum_{\substack{i_1<\cdots<i_k \\ a_1<\cdots<a_k}} \mathscr{M}_{a_1\ldots a_k}^{i_1\ldots i_k}(m_\mathrm{A})|\Phi_{i_1\ldots i_k}^{a_1\ldots a_k}\rangle \ . \tag{23}$$

Equation (21) states that one has to calculate quantities $C_{n-k}(m_\mathrm{A})$, Eq. (22), and moments $\mathscr{M}_{a_1\ldots a_k}^{i_1\ldots i_k}(m_\mathrm{A})$, with $k > m_\mathrm{A}$, to determine the noniterative energy correction $\delta_0^{(\mathrm{A})}$. The $C_{n-k}(m_\mathrm{A})$ terms are very easy to calculate. The zero-body term, $C_0(m_\mathrm{A})$, equals 1; the one-body term, $C_1(m_\mathrm{A})$, equals T_1; the two-body term, $C_2(m_\mathrm{A})$, equals $T_2 + \frac{1}{2}T_1^2$ if $m_\mathrm{A} \geq 2$; the three-body term, $C_3(m_\mathrm{A})$, equals $T_1T_2 + \frac{1}{6}T_1^3$ if $m_\mathrm{A} = 2$ and $T_3 + T_1T_2 + \frac{1}{6}T_1^3$ if $m_\mathrm{A} \geq 3$, etc. Determination of the generalized moments $\mathscr{M}_{a_1\ldots a_k}^{i_1\ldots i_k}(m_\mathrm{A})$ is relatively straightforward too, particularly for the lower-order CC methods, such as CCSD. We can write the following expressions for the CCSD moments $\mathscr{M}_{a_1\ldots a_k}^{i_1\ldots i_k}(2)$, $k = 3 - 6$, in terms of T_1 and T_2, assuming that the Hamiltonian does not contain higher–than–two-body interactions (cf. Eq. 20):

$$\begin{aligned}\mathscr{M}_{a_1a_2a_3}^{i_1i_2i_3}(2) = \langle\Phi_{i_1i_2i_3}^{a_1a_2a_3}|[H_\mathrm{N}(T_2 + T_1T_2 + \frac{1}{2}T_2^2 + \frac{1}{2}T_1^2T_2 \\ + \frac{1}{2}T_1T_2^2 + \frac{1}{6}T_1^3T_2)]_\mathrm{C}|\Phi\rangle \ ,\end{aligned} \tag{24}$$

$$\mathscr{M}^{i_1i_2i_3i_4}_{a_1a_2a_3a_4}(2) = \langle\Phi^{a_1a_2a_3a_4}_{i_1i_2i_3i_4}|[H_\mathrm{N}(\frac{1}{2}T_2^2 + \frac{1}{2}T_1T_2^2 + \frac{1}{6}T_2^3 + \frac{1}{4}T_1^2T_2^2)]_\mathrm{C}|\Phi\rangle \ , \quad (25)$$

$$\mathscr{M}^{i_1i_2i_3i_4i_5}_{a_1a_2a_3a_4a_5}(2) = \frac{1}{6}\langle\Phi^{a_1a_2a_3a_4a_5}_{i_1i_2i_3i_4i_5}|[H_\mathrm{N}(T_2^3 + T_1T_2^3)]_\mathrm{C}|\Phi\rangle \ , \quad (26)$$

$$\mathscr{M}^{i_1i_2i_3i_4i_5i_6}_{a_1a_2a_3a_4a_5a_6}(2) = \frac{1}{24}\langle\Phi^{a_1a_2a_3a_4a_5a_6}_{i_1i_2i_3i_4i_5i_6}|(H_\mathrm{N}T_2^4)_\mathrm{C}|\Phi\rangle \ . \quad (27)$$

Thus, the formula for $\delta_0^{(\mathrm{A})}$, Eq. (21), is a very good starting point for developing noniterative CC approaches, in which ground-state energies are calculated by adding $\delta_0^{(\mathrm{A})}$ to the CC energy $E_0^{(\mathrm{A})}$. For example, we can develop a variety of noniterative methods, in which we correct the results of the CCSD calculations. In this case, the formula for the correction $\delta_0^{(\mathrm{CCSD})}$, which must be added to the CCSD energy $E_0^{(\mathrm{CCSD})}$ to recover the exact energy E_0, is

$$\delta_0^{(\mathrm{CCSD})} \equiv E_0 - E_0^{(\mathrm{CCSD})} = \sum_{n=3}^{N}\sum_{k=3}^{\min(n,6)} \langle\Psi_0|C_{n-k}(2)M_k(2)|\Phi\rangle / \langle\Psi_0|\mathrm{e}^{T_1+T_2}|\Phi\rangle \ , \quad (28)$$

where

$$M_k(2)|\Phi\rangle = \sum_{\substack{i_1<\cdots<i_k \\ a_1<\cdots<a_k}} \mathscr{M}^{i_1\ldots i_k}_{a_1\ldots a_k}(2)|\Phi^{a_1\ldots a_k}_{i_1\ldots i_k}\rangle. \quad (29)$$

Interestingly enough, Eqs. (21) and (28) can be generalized to a situation where the truncated cluster operator $T^{(\mathrm{A})}$, Eq. (7), is not necessarily determined by solving the standard CC equations (Eq. 9). In this case, we can no longer assume that the generalized moments $\mathscr{M}^{i_1\ldots i_k}_{a_1\ldots a_k}(m_\mathrm{A})$ with $k = 1, \ldots, m_\mathrm{A}$ vanish. The resulting expression for the exact energy E_0 that uses all generalized moments $\mathscr{M}^{i_1\ldots i_k}_{a_1\ldots a_k}(m_\mathrm{A})$, Eq. (19), has the following form [12, 55, 56]:

$$E_0 = M_0(m_\mathrm{A}) + \sum_{n=1}^{N}\sum_{k=1}^{n}\langle\Psi_0|C_{n-k}(m_\mathrm{A})M_k(m_\mathrm{A})|\Phi\rangle / \langle\Psi_0|\mathrm{e}^{T^{(\mathrm{A})}}|\Phi\rangle, \quad (30)$$

where we define the zero-body moment $M_0(m_\mathrm{A})$ in the same way as we define the CC energy $E_0^{(\mathrm{A})}$, i.e., (cf. Eq. 14)

$$M_0(m_\mathrm{A}) = \langle\Phi|\bar{H}^{(\mathrm{A})}|\Phi\rangle \ . \quad (31)$$

The difference between $M_0(m_\mathrm{A})$ and $E_0^{(\mathrm{A})}$ lies in the fact that $E_0^{(\mathrm{A})}$ is determined using cluster amplitudes originating from the standard CC equations, Eq. (9), whereas $M_0(m_\mathrm{A})$ can be computed with any value of $T^{(\mathrm{A})}$, obtained by performing some nonstandard calculations, such as the ECC calculations mentioned in the Introduction (see the discussion later; see, also, Sect. 3.4). The $C_{n-k}(m_\mathrm{A})$ and $M_k(m_\mathrm{A})|\Phi\rangle$ quantities are still defined by Eqs. (22) and (23), respectively, with an exception that now we must consider all quantities $M_k(m_\mathrm{A})|\Phi\rangle$ with $k = 1, \ldots, N$, not just with $k > m_\mathrm{A}$. In the case of using only the T_1 and T_2 clusters to construct the exact energy E_0 (which are no longer determined by solving the standard CCSD equations), we can write

$$E_0 = M_0(2) + \sum_{n=1}^{N}\sum_{k=1}^{\min(n,6)} \langle\Psi_0|C_{n-k}(2)M_k(2)|\Phi\rangle / \langle\Psi_0|\mathrm{e}^{T_1+T_2}|\Phi\rangle \ , \quad (32)$$

where $M_k(2)|\Phi\rangle$ is defined by Eq. (29). Again, the only essential difference between Eqs. (32) and (28) is the presence of all moments $\mathscr{M}^{i_1\ldots i_k}_{a_1\ldots a_k}(2)$ in the former equation. Thus, for Hamiltonians containing up to two-body interactions, we must consider the singly and doubly excited moments, $\mathscr{M}^{i_1}_{a_1}(2)$ and $\mathscr{M}^{i_1i_2}_{a_1a_2}(2)$, respectively, which are no longer zeroed, along with moments $\mathscr{M}^{i_1\ldots i_k}_{a_1\ldots a_k}(2)$ with $k = 3 - 6$ considered in the standard CCSD case (cf. Eqs. 24, 25, 26, 27). The formulas for the $\mathscr{M}^{i_1}_{a_1}(2)$ and $\mathscr{M}^{i_1i_2}_{a_1a_2}(2)$ moments in terms of T_1 and T_2 are identical to the left-hand sides of the standard CCSD equations. We obtain (cf. Eqs. 11, 12)

$$\mathscr{M}^{i_1}_{a_1}(2) = \langle\Phi^{a_1}_{i_1}|[H_\mathrm{N}(1 + T_1 + T_2 + \frac{1}{2}T_1^2 + T_1T_2 + \frac{1}{6}T_1^3)]_\mathrm{C}|\Phi\rangle \quad (33)$$

and

$$\mathscr{M}^{i_1i_2}_{a_1a_2}(2) = \langle\Phi^{a_1a_2}_{i_1i_2}|[H_\mathrm{N}(1 + T_1 + T_2 + \frac{1}{2}T_1^2 + T_1T_2 + \frac{1}{6}T_1^3 + \frac{1}{2}T_2^2 + \frac{1}{2}T_1^2T_2 + \frac{1}{24}T_1^4)]_\mathrm{C}|\Phi\rangle \ . \quad (34)$$

Equation (21) or Eq. (28) and Eq. (30) or Eq. (32) define the ground-state MMCC formalism. Typically, we use Eq. (21) or Eq. (28). In this case, we solve first the standard CC equations to determine the truncated cluster operator $T^{(\mathrm{A})}$ defining the approximate CC method A. Once the cluster operator $T^{(\mathrm{A})}$ is determined, we calculate the relevant moments $\mathscr{M}^{i_1\ldots i_k}_{a_1\ldots a_k}(m_\mathrm{A})$ and calculate the noniterative correction $\delta_0^{(\mathrm{A})}$, Eq. (21), to improve the results obtained with method A. All previously published results of the MMCC calculations of ground-state PESs involving single and multiple bond breaking, including the results obtained with the renormalized and completely renormalized CCSD(T) and CCSD(TQ) methods and their QMMCC analogs [12, 55, 56, 57, 58, 59, 60, 61, 63, 64, 65, 66], were obtained with various approximate variants of the MMCC theory based on Eqs. (21) and (28). Examples of the applications of Eq. (28) to molecular PESs are discussed in Sect. 3. The general MMCC formulas, Eqs. (30) and (32), can be useful if we want to exploit the nonstandard values of the T_n cluster components defining $T^{(\mathrm{A})}$ (e.g., the nonstandard values of T_1 and T_2, which are not obtained with the CCSD method). We may wish to use the nonstandard T_n components to calculate the energy according to Eq. (30) or Eq. (32) in exceptionally difficult cases of multiple bond breaking, where the standard CCSD values of the T_1 and T_2 cluster components may be too poor to provide the desired improvements in the description of molecular PESs by the MMCC theory. A preliminary example of an application of the general MMCC formula (Eq. 32) to triple bond breaking in N_2, in which the T_1 and T_2 clusters needed to construct the generalized moments $\mathscr{M}^{i_1\ldots i_k}_{a_1\ldots a_k}(2)$ originate from the ECCSD [64, 65] rather than from the CCSD calculations, is discussed in Sect. 3.4.

There are two issues that have to be resolved before using Eqs. (21) and (28) (or their generalizations, Eqs. (30) and (32)) in practical calculations. First of all, the exact MMCC corrections $\delta_0^{(\mathrm{A})}$, Eq. (21), or $\delta_0^{(\mathrm{CCSD})}$, Eq. (28), have the form of the complete many-body expansions involving all n-tuply excited configurations with $n = m_{\mathrm{A}}, \ldots, N$, where N is the number of electrons in a system (see the summations over n in Eqs. (21), (28) or (30), (32)). Thus, in order to develop the computationally inexpensive MMCC methods, we must first truncate the many-body expansions for $\delta_0^{(\mathrm{A})}$ or $\delta_0^{(\mathrm{CCSD})}$ at some, preferably low, excitation level m_{B}. This leads to the MMCC($m_{\mathrm{A}}, m_{\mathrm{B}}$) schemes [12, 55, 56, 57, 61, 64] (see Sect. 3). For example, the renormalized and completely renormalized CCSD(T) and CCSD(TQ) methods discussed in Sect. 3.1 are the MMCC($m_{\mathrm{A}}, m_{\mathrm{B}}$) schemes with $m_{\mathrm{A}} = 2$ and $m_{\mathrm{B}} = 3$ [the CCSD(T) case] or $m_{\mathrm{B}} = 4$ [the CCSD(TQ) case]. Second, the wave function $|\Psi_0\rangle$ that enters the exact Eqs. (21) and (28) (or Eqs. (30), (32)) is the exact, full CI, ground state. Thus, in order to propose the computationally tractable approaches based on the MMCC theory, we must approximate $|\Psi_0\rangle$ in some way. Various ways of approximating $|\Psi_0\rangle$ in Eqs. (28) and (32), leading to the renormalized and completely renormalized CCSD(T) and CCSD(TQ) methods, the QMMCC methods, the CI-corrected MMCC approaches (all employing the CCSD values of T_1 and T_2 to construct the relevant energy corrections), and the MMCC methods employing the ECCSD values of T_1 and T_2, are discussed in Sect. 3.

2.2 The excited-state MMCC theory

The ground-state MMCC theory, described in Sect. 2.1, can be extended to excited electronic states [12, 61, 72, 73, 74]. In this case, the noniterative energy corrections $\delta_K^{(\mathrm{A})}$, Eq. (1), are added to the excitedstate energies, $E_K^{(\mathrm{A})}$, obtained in the EOMCC calculations (another possibility would be to use the genuine MRCC theory to calculate the $E_K^{(\mathrm{A})}$ energies and the multi-reference extension of the MMCC theory to calculate corrections $\delta_K^{(\mathrm{A})}$ [133]; in this article we focus on using the EOMCC method to calculate energies $E_K^{(\mathrm{A})}$). The MMCC formula for the excited-state corrections $\delta_K^{(\mathrm{A})}$ is very similar to the formula for the ground-state corrections $\delta_0^{(\mathrm{A})}$, Eq. (21). The only essential difference between the ground- and excited-state MMCC energy expressions is the presence of the generalized moments of the EOMCC equations in the formula for the excited-state corrections $\delta_K^{(\mathrm{A})}$ instead of the moments of the ground-state CC equations entering Eq. (21).

In order to properly define the generalized moments of the EOMCC equations, we must first describe the most essential elements of the EOMCC formalism. In the EOMCC theory, the excited states $|\Psi_K\rangle$ of a given N-electron system are obtained by applying the excitation operator R_K to the ground state obtained in the single-reference CC calculations, i.e.,

$$|\Psi_K\rangle = R_K|\Psi_0\rangle \ , \qquad (35)$$

where $|\Psi_0\rangle$ is defined by Eq. (3). In the exact EOMCC theory, the cluster operator T and the excitation operators R_K are sums of all relevant many-body components that can be written for a given N-electron system, including the N-body terms. In the standard EOMCC approximations, such as EOMCCSD, the many-body expansions of T and R_K are truncated at some excitation level $m_{\mathrm{A}} < N$ (again, A designates the standard EOMCC approximation). Thus, the cluster operator T is approximated by $T^{(\mathrm{A})}$, Eq. (7), whereas for the excitation operator R_K we write

$$R_K \simeq R_K^{(\mathrm{A})} = R_{K,0}^{(\mathrm{A})} + R_{K,\mathrm{open}}^{(\mathrm{A})} \ , \qquad (36)$$

where the "open" part of $R_K^{(\mathrm{A})}$ is defined as

$$R_{K,\mathrm{open}}^{(\mathrm{A})} = \sum_{n=1}^{m_{\mathrm{A}}} R_{K,n} \ , \qquad (37)$$

with

$$R_{K,n} = \sum_{\substack{i_1<\cdots<i_n\\ a_1<\cdots<a_n}} r^{i_1\ldots i_n}_{K,a_1\ldots a_n} E^{a_1\ldots a_n}_{i_1\ldots i_n} \qquad (38)$$

representing the n-body components of $R_K^{(\mathrm{A})}$. The standard EOMCCSD method is defined by setting $m_{\mathrm{A}} = 2$ in Eqs. (7) and (37). In the EOMCCSDT approach, $m_{\mathrm{A}} = 3$, etc. For the consistency of our discussion, operator $R_K^{(\mathrm{A})}$ is defined as a unit operator for $K = 0$. In the standard EOMCC calculations, the cluster operator $T^{(\mathrm{A})}$, Eq. (7), is obtained by solving the single-reference CC equations, Eq. (9). Once $T^{(\mathrm{A})}$ is determined, the excitation operators $R_K^{(\mathrm{A})}$ and the corresponding EOMCC energies $E_K^{(\mathrm{A})}$ are obtained by diagonalizing the similarity-transformed Hamiltonian $\bar{H}^{(\mathrm{A})}$, Eq. (10), in a space spanned by the reference configuration $|\Phi\rangle$ and the excited configurations $|\Phi^{a_1\ldots a_n}_{i_1\ldots i_n}\rangle$, $n = 1, \ldots, m_{\mathrm{A}}$, included in $T^{(\mathrm{A})}$ and $R_K^{(\mathrm{A})}$ (in practice, it is sufficient to diagonalize $\bar{H}^{(\mathrm{A})}$ in a space spanned by the excited configurations $|\Phi^{a_1\ldots a_n}_{i_1\ldots i_n}\rangle$, $n = 1, \ldots, m_{\mathrm{A}}$, since matrix elements of the $\langle\Phi^{a_1\ldots a_n}_{i_1\ldots i_n}|\bar{H}^{(\mathrm{A})}|\Phi\rangle$ type, which form the first column of the matrix representing $\bar{H}^{(\mathrm{A})}$, vanish for $n = 1, \ldots, m_{\mathrm{A}}$, if $T^{(\mathrm{A})}$ satifies the single-reference CC equations, Eq. (9); in this case, instead of energies $E_K^{(\mathrm{A})}$, we directly obtain the vertical excitation energies $\omega_K^{(\mathrm{A})} = E_K^{(\mathrm{A})} - E_0^{(\mathrm{A})}$).

Kowalski and Piecuch demonstrated that once the cluster and excitation operators, $T^{(\mathrm{A})}$ and $R_K^{(\mathrm{A})}$, respectively, and the ground- and excited-state energies $E_K^{(\mathrm{A})}$ are determined by solving the relevant CC/EOMCC equations, we can recover the exact, full CI, energies E_K by adding the following corrections $\delta_K^{(\mathrm{A})}$ to energies $E_K^{(\mathrm{A})}$ [12, 61, 72, 73, 74]:

$$\begin{aligned}\delta_K^{(\mathrm{A})} &\equiv E_K - E_K^{(\mathrm{A})} \\ &= \sum_{n=m_{\mathrm{A}}+1}^{N} \sum_{k=m_{\mathrm{A}}+1}^{n} \langle \Psi_K | C_{n-k}(m_{\mathrm{A}}) M_{K,k}(m_{\mathrm{A}}) | \Phi \rangle / \\ &\quad \langle \Psi_K | R_K^{(\mathrm{A})} \mathrm{e}^{T^{(\mathrm{A})}} | \Phi \rangle \ , \end{aligned} \tag{39}$$

where $C_{n-k}(m_{\mathrm{A}})$ is defined by Eq. (22) and

$$M_{K,k}(m_{\mathrm{A}}) |\Phi\rangle = \sum_{\substack{i_1 < \cdots < i_k \\ a_1 < \cdots < a_k}} \mathscr{M}_{K,a_1 \ldots a_k}^{i_1 \ldots i_k}(m_{\mathrm{A}}) |\Phi_{i_1 \ldots i_k}^{a_1 \ldots a_k}\rangle \ , \tag{40}$$

with $\mathscr{M}_{K,a_1 \ldots a_k}^{i_1 \ldots i_k}(m_{\mathrm{A}})$ representing the generalized moments of the EOMCC equations corresponding to the approximate method A. In analogy to the generalized moments of the ground-state CC equations, the generalized moments of the EOMCC equations are defined as projections of the left-hand side of the EOMCC eigenvalue problem involving $\bar{H}^{(\mathrm{A})}$ [the $(\bar{H}^{(\mathrm{A})} R_K^{(\mathrm{A})}) |\Phi\rangle$ term] on the excited configurations $|\Phi_{i_1 \ldots i_k}^{a_1 \ldots a_k}\rangle$ with $k > m_{\mathrm{A}}$,

$$\mathscr{M}_{K,a_1 \ldots a_k}^{i_1 \ldots i_k}(m_{\mathrm{A}}) = \langle \Phi_{i_1 \ldots i_k}^{a_1 \ldots a_k} | (\bar{H}^{(\mathrm{A})} R_K^{(\mathrm{A})}) | \Phi \rangle \ . \tag{41}$$

As shown in Ref. [72], the generalized moments of the EOMCC equations can be calculated using the following formula:

$$\begin{aligned}\mathscr{M}_{K,a_1 \ldots a_k}^{i_1 \ldots i_k}(m_{\mathrm{A}}) &= \langle \Phi_{i_1 \ldots i_k}^{a_1 \ldots a_k} | (\bar{H}_{\mathrm{open}}^{(\mathrm{A})} R_{K,\mathrm{open}}^{(\mathrm{A})})_{\mathrm{C}} | \Phi \rangle \\ &\quad + \sum_{p=m_{\mathrm{A}}+1}^{k-1} \langle \Phi_{i_1 \ldots i_k}^{a_1 \ldots a_k} | (\bar{H}_p^{(\mathrm{A})} R_{K,k-p}^{(\mathrm{A})})_{\mathrm{DC}} | \Phi \rangle \\ &\quad + r_{K,0}^{(\mathrm{A})} \mathscr{M}_{a_1 \ldots a_k}^{i_1 \ldots i_k}(m_{\mathrm{A}}) \ , \end{aligned} \tag{42}$$

where $r_{K,0}^{(\mathrm{A})}$ is the coefficient at the reference configuration $|\Phi\rangle$ in the many-body expansion of $R_K^{(\mathrm{A})}|\Phi\rangle$, subscripts open, C, and DC refer to open (i.e., having external lines), connected, and disconnected parts of a given operator expression, O_j represents the j-body component of operator O, and $\mathscr{M}_{a_1 \ldots a_k}^{i_1 \ldots i_k}(m_{\mathrm{A}})$ are the generalized moments of the single-reference CC equations defined by Eq. (19). Equation (42) is particularly useful when we want to implement the excited-state MMCC methods, since it allows us to express the relevant moments $\mathscr{M}_{K,a_1 \ldots a_k}^{i_1 \ldots i_k}(m_{\mathrm{A}})$ of the EOMCC equations in terms of the many-body components $R_{K,n}^{(\mathrm{A})}$ of the EOMCC excitation operator $R_K^{(\mathrm{A})}$, Eq. (36), and matrix elements of the similarity-transformed Hamiltonian $\bar{H}^{(\mathrm{A})}$. It should be noticed that Eq. (39) reduces to the ground-state MMCC formula, Eq. (21), when $K = 0$. Indeed, when $K = 0$, $R_K^{(\mathrm{A})}$ becomes a unit operator, so $r_{K,0}^{(\mathrm{A})} = 1$ and $R_{K,\mathrm{open}}^{(\mathrm{A})} = 0$ ($R_{K,n}^{(\mathrm{A})} = 0$ for $n > 0$). According to Eq. (42), we immediately obtain

$$\mathscr{M}_{K=0,a_1 \ldots a_k}^{i_1 \ldots i_k}(m_{\mathrm{A}}) = \mathscr{M}_{a_1 \ldots a_k}^{i_1 \ldots i_k}(m_{\mathrm{A}}) \ , \tag{43}$$

where $\mathscr{M}_{a_1 \ldots a_k}^{i_1 \ldots i_k}(m_{\mathrm{A}})$ are the generalized moments of the ground-state CC equations.

Equation (39) defines the excited-state MMCC formalism. This equation allows us to improve the CC/EOMCC results, in a state-selective manner, by adding the noniterative corrections $\delta_K^{(\mathrm{A})}$, obtained using information that can be extracted from the standard CC/EOMCC calculations (operators $T^{(\mathrm{A})}$ and $R_K^{(\mathrm{A})}$, matrix elements of $\bar{H}^{(\mathrm{A})}$, and generalized moments of the CC/EOMCC equations), to CC/EOMCC energies $E_K^{(\mathrm{A})}$. For example, if we want to recover the full CI energies E_K by adding corrections $\delta_K^{(\mathrm{A})}$ to the EOMCCSD energies $E_K^{(\mathrm{EOMCCSD})}$ (the $m_{\mathrm{A}} = 2$ case), we must determine the generalized moments of the EOMCCSD equations, i.e., the projections of the EOMCCSD equations on triply excited, quadruply excited, etc., configurations,

$$\begin{aligned}\mathscr{M}_{K,a_1 \ldots a_k}^{i_1 \ldots i_k}(2) &= \langle \Phi_{i_1 \ldots i_k}^{a_1 \ldots a_k} | (\bar{H}^{(\mathrm{CCSD})} R_K^{(\mathrm{CCSD})}) | \Phi \rangle \ , \\ &\quad k = 3, 4, \ldots , \end{aligned} \tag{44}$$

where $\bar{H}^{(\mathrm{CCSD})}$ is the similarity-transformed Hamiltonian of the CCSD method, defined by Eq. (13), and

$$R_K^{(\mathrm{CCSD})} = R_{K,0} + R_{K,1} + R_{K,2} = R_{K,0} + R_{K,\mathrm{open}}^{(\mathrm{CCSD})} \tag{45}$$

is the excitation operator of the EOMCCSD approach. These moments can easily be determined using Eq. (42). For example, the explicit formula for the leading moment $\mathscr{M}_{K,a_1 a_2 a_3}^{i_1 i_2 i_3}(2)$, entering the basic MMCC(2,3) [72, 73] and CR-EOMCCSD(T) [12, 74] approximations, in terms of the many-body components of $\bar{H}^{(\mathrm{CCSD})}$ and $R_K^{(\mathrm{CCSD})}$, is

$$\begin{aligned}\mathscr{M}_{K,a_1 a_2 a_3}^{i_1 i_2 i_3}(2) &= \langle \Phi_{i_1 i_2 i_3}^{a_1 a_2 a_3} | (\bar{H}_2^{(\mathrm{CCSD})} R_{K,2})_{\mathrm{C}} | \Phi \rangle \\ &\quad + \langle \Phi_{i_1 i_2 i_3}^{a_1 a_2 a_3} | [\bar{H}_3^{(\mathrm{CCSD})} (R_{K,1} + R_{K,2})]_{\mathrm{C}} | \Phi \rangle \\ &\quad + \langle \Phi_{i_1 i_2 i_3}^{a_1 a_2 a_3} | (\bar{H}_4^{(\mathrm{CCSD})} R_{K,1})_{\mathrm{C}} | \Phi \rangle \\ &\quad + r_{K,0}^{(\mathrm{CCSD})} \mathscr{M}_{a_1 a_2 a_3}^{i_1 i_2 i_3}(2) \ , \end{aligned} \tag{46}$$

where the ground-state $\mathscr{M}_{a_1 a_2 a_3}^{i_1 i_2 i_3}(2)$ moments are given by Eq. (24). Similar expressions can be given for the higher-order EOMCC moments $\mathscr{M}_{K,a_1 \ldots a_k}^{i_1 \ldots i_k}(2)$ with $k \geq 4$ [73]. The final formula for the corrections $\delta_K^{(\mathrm{EOMCCSD})}$, which must be added to the EOMCCSD energies $E_K^{(\mathrm{EOMCCSD})}$ to recover the exact energies E_K, is

$$\begin{aligned}\delta_K^{(\mathrm{EOMCCSD})} &= E_K - E_K^{(\mathrm{EOMCCSD})} \\ &= \sum_{n=3}^{N} \sum_{k=3}^{n} \langle \Psi_K | C_{n-k}(2) M_{K,k}(2) | \Phi \rangle / \\ &\quad \langle \Psi_K | R_K^{(\mathrm{CCSD})} \mathrm{e}^{T_1 + T_2} | \Phi \rangle \ , \end{aligned} \tag{47}$$

where

$$M_{K,k}(2) |\Phi\rangle = \sum_{\substack{i_1 < \cdots < i_k \\ a_1 < \cdots < a_k}} \mathscr{M}_{K,a_1 \ldots a_k}^{i_1 \ldots i_k}(2) |\Phi_{i_1 \ldots i_k}^{a_1 \ldots a_k}\rangle \ . \tag{48}$$

As in the ground-state MMCC theory, two issues must be resolved before applying Eq. (39) or Eq. (47) in practice. First, the exact MMCC corrections $\delta_K^{(\mathrm{A})}$, Eq. (39), or $\delta_K^{(\mathrm{EOMCCSD})}$, Eq. (47), are represented by complete many-body expansions, including the N-body contributions, where N is the number of electrons in a system, corresponding to all many-body components of the wave functions $|\Psi_K\rangle$ that enter Eqs. (39), (47) (see the summations over n in Eqs. (39), (47)). In order to develop practical MMCC methods, we must truncate the many-body expansions for $\delta_K^{(\mathrm{A})}$ or $\delta_K^{(\mathrm{EOMCCSD})}$, given by Eq. (39) or (47), at some, preferably low, excitation level m_{B}. This leads to the excited-state MMCC($m_{\mathrm{A}}, m_{\mathrm{B}}$) schemes [12, 72, 73, 74]. Examples of these schemes are the CI-corrected MMCC(2,3) and MMCC(2,4) methods discussed in Sect. 4.2 and the CR-EOMCCSD(T) approach described in Sect. 4.1, in which the suitably designed corrections $\delta_K^{(\mathrm{EOMCCSD})}$, based on Eq. (47), are added to the EOMCCSD energies. More importantly, the wave functions $|\Psi_K\rangle$ that enter the exact Eqs. (39) and (47) are the full CI states. Thus, we must approximate wave functions $|\Psi_K\rangle$ in some way. A few different methods of approximating $|\Psi_K\rangle$ in Eq. (47), leading to the aforementioned MMCC(2,3), MMCC(2,4), and CR-EOM-CCSD(T) schemes, are discussed in Sects. 4.1 and 4.2.

3 Approximate MMCC approaches to ground electronic states and their performance

Essentially all MMCC approximations proposed to date are based on an idea of limiting ourselves to the wave functions $|\Psi_0\rangle$ in Eq. (21) or Eq. (28) that do not contain higher–than–m_{B}-tuply excited components relative to $|\Phi\rangle$, where $m_{\mathrm{B}} > m_{\mathrm{A}}$ is not much higher than the excitation level m_{A} defining the CC method A, whose results we are trying to improve [12, 55, 56, 57, 61, 64]. This is, more or less, equivalent to restricting the summation over n in Eq. (21) to $\sum_{n=m_{\mathrm{A}}+1}^{m_{\mathrm{B}}}$. In the resulting MMCC($m_{\mathrm{A}}, m_{\mathrm{B}}$) approaches, we calculate the energy as follows [12, 55, 56, 57, 61, 64]:

$$E_0^{(\mathrm{MMCC})}(m_{\mathrm{A}}, m_{\mathrm{B}}) = E_0^{(\mathrm{A})} + \delta_0(m_{\mathrm{A}}, m_{\mathrm{B}}) \ , \tag{49}$$

where $E_0^{(\mathrm{A})}$ is the energy obtained with the CC method A and

$$\begin{aligned}\delta_0(m_{\mathrm{A}}, m_{\mathrm{B}}) = &\sum_{n=m_{\mathrm{A}}+1}^{m_{\mathrm{B}}} \sum_{k=m_{\mathrm{A}}+1}^{n} \langle\Psi_0|C_{n-k}(m_{\mathrm{A}}) \\ &\times M_k(m_{\mathrm{A}})|\Phi\rangle / \langle\Psi_0|\mathrm{e}^{T^{(\mathrm{A})}}|\Phi\rangle\end{aligned} \tag{50}$$

is the relevant MMCC correction. We can also contemplate the generalized MMCC($m_{\mathrm{A}}, m_{\mathrm{B}}$) [GMMCC($m_{\mathrm{A}}, m_{\mathrm{B}}$)] approaches, in which we no longer assume that the truncated cluster operator $T^{(\mathrm{A})}$, Eq. (7), is obtained by solving the standard CC equations, Eq. (9), so we can no longer assume that the generalized moments $\mathscr{M}_{a_1 \ldots a_k}^{i_1 \ldots i_k}(m_{\mathrm{A}})$ with $k = 1, \ldots, m_{\mathrm{A}}$ vanish. In this case, instead of using Eq. (21) and Eqs. (49) and (50) that result from it, we must use the more general Eq. (30). By limiting ourselves to the wave functions $|\Psi_0\rangle$ that do not contain higher–than–m_{B}-tuply excited components relative to $|\Phi\rangle$ and by restricting the summation over n in Eq. (30) accordingly, we obtain the following energy expression for the GMMCC($m_{\mathrm{A}}, m_{\mathrm{B}}$) methods:

$$\begin{aligned}E_0^{(\mathrm{GMMCC})}(m_{\mathrm{A}}, m_{\mathrm{B}}) = M_0(m_{\mathrm{A}}) + &\sum_{n=1}^{m_{\mathrm{B}}} \sum_{k=1}^{n} \langle\Psi_0|C_{n-k}(m_{\mathrm{A}}) \\ &\times M_k(m_{\mathrm{A}})|\Phi\rangle / \langle\Psi_0|\mathrm{e}^{T^{(\mathrm{A})}}|\Phi\rangle \ ,\end{aligned} \tag{51}$$

where $M_0(m_{\mathrm{A}})$ is defined by Eq. (31). Equation (51) is particularly useful, when the truncated cluster operator $T^{(\mathrm{A})}$ is obtained in a nonstandard fashion, for example, by performing the ECC calculations (see Sect. 3.4) that may provide better cluster amplitudes in severe cases of bond breaking than the standard CC calculations [64, 65]. The exact MMCC formalism, equivalent to calculating the full CI energies, is obtained when $|\Psi_0\rangle$ in Eqs. (50) and (51) is the full CI ground-state wave function and $m_{\mathrm{B}} = N$.

In this article, we focus on the MMCC($m_{\mathrm{A}}, m_{\mathrm{B}}$) and GMMCC($m_{\mathrm{A}}$, m_{B}) schemes with $m_{\mathrm{A}} = 2$, which can be used to correct the results of the CCSD or CCSD-like (e.g., ECCSD [64, 65]) calculations [for other MMCC($m_{\mathrm{A}}, m_{\mathrm{B}}$) approximations, including the MMCC(3, m_{B}) approaches which can be used to improve the results of the full CCSDT calculations, see Refs. [55, 56, 59, 61]]. The basic MMCC(2, m_{B}) methods are the MMCC(2,3) and MMCC(2,4) approximations, in which energies are calculated as follows [12, 55, 56, 57, 61, 64]:

$$\begin{aligned}E_0^{(\mathrm{MMCC})}(2,3) = E_0^{(\mathrm{CCSD})} &+ \langle\Psi_0|M_3(2)|\Phi\rangle / \\ &\langle\Psi_0|\mathrm{e}^{T_1+T_2}|\Phi\rangle \ ,\end{aligned} \tag{52}$$

$$\begin{aligned}E_0^{(\mathrm{MMCC})}(2,4) = E_0^{(\mathrm{CCSD})} &+ \langle\Psi_0|\{M_3(2) + [M_4(2) \\ &+ T_1 M_3(2)]\}|\Phi\rangle / \langle\Psi_0|\mathrm{e}^{T_1+T_2}|\Phi\rangle \ ,\end{aligned} \tag{53}$$

where $E_0^{(\mathrm{CCSD})}$ is the CCSD ground-state energy. The MMCC(2,3) approach requires that we determine moments $\mathscr{M}_{a_1 a_2 a_3}^{i_1 i_2 i_3}(2)$, Eq. (24), whereas the MMCC(2,4) method requires that we determine moments $\mathscr{M}_{a_1 a_2 a_3}^{i_1 i_2 i_3}(2)$ and $\mathscr{M}_{a_1 a_2 a_3 a_4}^{i_1 i_2 i_3 i_4}(2)$, Eqs. (24) and (25), respectively. If the T_1 and T_2 clusters are obtained in some nonstandard way rather than by performing the CCSD calculations, we must switch to the GMMCC(2,3) and GMMCC(2,4) approaches. According to Eq. (51), the GMMCC(2,4) energy is calculated as follows:

$$\begin{aligned}E_0^{(\mathrm{GMMCC})}(2,4) = M_0(2) &+ \langle\Psi_0|\{M_1(2) + [M_2(2) \\ &+ T_1 M_1(2)] + [M_3(2) + T_1 M_2(2) \\ &+ (T_2 + \tfrac{1}{2}T_1^2) M_1(2)] \\ &+ [M_4(2) + T_1 M_3(2) \\ &+ (T_2 + \tfrac{1}{2}T_1^2) M_2(2) \\ &+ (T_1 T_2 + \tfrac{1}{6}T_1^3) M_1(2)]\}|\Phi\rangle / \\ &\langle\Psi_0|\mathrm{e}^{T_1+T_2}|\Phi\rangle \ .\end{aligned} \tag{54}$$

If necessary, a similar expression can be written for the GMMCC(2,3) method (cf. Eq. 51). In the case of the GMMCC(2,4) approach, we must determine moments $\mathscr{M}_{a_1 a_2 a_3}^{i_1 i_2 i_3}(2)$ and $\mathscr{M}_{a_1 a_2 a_3 a_4}^{i_1 i_2 i_3 i_4}(2)$, Eqs. (24) and (25), respectively, along with moments $\mathscr{M}_{a_1}^{i_1}(2)$ and $\mathscr{M}_{a_1 a_2}^{i_1 i_2}(2)$, Eqs. (33) and (34), respectively. We can also consider the higher-order MMCC(2,5) and MMCC(2,6) methods and their GMMCC(2,5) and GMMCC(2,6) analogs, which are particularly useful in studies of multiple bond breaking [12, 64, 65, 66] (see Sects. 3.2, 3.3) and which require the consideration of the $\mathscr{M}^{i_1 i_2 i_3 i_4 i_5}_{a_1 a_2 a_3 a_4 a_5}(2)$ and $\mathscr{M}^{i_1 i_2 i_3 i_4 i_5 i_6}_{a_1 a_2 a_3 a_4 a_5 a_6}(2)$ moments, Eqs. (26) and (27), respectively, along with the lower-order moments $\mathscr{M}^{i_1 \ldots i_k}_{a_1 \ldots a_k}(2)$ with $k < 5$. Clearly, when moments $\mathscr{M}^{i_1}_{a_1}(2)$ and $\mathscr{M}^{i_1 i_2}_{a_1 a_2}(2)$ vanish, the GMMCC(2,4) energy expression, Eq. (54), reduces to the MMCC(2,4) formula, Eq. (53). This can only happen when the T_1 and T_2 clusters are obtained by solving the standard CCSD equations, Eqs. (11) and (12). In general, the GMMCC($m_{\mathrm{A}}, m_{\mathrm{B}}$) and MMCC($m_{\mathrm{A}}, m_{\mathrm{B}}$) approximations are identical, when the cluster operator $T^{(\mathrm{A})}$, Eq. (7), is obtained in the standard CC calculations.

In order to apply the MMCC(2,3), MMCC(2,4), GMMCC(2,4), and other (G)MMCC($m_{\mathrm{A}}, m_{\mathrm{B}}$) approaches in practice, we must suggest an approximate form of the wave function $|\Psi_0\rangle$ that enters Eqs. (50), (51), (52), (53), and (54). Our interest is in relatively inexpensive methods, so $|\Psi_0\rangle$ should be generated with one of the inexpensive ab initio approaches. So far, we have tested the following choices of $|\Psi_0\rangle$: (1) the low-order MBPT expressions, which result in the renormalized and completely renormalized CCSD(T) and CCSD(TQ) methods [12, 55, 56, 57, 58, 59, 60, 61, 63, 64, 65] and their most recent ECCSD-based GMMCC(2,4) analog, (2) the exponential, CC-like, expressions and their truncated forms, which lead to the linear MMCC (LMMCC) and QMMCC approaches [12, 64, 65, 66], and (3) the truncated CI-like expressions which lead to the CI-corrected MMCC methods [12, 55, 62, 72, 73]. The renormalized and completely renormalized CCSD(T) methods and the CI-corrected MMCC approaches have already been adopted by other groups [156, 157, 158, 161]. All of these methods and their performance in calculations involving bond breaking are discussed in Sects. 3.1, 3.2, 3.3 and 3.4.

3.1 The renormalized and completely renormalized CCSD(T) and CCSD(TQ) methods

In general, the R-CC and CR-CC methods are obtained when the wave function $|\Psi_0\rangle$ in the MMCC($m_{\mathrm{A}}, m_{\mathrm{B}}$) energy formulas, Eqs. (49) and (50), is approximated by the low-order MBPT expressions. For example, the CR-CCSD[T] and CR-CCSD(T) methods are examples of the MMCC(2,3) schemes, based on Eq. (52), in which the wave function $|\Psi_0\rangle$ is replaced by the following second-order-type, MBPT(2)[SDT]-like, expressions [12, 55, 56, 57, 58, 60, 61, 63, 64],

$$|\Psi_0^{\mathrm{CCSD[T]}}\rangle = (1 + T_1 + T_2 + T_3^{[2]})|\Phi\rangle \tag{55}$$

and

$$|\Psi_0^{\mathrm{CCSD(T)}}\rangle = |\Psi_0^{\mathrm{CCSD[T]}}\rangle + Z_3|\Phi\rangle \ , \tag{56}$$

where T_1 and T_2 are the singly and doubly excited clusters obtained in the CCSD calculations, the

$$T_3^{[2]}|\Phi\rangle = R_0^{(3)}(V_{\mathrm{N}}T_2)_{\mathrm{C}}|\Phi\rangle \tag{57}$$

term is an approximation of the connected triples (T_3) contribution, which is correct through second order, and

$$Z_3|\Phi\rangle = R_0^{(3)}V_{\mathrm{N}}T_1|\Phi\rangle \tag{58}$$

is the disconnected triples correction, which is responsible for the difference between the [T] and (T) triples corrections. We use the usual notation, in which $R_0^{(3)}$ designates the three-body component of the MBPT reduced resolvent and V_{N} is the two-body part of H_{N}. The CR-CCSD(TQ) methods [12, 55, 56, 57, 58, 59, 60, 61, 64] are obtained in a similar manner, by inserting the MBPT(2)[SDTQ]-like expressions for $|\Psi_0\rangle$ into the MMCC(2,4) formula, Eq. (53). For example, variant b of the CR-CCSD(TQ) approach (the CR-CCSD(TQ),b method [12, 55, 56, 57, 58, 59, 60, 61, 64]) is obtained by replacing $|\Psi_0\rangle$ in Eq. (53) by

$$|\Psi_0^{\mathrm{CCSD(TQ),b}}\rangle = |\Psi_0^{\mathrm{CCSD(T)}}\rangle + \frac{1}{2}T_2^2|\Phi\rangle \ , \tag{59}$$

where $|\Psi_0^{\mathrm{CCSD(T)}}\rangle$ is given by Eq. (56). Other variants of the CR-CCSD(TQ) approach (which we do not discuss here) are possible [12, 55, 56, 57, 58, 59, 60, 61, 64].

Based on Eqs. (52), (53), (55), (56), and (59), we can write the following compact formulas for the CR-CCSD[T], CR-CCSD(T), and CR-CCSD(TQ),b energies:

$$E_0^{(\mathrm{CR-CCSD[T]})} = E_0^{(\mathrm{CCSD})} + N^{\mathrm{CR[T]}}/D^{[\mathrm{T}]} \ , \tag{60}$$

$$E_0^{(\mathrm{CR-CCSD(T)})} = E_0^{(\mathrm{CCSD})} + N^{\mathrm{CR(T)}}/D^{(\mathrm{T})}, \tag{61}$$

and

$$E_0^{(\mathrm{CR-CCSD(TQ),b})} = E_0^{(\mathrm{CCSD})} + N^{\mathrm{CR(TQ),b}}/D^{(\mathrm{TQ}),\mathrm{b}}, \tag{62}$$

where the $N^{\mathrm{CR[T]}}$, $N^{\mathrm{CR(T)}}$, and $N^{\mathrm{CR(TQ),b}}$ numerators are defined as

$$N^{\mathrm{CR[T]}} = \langle\Phi|(T_3^{[2]})^\dagger M_3(2)|\Phi\rangle \ , \tag{63}$$

$$N^{\mathrm{CR(T)}} = N^{\mathrm{CR[T]}} + \langle\Phi|(Z_3)^\dagger M_3(2)|\Phi\rangle \ , \tag{64}$$

and

$$\begin{aligned} N^{\mathrm{CR(TQ),b}} = N^{\mathrm{CR(T)}} &+ \frac{1}{2}\langle\Phi|(T_2^\dagger)^2 \\ &\times [T_1 M_3(2) + M_4(2)]|\Phi\rangle \ , \end{aligned} \tag{65}$$

and the $D^{[\mathrm{T}]}$, $D^{(\mathrm{T})}$, and $D^{(\mathrm{TQ}),\mathrm{b}}$ denominators, representing the overlaps between the $|\Psi_0^{\mathrm{CCSD[T]}}\rangle$, $|\Psi_0^{\mathrm{CCSD(T)}}\rangle$, and $|\Psi_0^{\mathrm{CCSD(TQ),b}}\rangle$ wave functions, Eqs. (55), (56), and (59), respectively, with the CCSD ground state, are calculated as

$$\begin{aligned} D^{[\mathrm{T}]} &\equiv \langle\Psi_0^{\mathrm{CCSD[T]}}|\mathrm{e}^{T_1+T_2}|\Phi\rangle \\ &= 1 + \langle\Phi|T_1^\dagger T_1|\Phi\rangle + \langle\Phi|T_2^\dagger\left(T_2 + \frac{1}{2}T_1^2\right)|\Phi\rangle \\ &\quad + \langle\Phi|(T_3^{[2]})^\dagger(T_1T_2 + \frac{1}{6}T_1^3)|\Phi\rangle, \end{aligned} \tag{66}$$

$$\begin{aligned} D^{(\mathrm{T})} &\equiv \langle\Psi_0^{\mathrm{CCSD(T)}}|\mathrm{e}^{T_1+T_2}|\Phi\rangle \\ &= D^{[\mathrm{T}]} + \langle\Phi|Z_3^\dagger(T_1T_2 + \frac{1}{6}T_1^3)|\Phi\rangle, \end{aligned} \tag{67}$$

and

$$D^{(\mathrm{TQ}),\mathrm{b}} \equiv \langle \Psi_0^{\mathrm{CCSD(TQ)},\mathrm{b}} | \mathrm{e}^{T_1+T_2} | \Phi \rangle = D^{(\mathrm{T})} + \frac{1}{2} \langle \Phi | (T_2^\dagger)^2 (\frac{1}{2} T_2^2 + \frac{1}{2} T_1^2 T_2 + \frac{1}{24} T_1^4) | \Phi \rangle. \tag{68}$$

The R-CCSD[T], R-CCSD(T), and R-CCSD(TQ) approaches are obtained by replacing moments $\mathscr{M}_{a_1a_2a_3}^{i_1i_2i_3}(2)$ and $\mathscr{M}_{a_1a_2a_3a_4}^{i_1i_2i_3i_4}(2)$, entering Eqs. (60), (61), and (62) through the $M_3(2)|\Phi\rangle$ and $M_4(2)|\Phi\rangle$ quantities (cf. Eq. (29)), by their lowest-order estimates. For example, the R-CCSD[T] and R-CCSD(T) methods are obtained from the CR-CCSD[T] and CR-CCSD(T) formulas, Eqs. (60) and (61), by replacing moments $\mathscr{M}_{a_1a_2a_3}^{i_1i_2i_3}(2)$ defining $M_3(2)|\Phi\rangle$ in Eqs. (63) and (64), respectively, by $\langle \Phi_{i_1i_2i_3}^{a_1a_2a_3} | (V_N T_2)_C | \Phi \rangle$. Thus, the R-CCSD[T] and R-CCSD(T) energies are calculated as [12, 55, 56, 57, 58, 60, 61, 64]

$$E_0^{(\mathrm{R-CCSD[T]})} = E_0^{(\mathrm{CCSD})} + N^{[\mathrm{T}]}/D^{[\mathrm{T}]} \tag{69}$$

and

$$E_0^{(\mathrm{R-CCSD(T)})} = E_0^{(\mathrm{CCSD})} + N^{(\mathrm{T})}/D^{(\mathrm{T})}, \tag{70}$$

where

$$N^{[\mathrm{T}]} = \langle \Phi | (T_3^{[2]})^\dagger (V_N T_2)_C | \Phi \rangle, \tag{71}$$

$$N^{(\mathrm{T})} = N^{[\mathrm{T}]} + \langle \Phi | (Z_3)^\dagger (V_N T_2)_C | \Phi \rangle, \tag{72}$$

and $D^{[\mathrm{T}]}$ and $D^{(\mathrm{T})}$ are defined by Eqs. (66) and (67), respectively. The R-CCSD(TQ) energy expressions are obtained in an analogous manner by approximating moments $\mathscr{M}_{a_1a_2a_3}^{i_1i_2i_3}(2)$ and $\mathscr{M}_{a_1a_2a_3a_4}^{i_1i_2i_3i_4}(2)$, defining the $M_3(2)|\Phi\rangle$ and $M_4(2)|\Phi\rangle$ quantities in the CR-CCSD(TQ) formulas, such as Eq. (62), by their lowest-order estimates. We could, for example, use $\langle \Phi_{i_1i_2i_3}^{a_1a_2a_3} | (V_N T_2)_C | \Phi \rangle$ or $\langle \Phi_{i_1i_2i_3}^{a_1a_2a_3} | [V_N (T_2 + \frac{1}{2} T_2^2)]_C | \Phi \rangle$ instead of $\mathscr{M}_{a_1a_2a_3}^{i_1i_2i_3}(2)$ and $\langle \Phi_{i_1i_2i_3i_4}^{a_1a_2a_3a_4} | \{ V_N [\frac{1}{2} T_2^2 + T_3^{[2]}] \}_C | \Phi \rangle$ or $\langle \Phi_{i_1i_2i_3i_4}^{a_1a_2a_3a_4} | (\frac{1}{2} V_N T_2^2)_C | \Phi \rangle$ instead of $\mathscr{M}_{a_1a_2a_3a_4}^{i_1i_2i_3i_4}(2)$. We refer the reader to the original papers [55, 56, 57] for further information about the R-CCSD(TQ) methods.

It should be noticed that the $N^{[\mathrm{T}]}$ and $N^{(\mathrm{T})}$ numerators defining the R-CCSD[T] and R-CCSD(T) energies, Eqs. (69) and (70), respectively, which are obtained by simplifying the $N^{\mathrm{CR[T]}}$ and $N^{\mathrm{CR(T)}}$ numerators of the CR-CCSD[T] and CR-CCSD(T) methods, Eqs. (63) and (64), respectively, are identical to the noniterative triples corrections

$$E_{\mathrm{T}}^{[4]} = \langle \Phi | (T_3^{[2]})^\dagger (V_N T_2)_C | \Phi \rangle \tag{73}$$

and

$$E_{\mathrm{ST}}^{[5]} = \langle \Phi | (Z_3)^\dagger (V_N T_2)_C | \Phi \rangle, \tag{74}$$

defining the standard CCSD[T] and CCSD(T) energies [14, 15],

$$E_0^{(\mathrm{CCSD[T]})} = E_0^{(\mathrm{CCSD})} + E_{\mathrm{T}}^{[4]} \tag{75}$$

and

$$E_0^{(\mathrm{CCSD(T)})} = E_0^{(\mathrm{CCSD[T]})} + E_{\mathrm{ST}}^{[5]}, \tag{76}$$

respectively. Indeed, we can write

$$N^{[\mathrm{T}]} = E_{\mathrm{T}}^{[4]} \tag{77}$$

and

$$N^{(\mathrm{T})} = E_{\mathrm{T}}^{[4]} + E_{\mathrm{ST}}^{[5]}. \tag{78}$$

Thus, the R-CCSD[T] and R-CCSD(T) approximations, which are obtained by simplifying the CR-CCSD[T] and CR-CCSD(T) methods, reduce to the standard CCSD[T] and CCSD(T) approaches, when the $D^{[\mathrm{T}]}$ and $D^{(\mathrm{T})}$ denominators in Eqs. (69) and (70) are replaced by 1 [55, 56]. A very similar relationship exists between the R-CCSD(TQ) and CR-CCSD(TQ) methods on the one hand and the standard CCSD(TQ$_\mathrm{f}$) approximation of Kucharski and Bartlett [44] on the other hand. The latter approximation is immediately obtained by replacing the $D^{(\mathrm{TQ}),\mathrm{b}}$ denominator in Eq. (62) by 1 and by replacing the $N^{\mathrm{CR(TQ)},\mathrm{b}}$ numerator, Eq. (65), in the resulting equation by one of its lowest-order estimates that has the following form: $N^{(\mathrm{T})} + \frac{1}{2} \langle \Phi | T_2^\dagger (T_2^{(1)})^\dagger \{ V_N [\frac{1}{2} T_2^2 \ + T_3^{[2]}] \}_C | \Phi \rangle$, where $T_2^{(1)}$ is the first-order MBPT estimate of T_2. As we can see, one can view the standard CCSD[T], CCSD(T), and CCSD(TQ$_\mathrm{f}$) approaches as the simplified (C)R-CCSD[T], (C)R-CCSD(T), and (C)R-CCSD(TQ) methods. This analysis also shows how easy the derivations of various noniterative CC methods become, if we decide to employ the basic MMCC energy formula, Eq. (21).

As explained in the original papers on the R-CC and CR-CC methods by Piecuch and Kowalski [55, 56], the approximation of the $D^{[\mathrm{T}]}$, $D^{(\mathrm{T})}$, and $D^{(\mathrm{TQ}),\mathrm{b}}$ denominators by 1, as described earlier, has some merit to it from the point of view of MBPT, provided that the T_1 and T_2 cluster amplitudes are small, which is usually the case for the nondegenerate electronic states (e.g., molecules near their equilibrium geometries), for which the MBPT series rapidly converges. One can easily verify that the $D^{[\mathrm{T}]}$, $D^{(\mathrm{T})}$, and $D^{(\mathrm{TQ}),\mathrm{b}}$ denominators equal 1 plus terms that are at least of the second order in the perturbation V_N (see Eqs. 66, 67, 68; if we ignore 1, the lowest-order $\langle \Phi | T_2^\dagger T_2 | \Phi \rangle$ term in Eqs. 66, 67, and 68 contains the second- and higher-order contributions in V_N). The situation changes, when the configurational quasidegeneracy or nondynamic correlation effects become sizable and the MBPT series no longer converges, as is usually the case for stretched nuclear geometries. In this case, the T_1 and T_2 cluster components become large and the $D^{[\mathrm{T}]}$, $D^{(\mathrm{T})}$, and $D^{(\mathrm{TQ}),\mathrm{b}}$ denominators become substantially larger than 1 [56, 57]. This increase of the values of $D^{[\mathrm{T}]}$, $D^{(\mathrm{T})}$, and $D^{(\mathrm{TQ}),\mathrm{b}}$ at larger internuclear distances is one of the main reasons for the observed excellent performance of the CR-CCSD[T], CR-CCSD(T), and CR-CCSD(TQ) approaches at larger internuclear distances. One might state that the $D^{[\mathrm{T}]}$ and $D^{(\mathrm{T})}$ denominators damp or "renormalize" the excessively large values of the noniterative triples and quadruples corrections resulting from the standard CCSD[T], CCSD(T), and CCSD(TQ$_\mathrm{f}$) calculations at stretched nuclear geometries, which cause the poor description of bond breaking by the CCSD[T], CCSD(T), and CCSD(TQ$_{\mathrm{f}}$) methods (see the discussion later for the numerical examples). The presence of the $D^{[T]}$, $D^{(T)}$, and $D^{(TQ),b}$ denominators in the R-CCSD[T], R-CCSD(T), CR-CCSD[T], CR-CCSD(T), R-CCSD(TQ), and CR-CCSD(TQ) energy expressions, which renormalize the noniterative triples and quadruples corrections, particularly in the bond breaking region, was a primary reason for choosing the names "renormalized" or "completely renormalized" to describe these approaches in the original papers by Piecuch and Kowalski [55, 56, 57].

The apparently simple relationships between the renormalized and completely renormalized CCSD[T], CCSD(T), and CCSD(TQ) methods and their standard counterparts immediately imply that the computer costs of the R-CCSD[T], R-CCSD(T), CR-CCSD[T], CR-CCSD(T), R-CCSD(TQ), and CR-CCSD(TQ),b calculations are essentially identical to the costs of the standard CCSD[T], CCSD(T), and CCSD(TQ$_{\mathrm{f}}$) calculations. Thus, in analogy to the standard CCSD[T] and CCSD(T) methods, the R-CCSD[T], R-CCSD(T), CR-CCSD[T], and CR-CCSD(T) approaches are $n_{\mathrm{o}}^{3}n_{\mathrm{u}}^{4}$ procedures in the noniterative steps involving triples and $n_{\mathrm{o}}^{2}n_{\mathrm{u}}^{4}$ procedures in the iterative CCSD steps. The CR-CCSD[T] and CR-CCSD(T) approaches are twice as expensive as the standard CCSD[T] and CCSD(T) approaches in the steps involving noniterative triples corrections, whereas the costs of the R-CCSD[T] and R-CCSD(T) calculations are the same as the costs of the CCSD[T] and CCSD(T) calculations [162]. The memory and disk storage requirements characterizing the R-CCSD[T], R-CCSD(T), CR-CCSD[T], and CR-CCSD(T) methods are essentially identical to those characterizing the standard CCSD[T] and CCSD(T) approaches [162]. In complete analogy to the noniterative triples corrections, the costs of the R-CCSD(TQ) calculations are identical to the costs of the CCSD(TQ$_{\mathrm{f}}$) calculations [recall that CCSD(TQ$_{\mathrm{f}}$) is an $n_{\mathrm{o}}^{3}n_{\mathrm{u}}^{4}$ procedure in the triples part and an $n_{\mathrm{o}}^{2}n_{\mathrm{u}}^{5}$ procedure in the noniterative steps involving quadruples]. Again, the CR-CCSD(TQ),b approach and other variants of the CR-CCSD(TQ) method [12, 55, 56, 57, 58, 59, 60, 61, 64] are twice as expensive as the CCSD(TQ$_{\mathrm{f}}$) method in the steps involving the noniterative triples and quadruples corrections. The formal similarity of the standard, renormalized, and completely renormalized CCSD[T], CCSD(T), and CCSD(TQ) energy expressions greatly facilitates the efficient computer implementation of the R-CCSD[T], R-CCSD(T), CR-CCSD[T], CR-CCSD(T), R-CCSD(TQ), and CR-CCSD(TQ) methods. Our highly efficient R-CCSD[T], R-CCSD(T), CR-CCSD[T], and CR-CCSD(T) computer codes for ground-state PESs of singlet electronic states, described in detail in Ref. [162], fully exploiting the idea of recursively generated intermediates [117, 118], have already become an integral part of the popular GAMESS package [163]. The efficient implementation of the R-CCSD[T], R-CCSD(T), CR-CCSD[T], and CR-CCSD(T) methods for nonsinglet electronic states, based on the restricted open-shell Hartree–Fock (ROHF) and unrestricted Hartree–Fock (UHF) references, has largely been completed and will be described elsewhere (see the later part of this section for the preliminary results produced by these new open-shell codes). Work is in progress towards completing the highly efficient implementation of the R-CCSD(TQ) and CR-CCSD(TQ) methods.

Apart from the relatively low computer cost of the renormalized and completely renormalized CCSD[T], CCSD(T), and CCSD(TQ) approaches, the main practical advantage of these methods is the fact that they are as easy to use as the standard "black-box" approaches of the CCSD(T) type, while allowing us to considerably improve the description of the bond breaking region without the need to define active orbitals or using other elements of multireference theory. They are particularly well suited for the description of single and double bond breaking, including various examples of unimolecular dissociations [12, 55, 56, 58, 60, 61, 64, 162], highly excited vibrational term values near dissociation [12, 60, 61, 162], and exchange chemical reactions [12, 63]. Their performance for more complicated cases of bond breaking (e.g., the double bond breaking in C_2 or the triple bond breaking in N_2 [12, 57, 59, 61, 64]) is not as good as in various cases of single and double bond dissociations, although the results of the CR-CCSD(TQ) calculations for bond breaking in C_2 and N_2 are quite reasonable [12, 57, 59, 61, 64] (various ways of improving these CR-CCSD(TQ) results are discussed in Sects. 3.2, 3.3, 3.4).

Let us begin our discussion of the performance of the renormalized and completely renormalized CCSD[T], CCSD(T), and CCSD(TQ) methods, employing the spin- and symmetry-adapted RHF reference, with the unimolecular dissociations of three closed-shell molecules, namely, hydrogen fluoride, ethane, and methyl fluoride. In the case of ethane, we are interested in the C–C bond breaking and in the case of methyl fluoride, we study the C–F bond breaking. In the case of hydrogen fluoride, for which we used a small, double zeta (DZ) basis set [164], the R-CCSD[T], R-CCSD(T), CR-CCSD[T], CR-CCSD(T), and CR-CCSD(TQ),b results are compared with the results of the standard CC calculations, including CCSD, CCSD[T], CCSD(T), CCSD(TQ$_{\mathrm{f}}$), and CCSDT, and the exact, full CI, results (Table 1, Fig. 1a). In the case of ethane and methyl fluoride, for which we used the correlation-consistent polarized valence DZ (cc-pVDZ) basis [165] and for which the full CI results are not available, the CR-CCSD(T) results are compared with the results of accurate multireference CI (MRCI) and multireference MBPT (MRMBPT) calculations reported by Schütz [127], who used the internally contracted MRCI method of Werner and Knowles [166, 167] with quasidegenerate Davidson corrections [the MRCI(Q) approach] and the second-order MRMBPT approach employing the complete-active-space self-consistent-field (CASSCF) reference (CASPT2) [168, 169, 170, 171, 172, 173, 174, 175, 176, 177, 178], as implemented [179] in MOLPRO [180] (Fig. 1b, c).

As shown in Table 1 and Fig. 1, already the simple CR-CCSD[T] and CR-CCSD(T) methods eliminate the unphysical humps on the ground-state PESs of the HF, C_2H_6, and CH_3F molecules obtained with the standard CCSD[T], CCSD(T), and CCSD(TQ$_{\mathrm{f}}$) approaches at

Table 1. A comparison of the standard CC, renormalized and completely renormalized CCSD[T], CCSD(T), and CCSD(TQ), and CI-corrected MMCC(2,3) and MMCC(2,4) ground-state energies with the corresponding full CI results obtained for a few internuclear separations $R_{\mathrm{H-F}}$ of the HF molecule, as described by the double zeta (*DZ*) basis set [164]. The full CI total energies E are reported as $(E + 100)$ hartree. The CC, R-CC, CR-CC, and MMCC/CI energies are in millihartrees relative to the corresponding full CI energy values. See the Appendix for an explanation of the acronyms

Method	R_e^a	$2R_e$	$3R_e$	$5R_e$
Full CI[b]	−0.160300	−0.021733	0.014719	0.016707
CCSD	1.634	6.047	11.596	12.291
CCSDT[b]	0.173	0.855	0.957	0.431
CCSD[T][c]	−0.070	−2.725	−38.302	−75.101
CCSD(T)[c]	0.325	0.038	−24.480	−53.183
CCSD(TQ_f)[d]	0.218	−0.081	−18.351	−35.078
R-CCSD[T][c]	−0.010	−1.127	−13.526	−23.169
R-CCSD(T)[c]	0.371	1.137	−6.535	−14.246
CR-CCSD[T][c]	0.163	0.700	2.508	3.820
CR-CCSD(T)[c]	0.500	2.031	2.100	1.650
CR-CCSD(TQ),b[e]	0.060	0.299	0.316	0.689
MMCC(2,3)/CI[d,f]	1.195	2.708	3.669	3.255
MMCC(2,4)/CI[d,f]	1.207	2.225	3.015	3.066

[a] The equilibrium H–F bond length, $R_e = 1.7328$ bohr
[b] From Ref. [51]
[c] From Refs. [55, 56]
[d] From Ref. [62]
[e] From Ref. [12]
[f] The active space consisted of the 3σ, 1π, 2π, and 4σ orbitals

intermediate and larger internuclear separations. At the same time, the CR-CCSD[T] and CR-CCSD(T) methods provide great improvements in the poor CCSD results. For the HF, C_2H_6, and CH_3F molecules and several other examples of single bond breaking or simultaneous dissociation of two single bonds (e.g., both O–H bonds in the water molecule) [12, 56, 58, 60, 61, 64, 162], the CR-CCSD[T] and CR-CCSD(T) methods provide an approximately variational and uniformly accurate description of entire PESs, including the dissociation region. For example, the errors in the CR-CCSD[T] and CR-CCSD(T) results, relative to the full CI (HF) or MRCI(Q) (C_2H_6 and CH_3F) data, do not exceed a few millihartrees in the entire region of the H–F, C–C, and C–F distances considered in Table 1 and Fig. 1. This even applies to a complicated case of the C–F bond breaking in methyl fluoride, where for the C–F distances $R_{\mathrm{C-F}}$ less than or equal to 4.0 bohr and greater than 5.5 bohr, the differences between the CR-CCSD(T) and MRCI(Q) energies do not exceed 1–2 millihartree. For $R_{\mathrm{C-F}} \approx 5.0$ bohr, the differences between the CR-CCSD(T) and MRCI(Q) energies are around 4.5 millihartree. This should be compared with the large negative, around -100 millihartree, differences between the CCSD(T) and MRCI(Q) energies at larger values of $R_{\mathrm{C-F}}$. In consequence, the CR-CCSD[T] and CR-CCSD(T) methods, unlike their standard CCSD[T] and CCSD(T) counterparts, can be used to provide reasonable estimates of dissociation energies. For example, the CR-CCSD(T) dissociation energies D_e for ethane and methyl fluoride, calculated as differences between the CR-CCSD(T) energies at the largest C–C and C–F distances considered here ($R_{\mathrm{C-C}} = 10.0$ bohr for ethane and $R_{\mathrm{C-F}} = 6.5$ bohr for methyl fluoride) and at the corresponding equilibrium values of those distances ($R_{\mathrm{C-C}} = 2.9$ bohr for ethane and $R_{\mathrm{C-F}} = 2.6$ bohr for CH_3F), are 5.04 eV for C_2H_6 and 4.72 eV for CH_3F. These results should be compared with the MRCI(Q) values of D_e for ethane and methyl fluoride, which are 4.76 and 4.72 eV, respectively, or their CASPT2 counterparts, which are 4.77 and 4.74 eV, respectively. They should also be compared with the significantly worse D_e values produced by the single-reference CCSD approach (5.70 eV for ethane and 5.80 eV for methyl fluoride). Similar remarks apply to the DZ model of the HF molecule. For example, the CR-CCSD[T] and CR-CCSD(T) methods reduce the large positive, 11.596-millihartree, error in the CCSD result and the large negative, −38.302- and −24.480-millihartree, errors in the CCSD[T] and CCSD(T) results, respectively, at $R_{\mathrm{H-F}} = 3R_e$ ($R_{\mathrm{H-F}}$ is the H–F separation in HF and R_e is the equilibrium value of $R_{\mathrm{H-F}}$) to 2.508 and 2.100 millihartree, respectively. For the considerably larger augmented correlation-consistent polarized valence triple zeta (aug-cc-pVTZ) basis set [165, 181], the errors in the CR-CCSD(T) energies, relative to full CCSDT (the full CCSDT approach is almost exact for single bond breaking [51, 53]), do not exceed 3.9 millihartree [60]. In consequence, the spectroscopic description of the HF molecule by the CR-CCSD[T] and CR-CCSD(T) methods, including the dissociation energy D_e and all vibrational term values, including those located near the dissociation threshold, is excellent. As shown in Ref. [60], the CR-CCSD(T) method reduces the 0.725-eV error in the CCSD result for D_e, relative to the experimentally derived value of D_e of 6.120 eV [182, 183], to as little as 0.026 eV (one has to keep in mind that in this case, even the expensive full CCSDT approach gives a 0.056-eV error [54, 60]). The CR-CCSD(T) method reduces the 2881- and 325-cm^{-1} errors in the CCSD and full CCSDT results, respectively, for the $v = 19$ state of HF (the energy of this highest observed state is 49,027 cm^{-1} [183]) to 227 cm^{-1} [60]. This should be confronted with the fact that the standard CCSD[T] and

CCSD(T) approaches do not even support bound vibrational states of HF with $v > 12$ owing to the presence of the humps on the CCSD[T] and CCSD(T) potential energy curves [60].

Although we do not necessarily recommend using the R-CCSD[T] and R-CCSD(T) methods, particularly when the CR-CCSD[T] and CR-CCSD(T) calculations can be afforded, it is worth mentioning that the simplest ways of renormalizing the CCSD[T] and CCSD(T) approaches via the R-CCSD[T] and R-CCSD(T) approximations provide considerable improvements in the CCSD[T] and CCSD(T) results at larger internuclear separations (Table 1, Fig. 1a). The humps on the R-CCSD[T] and R-CCSD(T) PESs are much smaller, compared with the humps produced by the CCSD[T] and CCSD(T) methods. In the case of the DZ model of the HF molecule, the R-CCSD[T] and R-CCSD(T) methods reduce the −38.302- and −24.480-millihartree errors in the CCSD[T] and CCSD(T) results, respectively, at $R_{\mathrm{H-F}} = 3R_{\mathrm{e}}$ to −13.526 millihartree in the R-CCSD[T] case and −6.535 millihartree in the R-CCSD(T) case. For the larger aug-cc-pVTZ basis set, the vibrational term values resulting from the R-CCSD(T) calculations differ from the Rydberg–Klein–Rees (RKR) [184, 185, 186, 187] values [183] by as little as 1–9 cm^{-1} for $v \leq 13$ (the energy of the $v = 13$ level is $\sim 41,000\,\mathrm{cm}^{-1}$!) and we can use the R-CCSD(T) approach to study vibrational states with v as high as 16 [60]. None of this is possible when the standard CCSD[T] and CCSD(T) methods are applied to bond breaking in HF.

The CR-CCSD(TQ) approaches further improve the CR-CCSD[T] and CR-CCSD(T) results for single and double bond dissociations, while allowing us to obtain a fairly reasonable description of multiple bond breaking [12, 56, 57, 58, 60, 61, 64]. As shown in Table 1, the CR-CCSD(TQ),b approach is capable of reducing the 0.500-, 2.031-, 2.100- and 1.650-millihartree errors in the CR-CCSD(T) results for the DZ model of HF at $R_{\mathrm{H-F}} = R_{\mathrm{e}}$, $2R_{\mathrm{e}}$, $3R_{\mathrm{e}}$, and $5R_{\mathrm{e}}$ to the incredibly small errors of 0.060, 0.299, 0.316, and 0.689 millihartree, respectively. The description of the HF potential energy curve by the CR-CCSD(TQ),b approach is significantly better than the description of the same curve by the corresponding CCSD(TQ$_{\mathrm{f}}$) approach, which produces a hump and large negative errors on the order of 20–30 millihartree at larger values of $R_{\mathrm{H-F}}$ (Table 1). For the larger aug-cc-pVTZ basis set, the CR-CCSD(TQ),b method provides further improvement in the description of the dissociation energy of HF by the CR-CCSD(T) method, reducing the 0.026-eV error relative to the experimental D_{e} value of 6.120 eV, obtained with the CR-CCSD(T) approach, to 0.019 eV [60]. As in the CCSD(T) versus CR-CCSD(T) case and similarly to the calculations for the DZ basis set, the hump on the CCSD(TQ$_{\mathrm{f}}$) curve of HF is eliminated by the CR-CCSD(TQ),b approach and great improvements are observed in the calculated vibrational spectrum [60]. The CR-CCSD(TQ),b method reduces the 227-cm^{-1} error in the CR-CCSD(T) energy of the $v = 19$ state of HF, whose experimental or RKR energy is 49,027 cm^{-1}, to 159 cm^{-1} [60]. In fact, the CR-CCSD(TQ),b potential leads to the appearance of the $v = 20$ vibrational level to

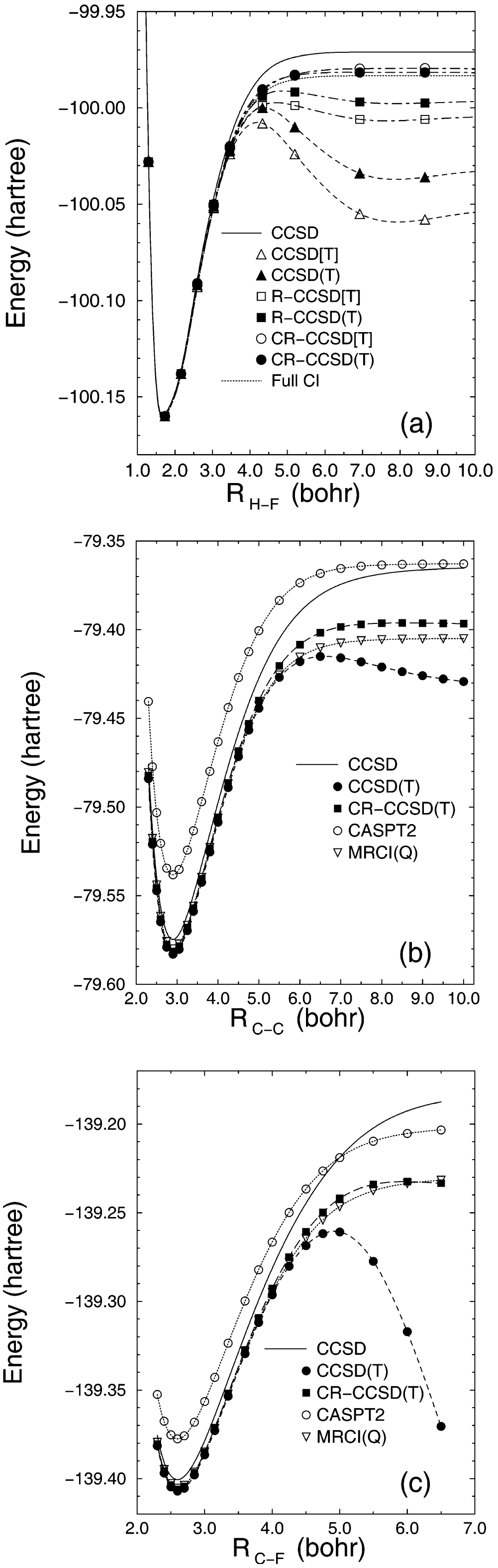

Fig. 1. Potential energy curves for the H–F bond breaking in **a** the double zeta (*DZ*) HF molecule, **b** the C–C bond breaking in the correlation-consistent polarized valence DZ (*cc-pVDZ*) model of ethane, and **c** the C–F bond breaking in the cc-pVDZ model of methyl fluoride (see the text for the remaining details and Refs. [12, 55, 56] for the original data; the CASPT2 and MRCI(Q) results for ethane and methyl fluoride taken from Ref. [127]). See the Appendix for an explanation of the acronyms

be located only 28 cm^{-1} below the corresponding dissociation threshold. The most accurate potential function for HF to date, obtained using the hybrid RKR-based theoretical approach (RKR plus improved long-range plus very accurate and expensive ab initio calculations), produces the $v = 20$ level with the energy of 23 cm^{-1} below the dissociation threshold [188, 189]. None of the existing ab initio approaches can provide results of similar quality with the ease of use characterizing the CR-CCSD(T) and CR-CCSD(TQ) methods.

The CR-CCSD(TQ),b and other variants [57] of the CR-CCSD(TQ) approach are particularly useful when multiple bonds are stretched or broken. This is shown in Table 2 and Fig. 2, where we present the results of the CR-CCSD(TQ),b and other calculations for the DZ model of the nitrogen molecule. In this case, the CR-CCSD(T) approach, which works great for single-bond breaking, fails at larger N–N separations (Table 2), which is a consequence of the fact that, as all multiply bonded systems, the N_2 molecule is characterized by the large T_3 and T_4 effects and, for the stretched nuclear geometries, by the nonnegligible contributions due to higher–than–quadruply excited clusters, in addition to huge contributions due to the T_3 and T_4 cluster components [57]. The large values of higher–than–doubly excited clusters are related to the significant nondynamic correlation effects in N_2, even in the vicinity of the equilibrium geometry ($R_{N-N} = R_e$; R_{N-N} is the N–N separation). The situation becomes particularly severe when the N–N bond is stretched. The combined effect of all higher–than–doubly excited clusters, as estimated by calculating the difference between the full CI and CCSD energies, dramatically increases with R_{N-N}, from 8.289 millihartree at $R_{N-N} = R_e$ to 33.545 millihartree at $R = 1.5R_e$ (Table 2). In consequence, the CCSD approach, in which higher–than–doubly excited clusters are ignored, completely fails, producing an unphysical hump on the potential energy curve of N_2 and energies that are significantly below the corresponding full CI energies at larger values of R_{N-N} (Fig. 2; cf., also, Sect. 3.4). The failure of the CCSD approach propagates into the poor performance of the CCSD(T) and CCSD(TQ$_f$) approximations. Indeed, the small, 2.156- and 0.323-millihartree, errors in the CCSD(T) and CCSD(TQ$_f$) results, relative to full CI, at $R_{N-N} = R_e$ increase (in absolute value) to 387.448 and 334.985 millihartree, respectively, at $R = 2.25R_e$ (Table 2). As shown in Fig. 2, the CCSD(T) approach produces a potential energy curve which falls significantly below the full CI curve, whereas the CCSD(TQ$_f$) potential energy curve is located significantly above the full CI curve. As a matter of fact, the nondynamic correlation effects are so big in N_2 that even the full CCSDT method and its CCSDT(Q$_f$) extension, in which noniterative correction due to T_4 clusters is added to the CCSDT energy, provide a completely erroneous description of the N_2 potential (Table 2, Fig. 2). The failure of the CCSD approach also propagates into the poor performance of the CR-CCSD(T) method. The CR-CCSD(T) method improves the CCSD results in the $R_{N-N} \leq 1.75R_e$ region, but the overall performance of the CR-CCSD(T) approach in the region of larger R_{N-N} values is poor. Because of the aforementioned importance of the higher–than–triply excited clusters in the region of larger N–N separations, we must go beyond the basic MMCC(2,3) approximation, on which the CR-CCSD(T) method is based, to achieve a satisfactory description of the N_2 dissociation within the single-reference MMCC framework.

As explained earlier, the CR-CCSD(TQ),b approach is the lowest-order MMCC approximation beyond MMCC(2,3) or CR-CCSD(T). The results in Table 2 and Fig. 2 show that the CR-CCSD(TQ),b approach,

Table 2. A comparison of the CCSD, CCSDT, CCSD(T), CCSD(TQ$_f$), CCSDT(Q$_f$), CR-CCSD(T), CR-CCSD(TQ),b, and CI-corrected and quadratic MMCC(2,4), MMCC(2,5), and MMCC(2,6) ground-state energies with the corresponding full CI results obtained for a few internuclear separations R_{N-N} of the N_2 molecule with the DZ basis set [164]. The full CI total energies E, reported as $(E + 108)$, are in hartrees. The CC, CR-CC, MMCC/CI and QMMCC energies are in millihartrees relative to the corresponding full CI energy values. The lowest two occupied and the highest two unoccupied orbitals were frozen in correlated calculations

Method	$0.75R_e$	R_e^a	$1.25R_e$	$1.5R_e$	$1.75R_e$	$2R_e$	$2.25R_e$
Full CI[b]	−0.549027	−1.105115	−1.054626	−0.950728	−0.889906	−0.868239	−0.862125
CCSD	3.132	8.289	19.061	33.545	17.714	−69.917	−120.836
CCSDT[c]	0.580	2.107	6.064	10.158	−22.468	−109.767	−155.656
CCSD(T)[b]	0.742	2.156	4.971	4.880	−51.869	−246.405	−387.448
CCSD(TQ$_f$)[b]	0.226	0.323	0.221	−2.279	−14.243	92.981	334.985
CCSDT(Q$_f$)[c]	0.047	−0.010	−0.715	−4.584	3.612	177.641	426.175
CR-CCSD(T)[b]	1.078	3.452	9.230	17.509	−2.347	−86.184	−133.313
CR-CCSD(TQ),b[b]	0.451	1.302	3.617	8.011	13.517	25.069	14.796
MMCC(2,4)/CI[d]	1.242	2.354	5.363	11.639	10.831	−16.086	−30.720
MMCC(2,5)/CI[d]	1.220	2.089	3.527	5.493	1.631	−24.410	−39.124
MMCC(2,6)/CI[d]	1.217	2.022	2.909	3.186	4.048	4.443	4.552
QMMCC(2,4)[e]	0.458	1.384	3.916	8.362	13.074	22.091	10.749
QMMCC(2,5)[e]	0.384	1.012	2.365	3.756	1.415	6.672	−2.638
QMMCC(2,6)[e]	0.384	1.012	2.373	3.784	1.380	6.230	−3.440

[a] The equilibrium bond length, $R_e = 2.068$ bohr

[b] From Ref. [57]

[c] From Ref. [59]

[d] From Ref. [12]. The active space consisted of the $3\sigma_g$, $1\pi_u$, $2\pi_u$, $1\pi_g$, $2\pi_g$, and $3\sigma_u$ orbitals

[e] From Ref. [66]

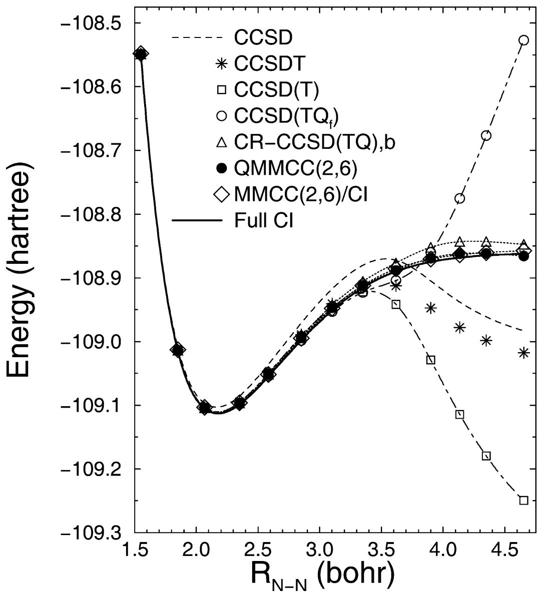

Fig. 2. Ground-state potential energy curves of the DZ N_2 molecule (see the text for the remaining details and Refs. [12, 57, 66] for the original data)

which is based on the MMCC(2,4) approximation and which accounts for the combined effect of the T_3 and T_4 clusters, provides considerable improvements in the poor description of the potential energy curve of N_2 by the standard CC and CR-CCSD(T) methods. As shown in Table 2 and Fig. 2, the CR-CCSD(TQ),b method, which, as explained earlier, is a rather simple modification of the conventional CCSD(TQ$_f$) approach and which uses, as the latter method, elements of MBPT to estimate the T_3 and T_4 contributions, provides a potential energy curve which is quite close to the exact, full CI curve. For example, the huge, 334.985-millihartree, error in the CCSD(TQ$_f$) energy at $R = 2.25R_e$ reduces to 14.796 millihartree when the CR-CCSD(TQ),b method is employed (see Table 2). The CR-CCSD(TQ),b curve is located above the full CI curve in the entire $R = 0.75R_e - 2.25R_e$ region and almost all pathologies observed in the standard single-reference CC calculations, including a nearly singular behavior of the CCSD(TQ$_f$) and CCSDT(Q$_f$) approaches at large R values, are eliminated when the CR-CCSD(TQ),b method is employed. There is a small, approximately 5-millihartree, hump on the CR-CCSD(TQ),b curve, but the overall performance of the CR-CCSD(TQ),b approach, when compared with other single-reference CC approaches, is very good. Although there are 10–25-millihartree errors in the CR-CCSD(TQ),b energies in the region of larger R_{N-N} values, the fact that we can obtain a reasonably accurate potential energy curve for the triply bonded N_2 molecule, with the ease characterizing the standard noniterative CC methods of the CCSD(TQ$_f$) type, demonstrates the type of improvements the CR-CC approaches can offer, even when multiple bonds are broken. Further improvements in the results for multiply bonded systems, such as N_2, via the QMMCC and CI-corrected MMCC(2,6) methods, are discussed in Sects. 3.2, 3.3, and 3.4.

The considerable improvements in the description of bond breaking by the CR-CC approaches are not limited to unimolecular dissociations. We can also use the CR-CC approaches to study ground-state PESs for exchange chemical reactions. This is shown in Figs. 3 and 4, where we compare the results of the CR-CCSD(T) calculations for the prototypical case of the $\mathrm{Be} + \mathrm{HF} \rightarrow \mathrm{BeF} + \mathrm{H}$ reaction, investigated earlier by others [190, 191, 192, 193, 194, 195, 196, 197, 198], with the results of the CCSD(T) and full CI calculations (all performed with the small, MIDI basis set [199]). The detailed description of these calculations, including the relevant numerical data, can be found elsewhere [63], so we limit our discussion to the most important observations. We have also performed the more realistic CR-CCSD(T) calculations with the larger basis sets of the cc-pVTZ and correlation-consistent polarized valence quadruple zeta (cc-pVQZ) quality, for which full CI calculations for the BeFH system on dense grids of nuclear geometries required to obtain a complete representation of the PES are too expensive [12]. Although we provide some information about these calculations, our discussion concentrates on the small basis set calculations reported in Ref. [63], since the main objective of this article is to assess the potential of the CR-CCSD(T) and other MMCC approaches by comparing, if possible, the CR-CC and MMCC data with the exact, full CI, data.

The results shown in Figs. 3 and 4 correspond to the collinear arrangement of the Be, F, and H atoms, with the Be atom approaching the HF molecule from the fluorine side. In this case, the ground electronic state of the BeFH system is a $^1\Sigma^+$ state correlating with the $\mathrm{Be}(2s^2\,{}^1\mathrm{S}) + \mathrm{HF}(\mathrm{X}\,{}^1\Sigma^+)$ state of reactants, the $\mathrm{BeF}(\mathrm{X}\,{}^2\Sigma^+) + \mathrm{H}(1s^1\,{}^2\mathrm{S})$ state of products, and the $\mathrm{Be}(2s^2\,{}^1\mathrm{S}) + \mathrm{F}(2p^5\,{}^2\mathrm{P}) + \mathrm{H}(1s^1\,{}^2\mathrm{S})$ state of noninteracting atoms. The $\mathrm{Be}(2s^2\,{}^1\mathrm{S}) + \mathrm{HF}(\mathrm{X}\,{}^1\Sigma^+)$ channel, corresponding to two closed-shell fragments, is adequately described by the RHF-based CC methods. This is no longer the case when the $\mathrm{BeF}(\mathrm{X}\,{}^2\Sigma^+) + \mathrm{H}(1s^1\,{}^2\mathrm{S})$ products and the noninteracting Be, F, and H atoms are examined. In these cases, the ground-state RHF configuration is no longer a good reference and all standard RHF-based CC methods fail. This is shown in Figs. 3a and 4a, which clearly demonstrate that the RHF-based CCSD(T) PES has the wrong topology. The differences between the CCSD(T) and full CI PESs are particularly large when the Be–F and H–F bonds are stretched. They are greater than 10 millihartree (6.3 kcal mol^{-1}) in the entire $R_{\mathrm{Be-F}} \geq 3.9$ bohr and $R_{\mathrm{H-F}} \geq 6.0$ bohr region and for $R_{\mathrm{Be-F}} \geq 3.3$ bohr and $R_{\mathrm{H-F}} = 8.0$ bohr. They exceed 5 millihartree (3.1 kcal mol^{-1}) in the $R_{\mathrm{Be-F}} > 3.0$ bohr and $R_{\mathrm{H-F}} \geq 5.0$ bohr region and for $R_{\mathrm{Be-F}} = 1.8 - 2.0$ bohr and $R_{\mathrm{H-F}} = 2.75 - 3.0$ bohr. For the larger, cc-pVTZ basis set, for which full CI results are not available, so comparisons have to be made with accurate multireference techniques, such as the aforementioned MRCI(Q) approach, the differences between the CCSD(T) and MRCI(Q) energies are as large as 120.140 millihartree (75.4 kcal mol^{-1}), exceeding 5 kcal mol^{-1} for almost all nuclear geometries from the $R_{\mathrm{Be-F}} < 2.5$ bohr and $R_{\mathrm{H-F}} \geq 2.5$ bohr region, for the majority of geometries from the $R_{\mathrm{Be-F}} \geq 3.5$ bohr and $R_{\mathrm{H-F}} \geq 3.5$ bohr

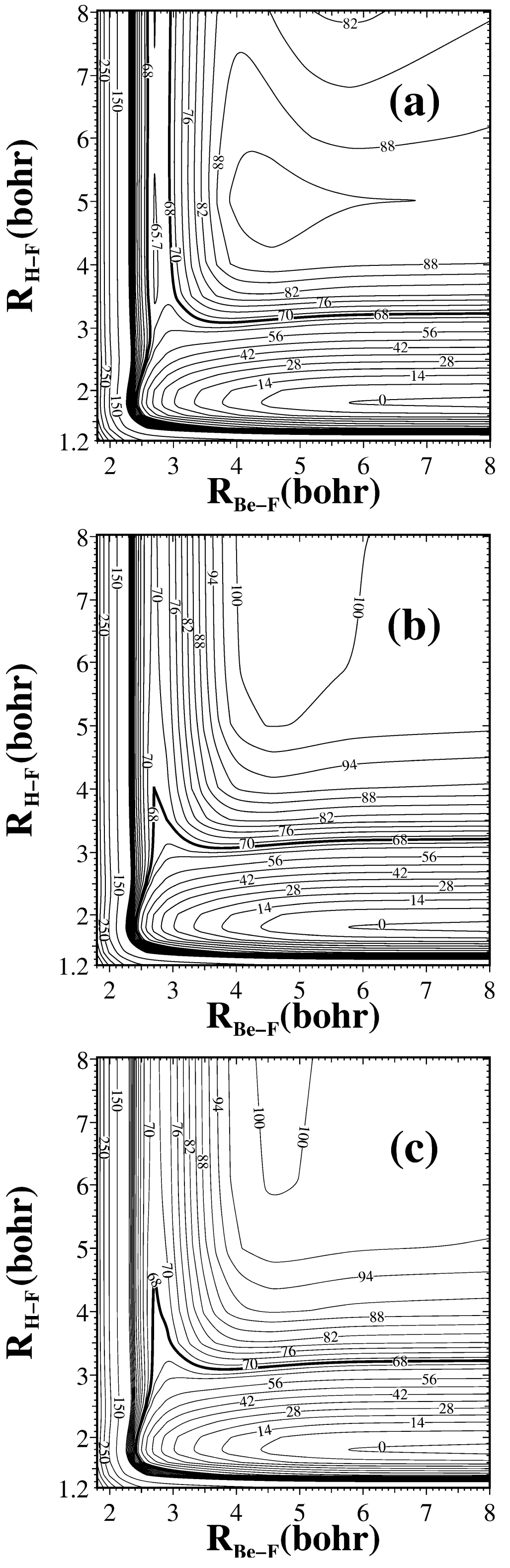

region, and for many geometries from the 2.5 bohr $\le R_{\mathrm{Be-F}} < 3.5$ bohr and $R_{\mathrm{H-F}} \approx 3.0$ bohr region. The differences between the CCSD(T) and MRCI(Q) energies resulting from the calculations with the cc-pVTZ basis set exceed 11 kcal mol^{-1} in the entire $R_{\mathrm{Be-F}} \ge 5.0$ bohr and $R_{\mathrm{H-F}} \ge 5.0$ bohr region [12]. For

◄

Fig. 3. The ground-state potential energy surfaces (*PESs*) of the collinear BeFH system resulting from the **a** CCSD(T), **b** CR-CCSD(T), and **c** full CI calculations with the MIDI basis set (see Ref. [63] for the original data). The energies are reported in kilocalorie per mole relative to the Be + HF reactants (the energy at $R_{\mathrm{Be-F}} = 8.0$ bohr and $R_{\mathrm{H-F}} = 1.7325$ bohr; $R_{\mathrm{H-F}} = 1.7325$ bohr is the equilibrium bond length in HF). The *thick contour line* corresponding to 68 kcal mol^{-1} separates the region where the contour spacing is 7 kcal mol^{-1} from the region where the contour spacing is 3 kcal mol^{-1}. An extra contour line corresponding to 65.7 kcal mol^{-1} emphasizes the presence of the exaggerated barrier and potential well in the product valley on the CCSD(T) PES and the absence of those features on the CR-CCSD(T) and full CI PESs

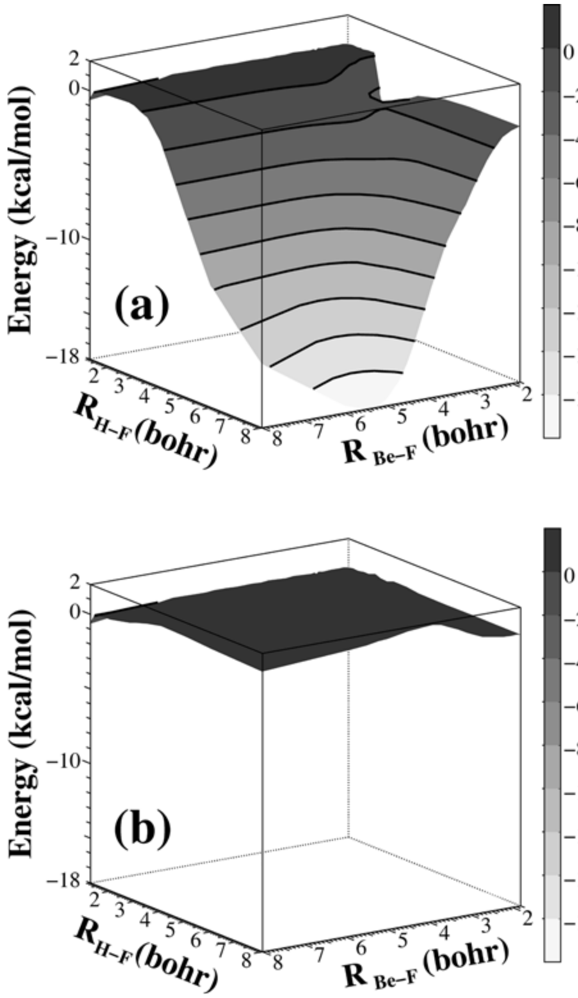

Fig. 4. The differences between the **a** CCSD(T) and **b** CR-CCSD(T) energies and the full CI energies (kcal mol^{-1}) for the collinear BeFH system, as described by the MIDI basis set, as functions of the H–F and Be–F internuclear separations, $R_{\mathrm{H-F}}$ and $R_{\mathrm{Be-F}}$, respectively (see Ref. [63] for the original data)

the MIDI basis set used to prepare Figs. 3 and 4, the maximum difference between the CCSD(T) and full CI energies is 28.605 millihartree (17.9 kcal mol^{-1}).

The CR-CCSD(T) PES, shown in Fig. 3b, is clearly much better than the CCSD(T) PES shown in Fig. 3a. The CR-CCSD(T) method reduces the maximum error in the CCSD(T) results of 28.605 millihartree to 3.122 millihartree (2.0 kcal mol^{-1}). As shown in Fig. 4b, for the vast majority of nuclear geometries, the errors in the CR-CCSD(T) results, relative to full CI, are on the order of 1 millihartree (0.6 kcal mol^{-1}) or smaller. For the cc-pVTZ basis set, the differences between the CR-CCSD(T) and MRCI(Q) energies typically are 0.2–2 kcal mol^{-1}, never exceeding 4.1 kcal mol^{-1} [12]. The CR-CCSD(T) PES is located above the exact, full CI, PES and both PESs are virtually parallel to each other. This should be contrasted with the nonvariational collapse of the standard CCSD(T) theory at larger Be–F and H–F distances. A comparison of the CR-CCSD(T) and full CI contour plots, shown in Fig. 3b and c, respectively, indicates that the overall description of the ground-state PES of the BeFH system, including the reactant and product valleys, the transition-state region, and the noninteracting atom limit, is excellent. This is emphasized in Fig. 3 by the thick contour lines corresponding to the energy of 68 kcal mol^{-1} and thin contour lines corresponding to 65.7 kcal mol^{-1}. These lines clearly indicate the presence of the exaggerated barrier and potential well in the product valley on the CCSD(T) PES and the absence of those features on the CR-CCSD(T) and full CI PESs. The contour lines corresponding to the energies above reactants of 88 and 91 kcal mol^{-1} indicate the presence of the well-pronounced unphysical hump on the CCSD(T) PES in the region of intermediate Be–F and H–F distances, the wrong description of the BeF + H and Be + F + H dissociation channels by the CCSD(T) method, and the absence of those kinds of problems in the CR-CCSD(T) calculations. Similar remarks apply to the CCSD(T) versus CR-CCSD(T) calculations for BeFH with the cc-pVTZ and cc-pVQZ basis sets [12] and the CCSD(T) and CR-CCSD(T) calculations for other arrangements of the Be, F, and H atoms, including the insertion of the Be atom into the H–F bond and the approach of HF by the Be atom from the H side, which will all be discussed in a future paper. For example, the CR-CCSD(T) barrier for the collinear Be + HF → BeF + H reaction, obtained with the cc-pVTZ basis set, is 32.2 kcal mol^{-1}, in very good agreement with the MRCI(Q) result of 31.1 kcal mol^{-1} [12] and the MRCI result for this barrier reported by Aguado et al. of 33.2 kcal mol^{-1} [192].

In all of these examples, we have considered bond breaking on singlet PESs. Clearly, the dissociation of closed-shell molecules into open-shell fragments, which requires the unpairing of one or more electron pairs, represents a very challenging problem for single-reference methods. However, many bond breaking phenomena and many exchange reactions of interest to chemists involve bond rearrangements in open-shell molecular systems. For this reason, we have recently started exploring the applicability of the renormalized and completely renormalized CCSD[T] and CCSD(T) methods to bond breaking on nonsinglet PESs. The efficient computer codes for the R-CCSD[T], R-CCSD(T), CR-CCSD[T], and CR-CCSD(T) methods have been written and several preliminary test calculations employing the UHF or ROHF references have been performed for bond breaking in small open-shell systems, including OH, CH, and F_2^+. Bond breaking in the OH and CH systems turned out to be trivial to describe by the CR-CCSD[T] and CR-CCSD(T) methods, so we do not discuss these results here (the results will be published elsewhere). The F_2^+ system turned out to be a lot more challenging for the R-CC and CR-CC methods and, thus, much more interesting for this discussion.

Just like its neutral F_2 counterpart [50, 58], the F_2^+ molecular ion is rather difficult to describe by the single-reference methods [200, 201, 202]. One of the interesting and challenging problems that the single-reference methods face, when bond breaking in F_2^+ is examined, is the possibility of the breakdown of the inversion symmetry (lowering of the symmetry from $D_{\infty h}$ to $C_{\infty v}$ or from D_{2h} to C_{2v}) by the UHF or ROHF calculations, which may significantly impact the results of the correlated single-reference calculations employing the UHF or ROHF references [201, 202]. The spin- and symmetry-adapted multi-reference methods employing the multi-configurational SCF (MCSCF), CASSCF, and other properly constructed multi-determinantal references do not have such problems (cf., e.g., the MRCI calculations for F_2^+, employing the generalized valence bond, GVB, references [203]), but in the single-reference calculations one must proceed with caution. In the specific case of F_2^+, the single-reference methods that strictly impose the $D_{\infty h}$ or D_{2h} symmetry on the reference configuration (preserving, in particular, the inversion symmetry) may experience severe difficulties in describing the dissociation of the ground-state F_2^+ molecule into $F(2p^5\ {}^2P)$ $+F^+(2p^4\ {}^3P)$. As in the case of bond breaking of closed-shell molecules into open-shell fragments, the description of bond breaking by the single-reference CC methods may significantly benefit from using the spin- and symmetry-broken UHF references [50]. This has been demonstrated by Watts and Bartlett [202], who showed that one can obtain a reasonable description of the entire potential energy curve of F_2^+ with the standard CC methods employing the symmetry-broken (C_{2v}-adapted) UHF reference. In analogy to the single-reference calculations for closed-shell systems employing the symmetry-adapted RHF references, this would not be possible if one employed the single-determinantal reference configurations adapted to the spin and point-group ($D_{\infty h}$ or D_{2h}) symmetries of the Hamiltonian of F_2^+. Indeed, the use of the symmetry-adapted references creates a situation, where the nondynamic correlation effects become large and difficult to describe by the single-reference methods, even in the region of the intermediate stretches of the F–F bond in F_2^+. This is shown in Fig. 5, where we compare the results of our preliminary CCSD, CCSD(T), and CR-CCSD(T) calculations, employing the D_{2h}-adapted ROHF reference, with the highly accurate potential energy curve of F_2^+ obtained by us with the MRCI(Q) approach (all calculations were performed with the relatively large aug-cc-pVTZ basis set [165, 181]). As we can see in Fig. 5, the CCSD approach produces a potential well which is 50 % deeper than that obtained with the MRCI(Q) approach. The MRCI(Q) approach provides a binding energy D_e of 3.35 eV, which compares very well with the experimental D_e value of 3.41 eV [182] and the GVB-based MRCI value of D_e of 3.00 eV reported in Ref. [203]. The CCSD method employing the symmetry-adapted ROHF refer-

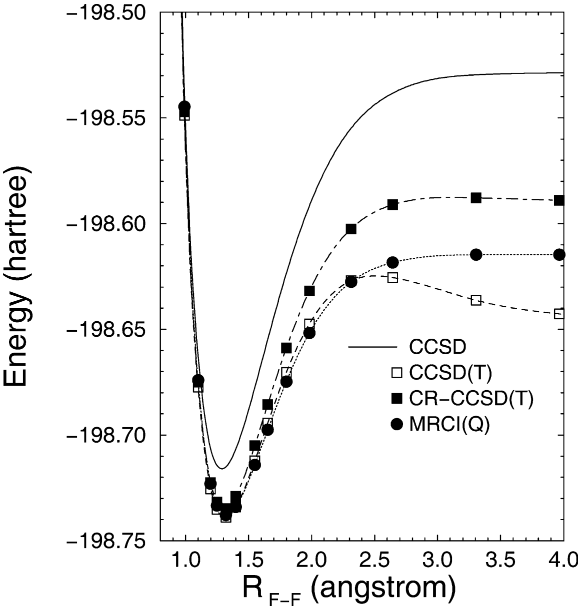

Fig. 5. Ground-state potential energy curves of F_2^+, as described by the augmented correlation-consitent polarized valence triple zeta basis set

ence gives 5.10 eV, which is a considerably worse result. The standard CCSD(T) approach, employing the D_{2h}-adapted ROHF reference, fails too, producing the well-pronounced unphysical hump at $R_{\mathrm{F-F}} \approx 2.5$ Å (cf. Fig. 5; the equilibrium bond length R_{e} of F_2^+ is 1.305 Å [204]). The depth of this hump, as measured by forming the difference between the CCSD(T) energies at the maximum corresponding to the hump and $R_{\mathrm{F-F}} = 5R_{\mathrm{e}}$, is around 25 millihartree. The hump on the CCSD[T] potential energy curve is even larger (approximately 28-millihartree deep). At larger F–F separations, the CCSD[T] and CCSD(T) potential energy curves are located significantly (more than 30 millihartree at $R_{\mathrm{F-F}} = 5R_{\mathrm{e}}$) below the MRCI(Q) curve. The differences between the CCSD and MRCI(Q) energies at larger values of $R_{\mathrm{F-F}}$ are almost 90 millihartree at $R_{\mathrm{F-F}} = 5R_{\mathrm{e}}$.

In view of the severe problems encountered by the CCSD, CCSD[T], and CCSD(T) methods employing the symmetry-adapted ROHF references, it is quite encouraging to see that the ROHF-based CR-CCSD(T) method, which produces the spin- and symmetry-adapted results, is capable of providing considerable improvements in the description of the potential energy curve of F_2^+. As shown in Fig. 5, the CR-CCSD(T) potential energy curve is located above the highly accurate MRCI(Q) curve and the well-pronounced, approximately 25-millihartree-deep, hump on the CCSD(T) curve is considerably reduced (to ≈ 4 millihartree) when the CR-CCSD(T) method is employed [we should mention that even the MRCI(Q) curve has a small, approximately 1-millihartree-deep, hump]. The R-CCSD[T], R-CCSD(T), and CR-CCSD[T] approaches provide very similar improvements. The CR-CCSD(T) dissociation energy D_{e}, obtained by forming the difference between the CR-CCSD(T) energy at the maximum corresponding to a tiny hump on the CR-CCSD(T) potential energy curve and the CR-CCSD(T) energy at $R_{\mathrm{F-F}} = R_{\mathrm{e}}$ is 4.00 eV. Similar calculations for the R-CCSD[T], R-CCSD(T), and CR-CCSD[T] methods give D_{e} values of 3.75, 3.86, and 3.92 eV, respectively, in reasonable agreement with the MRCI(Q) and experimental values of 3.35 and 3.41 eV, respectively. All of these R-CC and CR-CC values are much better than the CCSD D_{e} value of 5.10 eV. At the same time, the R-CCSD[T], R-CCSD(T), CR-CCSD[T], and CR-CCSD(T) potential energy curves for F_2^+ (which all look very similar) have essentially the same shape as the highly accurate MRCI(Q) curve shown in Fig. 5. The errors in the CR-CCSD(T) results, relative to MRCI(Q), are on the order of a fraction of a millihartree in the $R_{\mathrm{F-F}} = 1.15 - 1.20$-Å region and 2–3 millihartree in the $R_{\mathrm{F-F}} \approx R_{\mathrm{e}}$ region, while monotonically increasing to approximately 20 millihartree in the $R_{\mathrm{F-F}} \approx 5R_{\mathrm{e}}$ region. Although we may have to run the CR-CCSD(TQ) calculations to improve the CR-CCSD(T) results in the bond breaking region, the errors in the CR-CCSD(T) results are already a lot smaller than the approximately 90-millihartree errors in the CCSD results. At the same time, the CR-CCSD(T) description of the potential energy curve of F_2^+ is much more realistic than the description of this curve offered by the standard CCSD(T) approach. All of this indicates that the R-CC and CR-CC methods show a lot of promise for future studies of bond breaking in open-shell systems.

All of these examples show that the CR-CC methods are capable of eliminating or considerably reducing the failing of the standard CC methods at larger internuclear separations. Aside from the high accuracy and the approximately variational description that the CR-CC methods offer over wide ranges of nuclear geometries used in PES calculations, the major advantage of all CR-CC approaches is the fact that we do not have to select active orbitals in an ad hoc molecule–by–molecule manner, which characterizes all multireference approaches. We demonstrated that the CR-CCSD(T) approach is sufficient for PESs involving single bond breaking. Further improvements are offered by the higher-order CR-CCSD(TQ) approach. The CR-CCSD(TQ) method is also capable of providing substantial improvements in the description of multiple bond breaking, and is often sufficient to provide high accuracy, but the 10–25-millihartree errors that the CR-CCSD(TQ) approach produces at larger N–N separations in the N_2 molecule need to be addressed. This can be done in a few different ways, which are described in Sects. 3.2, 3.3, and 3.4.

3.2 The QMMCC methods

The QMMCC methods [12, 64, 65, 66] represent higher-order extensions of the basic CR-CCSD[T], CR-CCSD(T), and CR-CCSD(TQ) approximations, primarily designed to improve the description of molecular PESs involving multiple bond breaking by adding noniterative corrections to the CCSD energies (as in other MMCC methods, one might, of course, contemplate the QMMCC schemes in which similar corrections are added to the energies obtained in higher-level CC calculations; see Ref. [66] for further information). As one can imagine and as confirmed by us numerically, difficult cases of multiple bond breaking may require the explicit consideration of the pentuply and hextuply excited moments of the CCSD equations, $\mathscr{M}^{i_1i_2i_3i_4i_5}_{a_1a_2a_3a_4a_5}(2)$ and $\mathscr{M}^{i_1i_2i_3i_4i_5i_6}_{a_1a_2a_3a_4a_5a_6}(2)$, Eqs. (26) and (27), respectively, and the wave functions $|\Psi_0\rangle$ entering the MMCC equations that contain the pentuply and hextuply excited determinants, in addition to the triply and quadruply excited moments, $\mathscr{M}^{i_1i_2i_3}_{a_1a_2a_3}(2)$ and $\mathscr{M}^{i_1i_2i_3i_4}_{a_1a_2a_3a_4}(2)$, Eqs. (24) and (25), respectively, used by the CR-CCSD[T], CR-CCSD(T), and CR-CCSD(TQ) methods and other MMCC(2,3) and MMCC(2,4) approximations. In other words, we may have to consider the MMCC(2,5) and MMCC(2,6) schemes, in which energies are calculated as (cf. Eqs. (49) and (50))

$$
\begin{aligned}
E_0^{(\mathrm{MMCC})}(2,5) = E_0^{(\mathrm{CCSD})} &+ \langle\Psi_0|\{M_3(2) + [M_4(2) \\
&+ T_1M_3(2)] + [M_5(2) + T_1M_4(2) \\
&+ (T_2 + \frac{1}{2}T_1^2)M_3(2)]\}|\Phi\rangle / \\
&\langle\Psi_0|\mathrm{e}^{T_1+T_2}|\Phi\rangle
\end{aligned}
\tag{79}
$$

and

$$
\begin{aligned}
E_0^{(\mathrm{MMCC})}(2,6) = E_0^{(\mathrm{CCSD})} &+ \langle\Psi_0|\{M_3(2) + [M_4(2) \\
&+ T_1M_3(2)] + [M_5(2) + T_1M_4(2) \\
&+ (T_2 + \frac{1}{2}T_1^2)M_3(2)] + [M_6(2) \\
&+ T_1M_5(2) + (T_2 + \frac{1}{2}T_1^2)M_4(2) \\
&+ (T_1T_2 + \frac{1}{6}T_1^3)M_3(2)]\}|\Phi\rangle / \\
&\langle\Psi_0|\mathrm{e}^{T_1+T_2}|\Phi\rangle \ ,
\end{aligned}
\tag{80}
$$

respectively, and in which moments $\mathscr{M}^{i_1i_2i_3i_4i_5}_{a_1a_2a_3a_4a_5}(2)$ and $\mathscr{M}^{i_1i_2i_3i_4i_5i_6}_{a_1a_2a_3a_4a_5a_6}(2)$ enter the corresponding energy expressions through the $M_5(2)|\Phi\rangle$ and $M_6(2)|\Phi\rangle$ quantities (cf. Eq. 29). Based on the success of the perturbative CR-CCSD[T], CR-CCSD(T), and CR-CCSD(TQ) approximations described in Sect. 3.1, which use the simple MBPT(2)-like formulas for $|\Psi_0\rangle$ in the MMCC(2,3) and MMCC(2,4) energy expressions (cf. Eqs. 55, 56, 57, 58 and 59), one may try to design the higher-order MMCC schemes for multiple bond breaking, employing Eqs. (79) and (80), by replacing $|\Psi_0\rangle$ in Eqs. (79) and (80) by the MBPT(3)-like wave functions, since the MBPT(3) wave function is the lowest-order wave function which has the pentuply and hextuply excited components of the $T_2T_3^{[2]}$ and $\frac{1}{6}T_2^3$ type that can engage the pentuply and hextuply excited moments $\mathscr{M}^{i_1i_2i_3i_4i_5}_{a_1a_2a_3a_4a_5}(2)$ and $\mathscr{M}^{i_1i_2i_3i_4i_5i_6}_{a_1a_2a_3a_4a_5a_6}(2)$. As it turns out, the MMCC(2,5) and MMCC(2,6) methods employing MBPT(3)-like wave functions $|\Psi_0\rangle$ do not lead to the desired improvements in the CR-CCSD(TQ) results for triple bond breaking in N_2 and similar cases. A different choice of $|\Psi_0\rangle$ in Eqs. (79) and (80) has to be contemplated, if we want to improve the CR-CCSD(TQ) results via the MMCC(2,5) and MMCC(2,6) methods, while preserving the ease of use and black-box character of the noniterative CR-CCSD(TQ) and similar approaches.

The following analysis can help us to design the desired approach. A direct inspection of the CR-CCSD[T] equations, Eqs. (60), (63), and (66), and the formula for the wave function $|\Psi_0^{\mathrm{CCSD[T]}}\rangle$, Eq. (55), used to calculate the completely renormalized triples correction in the CR-CCSD[T] method, indicate that the CR-CCSD[T] approach is a special case of the MMCC$(2, m_\mathrm{B})$ approximation, in which the wave function $|\Psi_0\rangle$ entering Eq. (50) (where m_A is set at 2) is replaced by

$$
|\Psi_0^{\mathrm{LMMCC}}\rangle = (1+\Sigma)|\Phi\rangle \ , \tag{81}
$$

where the approximate cluster operator Σ is defined as

$$
\Sigma = T_1 + T_2 + T_3^{[2]} \ , \tag{82}
$$

with T_1 and T_2 representing the singly and doubly excited cluster components obtained in the CCSD calculations and $T_3^{[2]}$ defined by Eq. (57). It is worth mentioning that Σ, Eq. (82), represents a particularly interesting approximation to the exact cluster operator T, which is correct through the second order of the MBPT wave function (T_1 and T_3 contribute, for the first time, in the second order and T_2 contributes, for the first time, in the first order; T_4, T_5, etc. do not contribute in the first two orders of MBPT). We use the acronym LMMCC in designating the wave function $|\Psi_0^{\mathrm{LMMCC}}\rangle$ to emphasize the fact that the wave function ansatz used in Eq. (81) is linear in Σ. Clearly, one can view the wave function $|\Psi_0^{\mathrm{LMMCC}}\rangle$, Eq. (81), as the lowest-order approximation to the exponential wave function

$$
|\tilde{\Psi}_0\rangle = \mathrm{e}^{\Sigma}|\Phi\rangle \ . \tag{83}
$$

One might think of using $|\tilde{\Psi}_0\rangle$, Eq. (83), with Σ defined by Eq. (82), instead of $|\Psi_0\rangle$ in the basic MMCC formulas, Eqs. (21) and (28), but the resulting computational schemes would not be practical, since we would have to consider all many-body terms resulting from the presence of e^{Σ} in Eq. (83), including the N-body ones, where N is the number of electrons, to calculate the noniterative corrections $\delta_0^{(\mathrm{A})}$ or $\delta_0^{(\mathrm{CCSD})}$ to the CC (e.g., CCSD) energies. However, one can consider the MMCC approximations, in which the exponential wave function $|\tilde{\Psi}_0\rangle$, Eq. (83), is replaced by the truncated power series expansion in Σ. For example, we may be able to improve the CR-CCSD[T] and CR-CCSD(T) results by using the wave function

$$
|\Psi_0^{\mathrm{QMMCC}}\rangle = (1 + \Sigma + \frac{1}{2}\Sigma^2)|\Phi\rangle \ , \tag{84}
$$

instead of $|\Psi_0\rangle$, in the formula for the correction $\delta_0^{(\mathrm{CCSD})}$, Eq. (28). The $|\Psi_0^{\mathrm{QMMCC}}\rangle$ wave function, Eq. (84), represents a considerable improvement over the wave function $|\Psi_0^{\mathrm{LMMCC}}\rangle$, Eq. (81), or $|\Psi_0^{\mathrm{CCSD[T]}}\rangle$, Eq. (55), used to define the CR-CCSD[T] method, since it contains terms quadratic in Σ, in addition to the linear terms in Σ that are already present in $|\Psi_0^{\mathrm{LMMCC}}\rangle$ or $|\Psi_0^{\mathrm{CCSD[T]}}\rangle$. For the cluster operator Σ defined by Eq. (82), we obtain

$$
\begin{aligned}
|\Psi_0^{\mathrm{QMMCC}}\rangle \equiv |\Psi_0^{\mathrm{QMMCC}(2,6)}\rangle = [1 &+ T_1 + T_2 + \frac{1}{2}T_1^2 \\
&+ T_3^{[2]} + T_1T_2 + \frac{1}{2}T_2^2 + T_1T_3^{[2]} + T_2T_3^{[2]} \\
&+ \frac{1}{2}(T_3^{[2]})^2]|\Phi\rangle \ .
\end{aligned}
\tag{85}
$$

As one can see, $|\Psi_0^{\mathrm{QMMCC}}\rangle$, Eq. (85), contains singly (T_1), doubly ($T_2 + \frac{1}{2}T_1^2$), triply ($T_3^{[2]} + T_1T_2$), quadruply ($\frac{1}{2}T_2^2 + T_1T_3^{[2]}$), pentuply ($T_2T_3^{[2]}$), and hextuply ($\frac{1}{2}(T_3^{[2]})^2$) excited components that can engage all generalized moments of the CCSD equations in Eq. (80). In particular, the pentuply and hextuply excited components of $|\Psi_0^{\mathrm{QMMCC}}\rangle$ can engage the pentuply and hextuply excited moments $\mathscr{M}^{i_1i_2i_3i_4i_5}_{a_1a_2a_3a_4a_5}(2)$ and $\mathscr{M}^{i_1i_2i_3i_4i_5i_6}_{a_1a_2a_3a_4a_5a_6}(2)$, as we intended.

Equations (84) and (85) and their various approximate forms enable us to formulate the desired QMMCC corrections to the CCSD energies that improve the results of the CR-CCSD(TQ) calculations for multiple bond breaking through the presence of terms bilinear in the components of Σ. Thus, if we replace $|\Psi_0\rangle$ in the MMCC(2,6) energy formula, Eq. (80), by the wave function $|\Psi_0^{\mathrm{QMMCC}(2,6)}\rangle$, Eq. (85), we obtain the QMMCC(2,6) method. In the QMMCC(2,6) approach, which is the most complete way of correcting the CCSD results within the QMMCC formalism, we calculate the energy as follows [12, 64, 65, 66]:

$$E_0^{(\mathrm{QMMCC})}(2,6) = E_0^{(\mathrm{CCSD})} + N^{\mathrm{Q}(2,6)}/D^{\mathrm{Q}(2,6)}, \tag{86}$$

where

$$\begin{aligned} N^{\mathrm{Q}(2,6)} =& \sum_{n=3}^{6}\sum_{k=3}^{n}\langle\Psi_0^{\mathrm{QMMCC}}|C_{n-k}(2)M_k(2)|\Phi\rangle \\ =&\langle\Phi|\{[T_1^\dagger T_2^\dagger + (T_3^{[2]})^\dagger]M_3(2) \\ &+ [\frac{1}{2}(T_2^\dagger)^2 + T_1^\dagger(T_3^{[2]})^\dagger][M_4(2) + T_1M_3(2)] \\ &+ T_2^\dagger(T_3^{[2]})^\dagger[M_5(2) + T_1M_4(2) \\ &+ (T_2 + \frac{1}{2}T_1^2)M_3(2)] + \frac{1}{2}[(T_3^{[2]})^\dagger]^2[M_6(2) \\ &+ T_1M_5(2) + (T_2 + \frac{1}{2}T_1^2)M_4(2) \\ &+ (T_1T_2 + \frac{1}{6}T_1^3)M_3(2)]\}|\Phi\rangle \end{aligned} \tag{87}$$

and

$$\begin{aligned} D^{\mathrm{Q}(2,6)} =& \langle\Psi_0^{\mathrm{QMMCC}}|\mathrm{e}^{T_1+T_2}|\Phi\rangle \\ =& 1 + \langle\Phi|T_1^\dagger T_1|\Phi\rangle \\ &+ \langle\Phi|[T_2^\dagger + \frac{1}{2}(T_1^\dagger)^2](T_2 + \frac{1}{2}T_1^2)|\Phi\rangle \\ &+ \langle\Phi|[T_1^\dagger T_2^\dagger + (T_3^{[2]})^\dagger](T_1T_2 + \frac{1}{6}T_1^3)|\Phi\rangle \\ &+ \langle\Phi|[\frac{1}{2}(T_2^\dagger)^2 + T_1^\dagger(T_3^{[2]})^\dagger](\frac{1}{2}T_2^2 + \frac{1}{2}T_1^2T_2 \\ &+ \frac{1}{24}T_1^4)|\Phi\rangle + \langle\Phi|T_2^\dagger(T_3^{[2]})^\dagger(\frac{1}{2}T_1T_2^2 + \frac{1}{6}T_1^3T_2 \\ &+ \frac{1}{120}T_1^5)|\Phi\rangle + \langle\Phi|\frac{1}{2}[(T_3^{[2]})^\dagger]^2(\frac{1}{6}T_2^3 + \frac{1}{4}T_1^2T_2^2 \\ &+ \frac{1}{24}T_1^4T_2 + \frac{1}{720}T_1^6)|\Phi\rangle\ . \end{aligned} \tag{88}$$

As one can see, the QMMCC(2,6) energy expression contains essentially all terms of the CR-CCSD[T], CR-CCSD(T), and CR-CCSD(TQ),b methods (cf. Eqs. 86, 87 and 88 with Eqs. 60, 61, 62, 63, 64, 65, 66, 67 and 68), in addition to the selected higher-order terms involving the pentuply and hextuply excited $T_2^\dagger(T_3^{[2]})^\dagger$ and $\frac{1}{2}[(T_3^{[2]})^\dagger]^2$ bra components and moments $\mathscr{M}^{i_1i_2i_3i_4i_5}_{a_1a_2a_3a_4a_5}(2)$ and $\mathscr{M}^{i_1i_2i_3i_4i_5i_6}_{a_1a_2a_3a_4a_5a_6}(2)$. The presence of the $T_2^\dagger(T_3^{[2]})^\dagger$ and $\frac{1}{2}[(T_3^{[2]})^\dagger]^2$ terms in Eqs. (86), (87) and (88) [resulting from the $T_2T_3^{[2]}$ and $\frac{1}{2}(T_3^{[2]})^2$ contributions to $|\Psi_0^{\mathrm{QMMCC}(2,6)}\rangle$, Eq. 85] is absolutely essential for providing the desired improvements in the description of multiple bond breaking. As shown in Refs. [12, 64, 65, 66], these higher-order terms and a specific highly factorized many-body structure of the QMMCC(2,6) energy expression are more important than the actual presence of the pentuply and hextuply excited moments, $\mathscr{M}^{i_1i_2i_3i_4i_5}_{a_1a_2a_3a_4a_5}(2)$ and $\mathscr{M}^{i_1i_2i_3i_4i_5i_6}_{a_1a_2a_3a_4a_5a_6}(2)$, respectively, in Eqs. (86), (87) and (88).

Along with the complete QMMCC(2,6) scheme, we can also consider approximate QMMCC methods, such as QMMCC(2,5), QMMCC(2,4), and QMMCC(2,3). The QMMCC(2,5) method is obtained by neglecting the $\frac{1}{2}[(T_3^{[2]})^\dagger]^2$ terms in Eqs. (86), (87) and (88) or, simply, by replacing the wave function $|\Psi_0\rangle$ in the MMCC(2,5) energy formula, Eq. (79), by

$$\begin{aligned} |\Psi_0^{\mathrm{QMMCC}(2,5)}\rangle =& [1 + T_1 + T_2 + \frac{1}{2}T_1^2 + T_3^{[2]} + T_1T_2 \\ &+ \frac{1}{2}T_2^2 + T_1T_3^{[2]} + T_2T_3^{[2]}]|\Phi\rangle\ . \end{aligned} \tag{89}$$

As shown in a later part of this section, the apparent absence of the $\mathscr{M}^{i_1i_2i_3i_4i_5i_6}_{a_1a_2a_3a_4a_5a_6}(2)$ moments and the $\frac{1}{2}[(T_3^{[2]})^\dagger]^2$ components in the QMMCC(2,5) energy expression has almost no effect on the excellent results of the QMMCC calculations for multiple bond breaking in N_2. The QMMCC(2,4) approach is obtained by neglecting the $T_2^\dagger(T_3^{[2]})^\dagger$ terms in the QMMCC(2,6) energy formulas, Eqs. (86), (87) and (88), and the $\frac{1}{2}[(T_3^{[2]})^\dagger]^2$ terms that have already been neglected in the QMMCC(2,5) approach or, simply, by replacing the wave function $|\Psi_0\rangle$ in the MMCC(2,4) energy formula, Eq. (53), by

$$\begin{aligned} |\Psi_0^{\mathrm{QMMCC}(2,4)}\rangle =& [1 + T_1 + T_2 + \frac{1}{2}T_1^2 + T_3^{[2]} + T_1T_2 \\ &+ \frac{1}{2}T_2^2 + T_1T_3^{[2]}]|\Phi\rangle\ . \end{aligned} \tag{90}$$

In analogy to the CR-CCSD(TQ),b approach, the QMMCC(2,4) method requires that we only consider the tri- and tetraexcited moments of the CCSD equations, $\mathscr{M}^{i_1i_2i_3}_{a_1a_2a_3}(2)$ and $\mathscr{M}^{i_1i_2i_3i_4}_{a_1a_2a_3a_4}(2)$, respectively. In fact, the QMMCC(2,4) and CR-CCSD(TQ),b energy expressions and the results of the QMMCC(2,4) and CR-CCSD(TQ),b calculations are almost identical. Finally, the QMMCC(2,3) approach is obtained by ignoring the $[\frac{1}{2}(T_2^\dagger)^2 + T_1^\dagger(T_3^{[2]})^\dagger]$ terms in the QMMCC(2,4) approximation, i.e. by replacing the wave function $|\Psi_0\rangle$ in the MMCC(2,3) energy formula, Eq. (52), by

$$|\Psi_0^{\mathrm{QMMCC}(2,3)}\rangle = [1 + T_1 + T_2 + \frac{1}{2}T_1^2 + T_3^{[2]} + T_1 T_2]|\Phi\rangle \ . \qquad (91)$$

It is easy to verify that the QMMCC(2,3) and CR-CCSD[T] or CR-CCSD(T) energy formulas are practically identical. In particular, the only moments of the CCSD equations that are included in the QMMCC(2,3) calculations are the triply excited $\mathscr{M}_{a_1a_2a_3}^{i_1i_2i_3}(2)$ moments. The QMMCC(2,3) results are virtually identical to the CR-CCSD[T] or CR-CCSD(T) results. In particular, in analogy to the CR-CCSD[T] and CR-CCSD(T) approaches, the QMMCC(2,3) method is not sufficient to describe multiple bond breaking, although the QMMCC(2,3) results for single bond breaking are as good as those obtained with the CR-CCSD[T] and CR-CCSD(T) approaches. Because of the similarity of the QMMCC(2,3) and CR-CCSD[T] or CR-CCSD(T) results, we do not discuss the results of the QMMCC(2,3) calculations in this article.

The formal similarity of the QMMCC(2,4) and CR-CCSD(TQ),b approximations implies that the computer costs of the QMMCC(2,4) and CR-CCSD(TQ),b calculations are essentially identical. Thus, in analogy to the CR-CCSD(TQ),b method and its standard CCSD(TQ$_\mathrm{f}$) counterpart, the cost of calculating the QMMCC(2,4) correction to CCSD energy is $n_\mathrm{o}^2 n_\mathrm{u}^5$. The QMMCC(2,5) and QMMCC(2,6) methods are somewhat more expensive, although, as already mentioned, we can ignore the most expensive pentuply and hextuply excited moments, $\mathscr{M}_{a_1a_2a_3a_4a_5}^{i_1i_2i_3i_4i_5}(2)$ and $\mathscr{M}_{a_1a_2a_3a_4a_5a_6}^{i_1i_2i_3i_4i_5i_6}(2)$, respectively, in the QMMCC(2,5) and QMMCC(2,6) energy expressions without affecting the excellent QMMCC(2,5) and QMMCC(2,6) results. The most expensive steps of the full QMMCC(2,6) approximation, on which all other QMMCC methods are based, scale as $n_\mathrm{o}^3 n_\mathrm{u}^5$. The relatively low, n^8-like, cost of computing the noniterative QMMCC(2,6) energy correction may be somewhat surprising, since the hextuply excited moments $\mathscr{M}_{a_1a_2a_3a_4a_5a_6}^{i_1i_2i_3i_4i_5i_6}(2)$ entering Eq. (87) through $M_6(2)|\Phi\rangle$ are 12-index quantities with a few additional internal summations, but one has to recognize the highly factorized character of the QMMCC(2,6) energy corrections. For example, the most expensive $\frac{1}{2}\langle\Phi|[(T_3^{[2]})^\dagger]^2 M_6(2)|\Phi\rangle$ term of the QMMCC(2,6) approach can be rewritten as

$$\frac{1}{2}\langle\Phi|[(T_3^{[2]})^\dagger]^2 M_6(2)|\Phi\rangle = \frac{1}{48}\langle\Phi|[(T_3^{[2]})^\dagger]^2 (V_\mathrm{N} T_2^4)_\mathrm{C}|\Phi\rangle \ , \qquad (92)$$

since (cf. Eq. 27)

$$\mathscr{M}_{a_1a_2a_3a_4a_5a_6}^{i_1i_2i_3i_4i_5i_6}(2) = \frac{1}{24}\langle\Phi_{i_1i_2i_3i_4i_5i_6}^{a_1a_2a_3a_4a_5a_6}|(V_\mathrm{N} T_2^4)_\mathrm{C}|\Phi\rangle \ . \qquad (93)$$

The highly factorized character of Eq. (92), resulting from the factorization of the hextuple excitations in $|\Psi_0^{\mathrm{QMMCC}(2,6)}\rangle$, Eq. (85), into a product of two $T_3^{[2]}$ clusters, allows us to form the intermediates from the $(T_3^{[2]})^\dagger$ deexcitation and T_2 excitation cluster amplitudes by connecting the $(T_3^{[2]})^\dagger$ and T_2 diagrams with at least two fermion lines. In consequence, we do not have to construct and store the 12-index hextuply excited moments $\mathscr{M}_{a_1a_2a_3a_4a_5a_6}^{i_1i_2i_3i_4i_5i_6}(2)$ to calculate terms such as Eq. (92). This leads to a considerable reduction of the computer cost to the $n_\mathrm{o}^3 n_\mathrm{u}^5$ or less expensive noniterative steps. Similar remarks apply to the QMMCC(2,5) theory. Again, all terms entering the QMMCC(2,5) energy formula are highly factorized and we can completely eliminate the need for calculating and storing the ten-index quantities, such as $\mathscr{M}_{a_1a_2a_3a_4a_5}^{i_1i_2i_3i_4i_5}(2)$, by connecting the $T_2^\dagger$ and $(T_3^{[2]})^\dagger$ deexcitation vertices of the $T_2^\dagger(T_3^{[2]})^\dagger$ term, resulting from the presence of $T_2 T_3^{[2]}$ in $|\Psi_0^{\mathrm{QMMCC}(2,5)}\rangle$, Eq. (89), with the T_1 and T_2 excitation vertices entering $\mathscr{M}_{a_1a_2a_3a_4a_5}^{i_1i_2i_3i_4i_5}(2)$, Eq. (26), to form the relevant intermediates.

Let us illustrate the performance of the QMMCC approximations using a difficult case of triple bond breaking in N_2 as an example. The results of the QMMCC calculations for the DZ model of N_2 are shown in Table 2 and Fig. 2. As we can see, the QMMCC(2,5) and QMMCC(2,6) methods provide an excellent description of the entire $R_{\mathrm{N-N}} = 0.75R_\mathrm{e} - 2.25R_\mathrm{e}$ region of the N_2 potential energy curve. The large negative errors in the CCSD results for N_2 in the $R_{\mathrm{N-N}} > 1.75R_\mathrm{e}$ region and the 13.517-, 25.069-, and 14.796-millihartree errors in the CR-CCSD(TQ),b results at $R_{\mathrm{N-N}} = 1.75R_\mathrm{e}$, $2R_\mathrm{e}$, and $2.25R_\mathrm{e}$ are reduced by the QMMCC(2,6) method to 1.380, 6.230, and −3.440 millihartree, respectively. This is quite remarkable, considering the single-reference and noniterative character of the QMMCC energy corrections, their relatively low, $n_\mathrm{o}^3 n_\mathrm{u}^5$-like, computer cost, and the complete failure of the CCSD and other standard CC methods at larger internuclear separations. What is even more interesting is the excellent performance of the QMMCC(2,5) method, in which the $\mathscr{M}_{a_1a_2a_3a_4a_5a_6}^{i_1i_2i_3i_4i_5i_6}(2)$ moments are not considered. As shown in Table 2, the QMMCC(2,5) and QMMCC(2,6) results are essentially identical. One can, in fact, show that the QMMCC(2,5) and QMMCC(2,6) results almost do not change if we ignore the pentuply and hextuply excited moments of the CCSD equations in the QMMCC(2,5) and QMMCC(2,6) energy expressions and retain the specific many-body structure of these expressions [12, 64, 65, 66].

Interestingly enough, the QMMCC(2,5) and QMMCC(2,6) potential energy curves for N_2 are located above the full CI curve in the entire $R_{\mathrm{N-N}} < 2.25R_\mathrm{e}$ region, in spite of the apparently nonvariational behavior of the CCSD method at larger N–N separations. The approximate dissociation energies, calculated by forming the difference between the QMMCC(2,5) and QMMCC(2,6) energies at $R_{\mathrm{N-N}} = 4.35$ bohr and $R_{\mathrm{N-N}} = R_\mathrm{e} = 2.068$ bohr, are 6.61 and 6.59 eV, in excellent agreement with the full CI value of D_e of 6.61 eV [the QMMCC(2,5) and QMMCC(2,6) potentials are monotonically increasing functions of R in the entire 2.068 bohr $\leq R \leq$ 4.35 bohr region]. Thus, the QMMCC(2,5) and QMMCC(2,6) methods are the quasivariational approaches, which are capable of providing an excellent description of the large portion of the potential energy curve of N_2. The formal explanation of this quasivariational character of the QMMCC results can be found in Refs. [12, 65, 66].

As expected, the QMMCC(2,4) results for N_2 are essentially identical to those obtained with the CR-CCSD(TQ),b approach (Table 2). This finding implies that we cannot neglect the $T_2^\dagger (T_3^{[2]})^\dagger$ terms in the QMMCC(2,6) or QMMCC(2,5) energy expressions if we want to obtain an accuracy of a few millihartrees for triple bond breaking. Similar findings are true for other cases of bond breaking. For example, the errors in the QMMCC(2,5) and QMMCC(2,6) results for the double dissociation of the water molecule, where both O–H bonds are simultaneously stretched by a factor of 1.5 or 2, are on the order of 0.2–0.7 millihartree. These very small errors increase to 2–3-millihartree, when the CR-CCSD(TQ),b and QMMCC(2,4) methods are applied to a situation where both O–H bonds in water are stretched by a factor of 2 [12, 64, 66]. The 2–3-millihartree errors in the CR-CCSD(TQ),b and QMMCC(2,4) results are much smaller than the errors obtained in the standard CCSD[T], CCSD(T), and CCSD(TQ$_\mathrm{f}$) calculations, but they are considerably bigger than the 0.2–0.7-millihartree errors produced by the higher-order QMMCC(2,5) and QMMCC(2,6) calculations.

In summary, we can state that the QMMCC(2,4) approach is similar in content and computer cost to the CR-CCSD(TQ),b method discussed in Sect. 3.1. The higher-order and more complete QMMCC(2,5) and QMMCC(2,6) approximations are clearly superior compared with the CR-CCSD(TQ),b or QMMCC(2,4) approaches in studies of multiple bond breaking. Thus, the CR-CCSD(TQ),b or QMMCC(2,4) methods can be regarded as intermediate steps between the less accurate CR-CCSD[T] or CR-CCSD(T) approaches, which work well for single bond breaking, and the more accurate QMMCC(2,5) and QMMCC(2,6) approaches, which are capable of providing an accurate description of the PESs involving multiple bond stretching or breaking. The QMMCC methods provide us with a systematic way of improving the accuracy of the CR-CC calculations. This can be summarized by the following accuracy patterns that are clearly reflected in the actual calculations:

$$\begin{aligned}\text{CR-CCSD[T]} \leq &\text{CR-CCSD(T)} \approx \text{QMMCC}(2,3)\\ &<\text{CR-CCSD(TQ), b} \approx \text{QMMCC}(2,4)\\ &<\text{QMMCC}(2,5) \leq \text{QMMCC}(2,6)\\ &<\text{full CI.} \qquad (94)\end{aligned}$$

In analogy to the CR-CCSD[T], CR-CCSD(T), and CR-CCSD(TQ) methods, the QMMCC approaches can be viewed as black-box computational schemes, which are as easy to use as the standard noniterative CC approximations of the CCSD(T) or CCSD(TQ$_\mathrm{f}$) type. The QMMCC(2,5) and QMMCC(2,6) approaches are more expensive than the CR-CCSD[T], CR-CCSD(T), and CR-CCSD(TQ) methods, although the noniterative $n_\mathrm{o}^3 n_\mathrm{u}^5$ steps used to define the QMMCC(2,5) and QMMCC(2,6) energy corrections are relatively inexpensive, particularly considering the fact that one can use these methods to accurately describe multiple bond stretching or breaking. One should keep in mind that the full CCSDT approach, which is an iterative $n_\mathrm{o}^3 n_\mathrm{u}^5$ method, fails to describe bond breaking in N_2, providing results which are considerably worse than those obtained with the QMMCC(2,5) and QMMCC(2,6) approaches at all N–N separations; see Table 2 and Fig. 2. A potentially less expensive alternative to the QMMCC methods, based on combining the MMCC and ECC concepts, is described in Sect. 3.4. In the next section, we discuss the CI-corrected MMCC methods, where savings in the computer costs in studies involving single and multiple bond breaking are achieved by combining the MMCC theory with the limited CI approximations of the multireference type.

3.3 The CI-corrected MMCC methods

The MMCC theory is a flexible formalism, in which the wave function $|\Psi_0\rangle$, entering Eq. (21), (28), or (50), does not have to originate from the CC or MBPT calculations. The possibility of using the non-CC or non-MBPT wave functions $|\Psi_0\rangle$ in the MMCC equations gives us an opportunity of improving the MMCC results in all these cases where the MBPT/CC-like choices of $|\Psi_0\rangle$ defining the CR-CC and QMMCC approximations do not lead to the desired accuracies.

In the spirit of the externally corrected CC methods introduced by Paldus and coworkers [9, 20, 21, 108, 109, 110, 111, 112, 113, 205, 206, 207, 208] (see, also, Ref. [209]), we can develop a wide category of the externally corrected MMCC approximations, in which the wave functions $|\Psi_0\rangle$ entering the MMCC($m_\mathrm{A}, m_\mathrm{B}$) energy expressions, Eqs. (49) and (50), are obtained in some relatively inexpensive ab initio calculations that are not related to a CC calculation whose results we are trying to improve with the MMCC($m_\mathrm{A}, m_\mathrm{B}$) correction $\delta_0(m_\mathrm{A}, m_\mathrm{B})$. We can, for example, consider the MMCC($m_\mathrm{A}, m_\mathrm{B}$) methods, in which the wave function $|\Psi_0\rangle$ entering Eqs. (49) and (50) is obtained in relatively inexpensive limited CI calculations. All externally corrected MMCC approximations, in which the wave function $|\Psi_0\rangle$ is a limited CI wave function of the single-reference or multireference type, are referred to as the CI-corrected MMCC (MMCC/CI) approaches. We can also contemplate the CASSCF- or CASPT2-corrected MMCC($m_\mathrm{A}, m_\mathrm{B}$) approaches, in which the wave function $|\Psi_0\rangle$ entering Eqs. (49) and (50) is obtained in CASSCF or CASPT2 calculations (P. Piecuch, K. Kowalski, M. Lodriguito, unpublished results).

The CI-corrected MMCC methods were originally proposed and tested in Ref. [55]. They were further developed and extended to excited electronic states in Refs. [12, 62, 72, 73]. A few types of the CI-corrected MMCC methods, limited to the ground-state problem, based on the general recipes described earlier in Refs. [55, 56], have recently been implemented by Li and Paldus [156, 157, 158] (somewhat unfortunately, under a different name of the "energy-corrected CC approaches"). In this section, we discuss the CI-corrected MMCC methods for ground electronic states. The CI-corrected MMCC approaches for excited states are discussed in Sect. 4.2.

A variety of limited CI techniques could be used to generate $|\Psi_0\rangle$ in the MMCC($m_{\mathrm{A}}, m_{\mathrm{B}}$) energy expressions. Because of our interest in the bond breaking problem, in this section we focus on a few simple choices of $|\Psi_0\rangle$ resulting from performing the multireference-like, but really single-reference, CI calculations that guarantee the qualitatively correct description of bond breaking. We might, of course, use the traditional MRCI approaches to generate $|\Psi_0\rangle$. The problem with this is that MRCI calculations are usually a lot more expensive than the CC calculations we are trying to improve. Thus, in the following, we focus on the idea of defining $|\Psi_0\rangle$ via the so-called active-space CI methods [55], in which we use the concept of active orbitals, originating from the multireference formalism, to select the dominant higher–than–doubly excited components of the single-reference CI wave function.

Our main interest is in improving poor CCSD results in the bond breaking region by adding the MMCC(2,3), MMCC(2,4), MMCC(2,5), and MMCC(2,6) corrections to the CCSD energies, as described by Eqs. (52), (53), (79), and (80), respectively. In order to define the corresponding wave functions $|\Psi_0\rangle$ that can be used to determine the MMCC(2,3), MMCC(2,4), MMCC(2,5), and MMCC(2,6) energies and that guarantee the qualitatively correct description of bond breaking, we divide the available spin-orbitals into four groups (Fig. 6) of core spin-orbitals ($\mathbf{i}_1$, $\mathbf{i}_2$, ...), active spin-orbitals occupied in reference $|\Phi\rangle$ ($\mathbf{I}_1$, $\mathbf{I}_2$, ...), active spin-orbitals unoccupied in reference $|\Phi\rangle$ ($\mathbf{A}_1$, $\mathbf{A}_2$, ...), and virtual spin-orbitals ($\mathbf{a}_1$, $\mathbf{a}_2$, ...). The choice of active spin-orbitals (typically, a few highest-energy occupied spin-orbitals and a few lowest-energy unoccupied spin-orbitals) is dictated by the type of bond breaking (single, double, etc.) that we are trying to describe. For example, the qualitatively correct description of single bond breaking in the HF molecule is obtained if the 3σ, 1π, and 2π occupied and 4σ unoccupied orbitals, correlating with the $1s$ and $2p$ shells of the H and F atoms, respectively, are chosen as active orbitals. The qualitatively correct description of triple bond breaking in N_2 requires the presence of the $3\sigma_g$, $1\pi_{\mathrm{u}}$, $2\pi_{\mathrm{u}}$, $1\pi_g$, $2\pi_g$, and $3\sigma_{\mathrm{u}}$ orbitals, correlating with the $2p$ shells of the N atoms, in the active orbital space, etc.

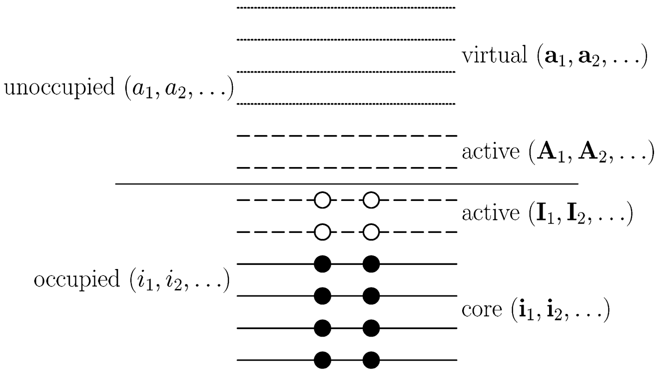

Fig. 6. The orbital classification used in the active-space CI and the CI-corrected MMCC(2,3), MMCC(2,4), MMCC(2,5), and MMCC(2,6) approaches discussed in this article. Core, active, and virtual orbitals are represented by *solid*, *dashed*, and *dotted lines*, respectively. *Full* and *open circles* represent core and active electrons of the reference configuration $|\Phi\rangle$ (the closed-shell reference is assumed)

Once active spin-orbitals are selected, we can define the following CI wave functions $|\Psi_0\rangle$ for the CI-corrected MMCC(2,3), MMCC(2,4), MMCC(2,5), and MMCC(2,6) calculations:

$$|\Psi_0^{\mathrm{CISDt}}\rangle = (C_0 + C_1 + C_2 + c_3)|\Phi\rangle \ , \tag{95}$$

$$|\Psi_0^{\mathrm{CISDtq}}\rangle = (C_0 + C_1 + C_2 + c_3 + c_4)|\Phi\rangle \ , \tag{96}$$

$$|\Psi_0^{\mathrm{CISDtqp}}\rangle = (C_0 + C_1 + C_2 + c_3 + c_4 + c_5)|\Phi\rangle \ , \tag{97}$$

$$|\Psi_0^{\mathrm{CISDtqph}}\rangle = (C_0 + C_1 + C_2 + c_3 + c_4 + c_5 + c_6)|\Phi\rangle \ , \tag{98}$$

where $C_0|\Phi\rangle$, $C_1|\Phi\rangle$, and $C_2|\Phi\rangle$ are the usual reference, singly excited, and doubly excited contributions, respectively, and

$$c_3|\Phi\rangle = \sum_{\substack{i_1<i_2<\mathbf{I}_3 \\ a_1>a_2>\mathbf{A}_3}} c_{a_1 a_2 \mathbf{A}_3}^{i_1 i_2 \mathbf{I}_3} E_{i_1 i_2 \mathbf{I}_3}^{a_1 a_2 \mathbf{A}_3} \ , \tag{99}$$

$$c_4|\Phi\rangle = \sum_{\substack{i_1<i_2<\mathbf{I}_3<\mathbf{I}_4 \\ a_1>a_2>\mathbf{A}_3>\mathbf{A}_4}} c_{a_1 a_2 \mathbf{A}_3 \mathbf{A}_4}^{i_1 i_2 \mathbf{I}_3 \mathbf{I}_4} E_{i_1 i_2 \mathbf{I}_3 \mathbf{I}_4}^{a_1 a_2 \mathbf{A}_3 \mathbf{A}_4} \ , \tag{100}$$

$$c_5|\Phi\rangle = \sum_{\substack{i_1<i_2<\mathbf{I}_3<\mathbf{I}_4<\mathbf{I}_5 \\ a_1>a_2>\mathbf{A}_3>\mathbf{A}_4>\mathbf{A}_5}} c_{a_1 a_2 \mathbf{A}_3 \mathbf{A}_4 \mathbf{A}_5}^{i_1 i_2 \mathbf{I}_3 \mathbf{I}_4 \mathbf{I}_5} E_{i_1 i_2 \mathbf{I}_3 \mathbf{I}_4 \mathbf{I}_5}^{a_1 a_2 \mathbf{A}_3 \mathbf{A}_4 \mathbf{A}_5} \ , \tag{101}$$

and

$$c_6|\Phi\rangle = \sum_{\substack{i_1<i_2<\mathbf{I}_3<\mathbf{I}_4<\mathbf{I}_5<\mathbf{I}_6 \\ a_1>a_2>\mathbf{A}_3>\mathbf{A}_4>\mathbf{A}_5>\mathbf{A}_6}} c_{a_1 a_2 \mathbf{A}_3 \mathbf{A}_4 \mathbf{A}_5 \mathbf{A}_6}^{i_1 i_2 \mathbf{I}_3 \mathbf{I}_4 \mathbf{I}_5 \mathbf{I}_6} E_{i_1 i_2 \mathbf{I}_3 \mathbf{I}_4 \mathbf{I}_5 \mathbf{I}_6}^{a_1 a_2 \mathbf{A}_3 \mathbf{A}_4 \mathbf{A}_5 \mathbf{A}_6} \tag{102}$$

are the excitation operators generating the relevant higher–than–doubly excited components of $|\Psi_0^{\mathrm{CISDt}}\rangle$, $|\Psi_0^{\mathrm{CISDtq}}\rangle$, $|\Psi_0^{\mathrm{CISDtqp}}\rangle$, and $|\Psi_0^{\mathrm{CISDtqph}}\rangle$. As one can see, the CISDt wave function $|\Psi_0^{\mathrm{CISDt}}\rangle$, Eq. (95), used in the CI-corrected MMCC(2,3) [MMCC(2,3)/CI] calculations, includes all singles and doubles from the reference configuration $|\Phi\rangle$ and a relatively small set of internal and semiinternal triples containing at least one active occupied and one active unoccupied spin-orbital indices (cf. Eq. 99). The CISDtq wave function $|\Psi_0^{\mathrm{CISDtq}}\rangle$, Eq. (96), used in the CI-corrected MMCC(2,4) [MMCC(2,4)/CI] calculations, includes all singles and doubles from $|\Phi\rangle$, a relatively small set of internal and semiinternal triples containing at least one active occupied and one active unoccupied spin-orbital indicies and a relatively small set of quadruples containing at least two active occupied and two active unoccupied spin-orbital indices (cf. Eqs. 99, 100). The

CISDtqp wave function $|\Psi_0^{\text{CISDtqp}}\rangle$, Eq. (97), used in the CI-corrected MMCC(2,5) [MMCC(2,5)/CI] calculations includes a relatively small set of internal and semiinternal pentuples, defined by Eq. (101), in addition to singles, doubles, triples, and quadruples included in $|\Psi_0^{\text{CISDtq}}\rangle$, Eq. (96). Finally, the CISDtqph wave function $|\Psi_0^{\text{CISDtqph}}\rangle$, Eq. (98), used in the CI-corrected MMCC(2,6) [MMCC(2,6)/CI] calculations includes a relatively small set of internal and semiinternal pentuples and hextuples, defined by Eqs. (101) and (102), respectively, in addition to singles, doubles, triples, and quadruples included in $|\Psi_0^{\text{CISDtq}}\rangle$, Eq. (96). The CI coefficients defining the CISDt, CISDtq, CISDtqp, and CISDtqph wave functions are determined variationally. It is worth mentioning that this selection of higher–than–doubly excited determinants in the CISDt, CISDtq, CISDtqp, and CISDtqph wave functions is analogous to the selection of higher–than–doubly excited cluster amplitudes in the highly successful active-space CC or state-selective MRCC methods developed by Adomowicz, Piecuch, Oliphant, and their coworkers [51, 53, 54, 58, 69, 70, 71, 95, 96, 97, 98, 99, 100, 101, 102, 103, 104].

Although the CI-corrected MMCC methods are not as easy to use as the CR-CC and QMMCC approaches, since one has to define active orbitals to select higher–than–doubly excited components of $|\Psi_0\rangle$, they offer several advantages that can be very useful in calculations of molecular PESs involving bond breaking. One of the main advantages of the CI-corrected MMCC schemes is a very good control of the quality of the wave function $|\Psi_0\rangle$, used to construct the noniterative corrections $\delta_0(m_{\text{A}}, m_{\text{B}})$, which is accomplished through the judicious choice of active orbitals that can always be adjusted to a given type of bond breaking. Another advantage of the CI-corrected MMCC methods is their relatively low computer cost, which is a consequence of the fact that it is usually sufficient to use very small active orbital spaces to obtain an accurate description of bond breaking. The relatively low cost of the CI-corrected MMCC calculations is illustrated here by using the CI-corrected MMCC(2,3) approach as an example. In this case, we use the CISDt wave function $|\Psi_0^{\text{CISDt}}\rangle$, Eq. (95), to construct the MMCC(2,3) correction $\delta_0(2,3)$ to the CCSD energy. By replacing the wave function $|\Psi_0\rangle$ in the general MMCC(2,3) formula, Eq. (52), by $|\Psi_0^{\text{CISDt}}\rangle$, we obtain the following expression for the MMCC(2,3)/CI energy:

$$E_0^{(\text{MMCC/CI})}(2,3) = E_0^{(\text{CCSD})} + \sum_{\substack{i_1<i_2<\mathbf{I}_3 \\ a_1>a_2>\mathbf{A}_3}} c_{a_1 a_2 \mathbf{A}_3}^{i_1 i_2 \mathbf{I}_3} \mathscr{M}_{a_1 a_2 \mathbf{A}_3}^{i_1 i_2 \mathbf{I}_3}(2) / \langle \Psi_0^{\text{CISDt}} | \mathrm{e}^{T_1+T_2} | \Phi \rangle, \tag{103}$$

where $c_{a_1 a_2 \mathbf{A}_3}^{i_1 i_2 \mathbf{I}_3}$ are the CI coefficients obtained in the CISDt calculations, $\mathscr{M}_{a_1 a_2 \mathbf{A}_3}^{i_1 i_2 \mathbf{I}_3}(2)$ are the triexcited moments of the CCSD equations defined by Eq. (24), and T_1 and T_2 are the singly and doubly excited cluster components obtained in the CCSD calculations. As one can see, we do not have to determine the entire set of the triexcited moments $\mathscr{M}_{a_1 a_2 a_3}^{i_1 i_2 i_3}(2)$ in the MMCC(2,3)/CI calculations. This alone leads to considerable savings in the computer effort. Indeed, if N_{o} (N_{u}) is the number of active orbitals occupied (unoccupied) in $|\Phi\rangle$, we only have to construct $N_{\text{o}} N_{\text{u}} n_{\text{o}}^2 n_{\text{u}}^2$ moments $\mathscr{M}_{a_1 a_2 \mathbf{A}_3}^{i_1 i_2 \mathbf{I}_3}(2)$, which is a small fraction of all $n_{\text{o}}^3 n_{\text{u}}^3$ moments $\mathscr{M}_{a_1 a_2 a_3}^{i_1 i_2 i_3}(2)$ when $N_{\text{o}} \ll n_{\text{o}}$ and $N_{\text{u}} \ll n_{\text{u}}$. Moreover, the $n_{\text{o}}^3 n_{\text{u}}^4$ steps related to the construction of all moments $\mathscr{M}_{a_1 a_2 a_3}^{i_1 i_2 i_3}(2)$ reduce to the n^5-like $N_{\text{o}} N_{\text{u}} n_{\text{o}}^2 n_{\text{u}}^3$ steps in the MMCC(2,3)/CI calculations. There is an additional cost related to the CISDt calculations, needed to generate the $|\Psi_0^{\text{CISDt}}\rangle$ wave function, but again the usual $n_{\text{o}}^3 n_{\text{u}}^5$ steps of the parent CI singles, doubles, and triples (CISDT) approach reduce to considerably less expensive $N_{\text{o}} N_{\text{u}} n_{\text{o}}^2 n_{\text{u}}^4$ steps in the CISDt case. All these factors contribute to the relatively low cost of the MMCC(2,3)/CI calculations. The number of triples used in the CI-corrected MMCC(2,3) calculations is usually very small (no more than 30% of all triples; sometimes even less than that [12, 62, 72, 73]). The CPU times required to construct the relevant corrections $\delta_0(2,3)$ to CCSD energies are often on the order of the CPU time of a single CCSD iteration [12, 62, 72, 73]. The CI-corrected MMCC(2,4), MMCC(2,5), and MMCC(2,6) calculations are obviously more expensive, but again a considerable reduction in the computer effort is observed when the MMCC(2,4)/CI, MMCC(2,5)/CI, and MMCC(2,6)/CI methods are used in practice. It is also worth mentioning that the CI-corrected MMCC methods can be generalized to excited states in a rather straightforward fashion via the EOMCC formalism (see Sect. 4.2), which is another advantage of the CI-corrected MMCC approaches.

Our experience to date indicates that it is sufficient to use the simplest MMCC(2,3)/CI approach in studies of PESs involving single bond breaking [12, 55, 62, 72]. This is illustrated in Table 1, where we examine the MMCC/CI results for single bond breaking in the HF molecule, as described by the DZ basis set. As one can see, the MMCC(2,3)/CI approach, employing a very small active space consisting of only four valence orbitals of HF and the ground-state RHF determinant as a reference, reduces the 12 and 24–53-millihartree unsigned errors in the CCSD and CCSD(T) results in the $R_{\text{H-F}} = 3R_{\text{e}} - 5R_{\text{e}}$ region to 3–4 millihartree. The CISDt approach, on which the MMCC(2,3)/CI method is based, produces much larger errors (29–34 millihartree). In analogy to the CR-CCSD[T] and CR-CCSD(T) approaches, which are also based on the MMCC(2,3) approximation, the MMCC(2,3)/CI method eliminates the well-pronounced humps on the CCSD[T] and CCSD(T) potential energy curves. Thus, the MMCC(2,3)/CI method combines two relatively poor pieces of information (the T_1 and T_2 cluster components obtained in the CCSD calculations and the CISDt wave function) to produce an excellent description of the entire potential energy curve of HF. The MMCC(2,4)/CI approach provides some improvements in the MMCC(2,3)/CI results, but these improvements are not particularly impressive, particularly considering the fact that the MMCC(2,4)/CI calculations are more expensive than the MMCC(2,3)/CI calculations. This seems to be the case in other cases of single bond breaking. The CI-corrected MMCC(2,4) approach becomes more important when double bond dissociation is examined, providing a more balanced description of the ground-state potential energy curves in the region of stretched nuclear geometries [12, 62], but neither the MMCC(2,3)/CI theory nor its MMCC(2,4)/CI extension is sufficient when more complicated types of multiple bond breaking are examined. This is shown in Table 2 (see, also, Fig. 2), where we examine the results of the MMCC/CI calculations for a challenging case of triple bond breaking in N_2.

As demonstrated in Table 2, the MMCC(2,4)/CI method works well for the N–N separations $R_{\mathrm{N-N}}$ not exceeding $1.75R_{\mathrm{e}}$, but the MMCC(2,4)/CI results for $R_{\mathrm{N-N}} > 1.75R_{\mathrm{e}}$ are not good (we do not show the MMCC(2,3)/CI results, since they are even worse than those obtained with the MMCC(2,4)/CI approach in the $R_{\mathrm{N-N}} > 1.75R_{\mathrm{e}}$ region). In particular, the MMCC(2,4)/CI method suffers from the nonvariational collapse in the $R_{\mathrm{N-N}} > 1.75R_{\mathrm{e}}$ region, similar to that characterizing the CCSD and CCSD(T) approximations, although the MMCC(2,4)/CI results for $R_{\mathrm{N-N}} > 1.75R_{\mathrm{e}}$, characterized by the unsigned errors of 16–31 millihartree, are a lot better than the results of the CCSD, CCSDT, CCSD(T), CCSD(TQ$_{\mathrm{f}}$), and CCSDT(Q$_{\mathrm{f}}$) calculations, which give huge errors on the order of 100 millihartree at larger N–N distances. The CR-CCSD(TQ),b and QMMCC(2,4) methods discussed in the earlier sections, which are also based on the MMCC(2,4) approximation, seem to provide a more balanced description of the potential energy curve of N_2 when compared with the MMCC(2,4)/CI approach.

On the basis of our positive experience with the QMMCC(2,5) method, which we discussed in Sect. 3.2 and which is based on the MMCC(2,5) approximation, one might expect that the CI-corrected MMCC(2,5) approach should provide a good description of the $R_{\mathrm{N-N}} > 1.75R_{\mathrm{e}}$ region of the potential-energy curve of N_2. Apparently, this is not the case. The MMCC(2,5)/CI results are considerably better than the MMCC(2,4)/CI results in the $R_{\mathrm{N-N}} \leq 1.75R_{\mathrm{e}}$ region, but there is practically no difference in the performance of the MMCC(2,4)/CI and MMCC(2,5)/CI approximations for $R_{\mathrm{N-N}} > 1.75R_{\mathrm{e}}$. This shows that the CI-corrected MMCC methods are less effective than the QMMCC approaches in bringing the higher-order terms required to improve the description of multiple bond breaking.

The failure of the MMCC(2,4)/CI and MMCC(2,5)/CI theories at larger internuclear separations in N_2 shows that one cannot ignore the pentuply and hextuply excited components in the wave function $|\Psi_0\rangle$ and the corresponding moments $\mathscr{M}^{i_1i_2\mathbf{I}_3\mathbf{I}_4\mathbf{I}_5}_{a_1a_2\mathbf{A}_3\mathbf{A}_4\mathbf{A}_5}(2)$ and $\mathscr{M}^{i_1i_2\mathbf{I}_3\mathbf{I}_4\mathbf{I}_5\mathbf{I}_6}_{a_1a_2\mathbf{A}_3\mathbf{A}_4\mathbf{A}_5\mathbf{A}_6}(2)$, if we are interested in a highly accurate description of multiple bond breaking. This behavior of the MMCC/CI methods is in sharp contrast with the behavior of the QMMCC approximations discussed in the previous section, which can provide errors of a few millihartrees in the entire $R_{\mathrm{N-N}} = 0.75R_{\mathrm{e}} - 2.25R_{\mathrm{e}}$ region of the N_2 PES. On the other hand, once the pentuply and hextuply excited components in the wave function $|\Psi_0\rangle$ and the corresponding moments $\mathscr{M}^{i_1i_2\mathbf{I}_3\mathbf{I}_4\mathbf{I}_5}_{a_1a_2\mathbf{A}_3\mathbf{A}_4\mathbf{A}_5}(2)$ and $\mathscr{M}^{i_1i_2\mathbf{I}_3\mathbf{I}_4\mathbf{I}_5\mathbf{I}_6}_{a_1a_2\mathbf{A}_3\mathbf{A}_4\mathbf{A}_5\mathbf{A}_6}(2)$ are included in the CI-corrected MMCC calculations, the description of the entire potential energy curve of N_2 becomes extremely good. As shown in Table 2 and Fig. 2, the MMCC(2,6)/CI approach reduces the huge errors, on the order of 100 millihartree, in the results of the CCSD, CCSDT, CCSD(T), CCSD(TQ$_{\mathrm{f}}$), and similar calculations at larger N–N distances to 4.443 millihartree at $R_{\mathrm{N-N}} = 2R_{\mathrm{e}}$ and 4.552 millihartree at $R_{\mathrm{N-N}} = 2.25R_{\mathrm{e}}$. The dissociation energy D_{e}, obtained by forming the difference of the MMCC(2,6)/CI energies at $R = 2.25R_{\mathrm{e}}$ and $R = R_{\mathrm{e}}$, is 6.68 eV, in very good agreement with the full CI D_{e} value of 6.61 eV. The small, 1–5-millihartree, errors in the MMCC(2,6)/CI description of the entire potentialenergy curve of N_2, which are obtained with the generalized moments of the failing CCSD method, clearly show that the MMCC theory is a robust formalism which can be applied to single as well as multiple bond breaking. Although QMMCC methods are more effective in bringing higher-order effects, required to describe multiple bond breaking, at the lower level of theory, when compared with the CI-corrected MMCC approaches, the overall description of the potential energy curve of N_2 by the MMCC(2,6)/CI method is better than the description of the same curve by all QMMCC approximations. The small unsigned errors in the MMCC(2,6)/CI and QMMCC(2,6) results, on the order of a few millihartrees, in the region of large N–N separations are almost identical, but the MMCC(2,6)/CI potential energy curve is located above the full CI curve for all $R_{\mathrm{N-N}}$ values, whereas the QMMCC(2,6) approach suffers from a minor nonvariational collapse in the $R_{\mathrm{N-N}} > 2R_{\mathrm{e}}$ region. This means that we can always improve the CR-CC and QMMCC results for difficult cases of bond breaking, where none of the simpler MMCC methods work, by performing the CI-corrected MMCC calculations, using the MMCC(2,6)/CI and similar approaches.

As mentioned earlier, the CI-corrected MMCC methods are useful in describing ground as well as excited states. Before discussing the performance of the MMCC methods in excited-state calculations (see Sect. 4), we address another important issue: Can one improve the results of the MMCC calculations in the bond breaking region by improving the quality of the T_1 and T_2 cluster components?

3.4 The MMCC methods employing the ECC theory

Until now, our discussion of the MMCC approaches has focused on improving the results of the standard CCSD calculations by adding one of the approximate forms of the noniterative correction $\delta_0^{(\mathrm{CCSD})}$, Eq. (28), to the CCSD energy. In constructing the relevant MMCC corrections to the CCSD energies, we used the CCSD values of the T_1 and T_2 cluster components, obtained with the symmetry-adapted RHF or ROHF references, which are usually very poor in the bond breaking region, particularly when multiple bond breaking is involved. As shown in Sects. 3.1, 3.2, and 3.3, the MMCC formalism allows us to considerably improve the results of the standard CC calculations, even when poor CCSD values of the T_1 and T_2 cluster amplitudes are used in constructing corrections $\delta_0^{(\mathrm{CCSD})}$, but an interesting question arises if we could improve the MMCC results further or with a smaller computational effort by using better T_1 and T_2 cluster amplitudes, obtained, for example, in some nonstandard CCSD-like (but not CCSD) calculations. The bond breaking case, which is particularly challenging for the single-reference CC and MMCC methods and which should help us to address the question, is the case of triple bond breaking in N_2.

We have already demonstrated that we can obtain a very accurate description of the potential energy curve for N_2, if we use the more expensive MMCC schemes, such as QMMCC(2,5), QMMCC(2,6), or MMCC(2,6)/CI. We have shown that the MMCC(2,6)/CI results, employing the pentuply and hextuply excited moments of the CCSD equations, are particularly impressive, although we must not forget that we had to perform additional multireference-like CI calculations to obtain these excellent results. From the practical point of view, one would prefer to use the lower-order MMCC approaches of the CR-CCSD(TQ),b or QMMCC(2,4) type, since they do not require any additional non-CC calculations to construct the relevant corrections $\delta_0^{(\mathrm{CCSD})}$ and since they only use the triply and quadruply excited moments of the CCSD equations, thereby reducing the costs of calculating the $\delta_0^{(\mathrm{CCSD})}$ corrections to the manageable $n_o^2 n_u^5$ steps. Unfortunately, as shown in Table 2 and Fig. 2, the accuracy of the CR-CCSD(TQ),b or QMMCC(2,4) calculations for the DZ model of N_2, which give errors on the order of 11–25 millihartree in the $R_{\mathrm{N-N}} > 1.75 R_e$ region, and the presence of small humps on the CR-CCSD(TQ),b and QMMCC(2,4) potential energy curves make the CR-CCSD(TQ),b and QMMCC(2,4) methods hardly usable in quantitative studies of triple bond dissociation.

Undoubtedly, the main problem that the MMCC methods face, when dealing with complicated cases of multiple bond breaking, is the very low quality of the T_1 and T_2 cluster amplitudes used to construct the noniterative MMCC corrections. The low quality of the T_1 and T_2 cluster components resulting from the standard CCSD calculations can be seen by looking at the CCSD potential energy curve shown in Fig. 2 or at the larger portion of the CCSD potential energy curve, obtained with the STO-3G basis set [210], shown in Fig. 7 (see Table 3 for the corresponding numerical data). As one can see, the collapse of the CCSD theory at larger internuclear separations, with unsigned errors in the CCSD results exceeding 200 millihartree in the $R_{\mathrm{N-N}} \geq 5.0$-bohr region, is really severe. As shown in Refs. [64, 65], the quality of the CCSD wave function, as measured by forming overlaps of the normalized CCSD and full CI states at various values of $R_{\mathrm{N-N}}$, and the quality of the corresponding T_1 and T_2 components dramatically deteriorate in the bond breaking region. In consequence, the lower-order MMCC methods, such as CR-CCSD(TQ),b, eventually break down when multiple bonds are broken (Fig. 7, Table 3; see, also, Sects. 3.1, 3.2).

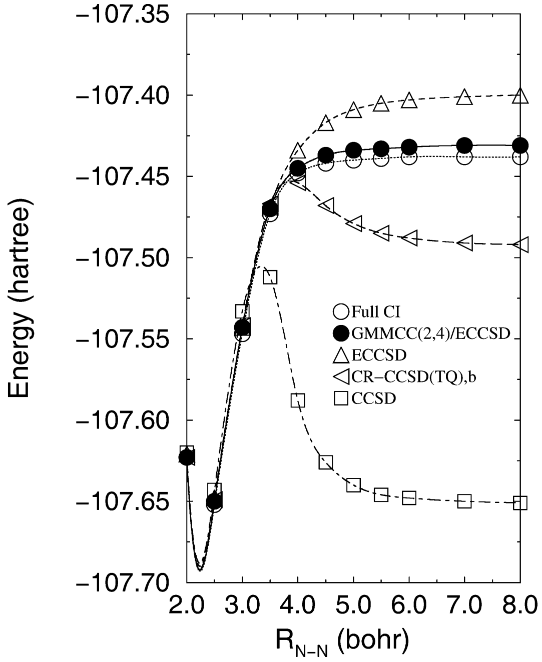

Fig. 7. Ground-state potential-energy curves of the N_2 molecule, as described by the STO-3G basis set (see the text for the remaining details and Refs. [64, 65] for the original data)

We can think of several ways of improving the quality of the T_1 and T_2 clusters that may help the MMCC results in complicated cases of multiple bond breaking. For example, instead of solving the standard CCSD equations, Eqs. (11) and (12), we could minimize the expectation value of the Hamiltonian with the CCSD wave function, i.e.,

$$E_0^{(\mathrm{VCC})}(T_1, T_2) = \langle\Phi|e^{T_1^\dagger + T_2^\dagger} H e^{T_1+T_2}|\Phi\rangle / \langle\Phi|e^{T_1^\dagger + T_2^\dagger} e^{T_1+T_2}|\Phi\rangle \;, \qquad (104)$$

with respect to cluster amplitudes $t_{a_1}^{i_1}$ and $t_{a_1 a_2}^{i_1 i_2}$ defining T_1 and T_2. This would enable us to obtain the variationally best T_1 and T_2 operators, which might be better for the MMCC calculations, while eliminating the apparently nonvariational behavior of the standard CCSD method at larger internuclear separations of multiply bonded systems [138, 211]. Unfortunately, it is very difficult to propose an efficient algorithm for calculating the energy expressions of the type of Eq. (104), since the expectation value of the Hamiltonian with a CC wave function represents a nonterminating series in cluster components [4]. A different approach is called for if we wish to improve the quality of T_1 and T_2 clusters for MMCC calculations at the relatively low level of theory that uses only one- and two-body cluster components.

We have recently demonstrated [64, 65] that one can obtain reasonably good T_1 and T_2 cluster amplitudes, in a computationally tractable fashion, which may be very well suited for studies of multiple bond breaking, i.e., without resorting to the nonterminating series in cluster components resulting from Eq. (104), by switching to

Table 3. A comparison of the CCSD, ECCSD, CR-CCSD(TQ),b, GMMCC(2,4)/ECCSD, and GMMCC(2,4)/BECCSD ground-state energies with the corresponding full CI results obtained for several internuclear separations $R_{\mathrm{N-N}}$ of the N_2 molecule with the STO-3G basis set [210]. The full CI total energies are in hartrees. The remaining energies are in millihartrees relative to the corresponding full CI energy values. The lowest two occupied orbitals were frozen in correlated calculations

$R_{\mathrm{N-N}}$[a]	Full CI[b]	CCSD[b]	ECCSD[b,c]	$M_0(2)$/ECCSD[d]	CR-CCSD(TQ),b[e]	GMMCC(2,4)/ ECCSD[f]	GMMCC(2,4)/ BECCSD[g]
1.0	−101.791600	0.319	0.298	0.278	0.062	0.061	0.061
1.5	−106.720117	1.102	0.885	0.666	0.202	0.195	0.195
2.0	−107.623240	3.295	1.897	0.443	0.687	0.613	0.626
2.5	−107.651880	9.220	3.427	−2.853	2.497	1.970	1.971
3.0	−107.546614	13.176	3.758	−6.778	4.483	3.490	3.490
3.5	−107.473442	−38.645	4.476	14.930	6.168	3.126	3.074
4.0	−107.447822	−140.376	14.117	63.870	−5.820	3.356	2.141
4.5	−107.441504	−184.984	24.039	109.058	−26.557	4.870	1.190
5.0	−107.439549	−200.857	30.390	138.799	−39.221	5.543	0.190
5.5	−107.438665	−206.974	33.867	157.333	−46.162	6.164	−0.535
6.0	−107.438265	−209.538	35.746	167.731	−49.962	6.450	−0.932
7.0	−107.438054	−211.915	37.306	176.197	−53.158	6.649	−1.166
8.0	−107.438029	−213.431	37.799	178.312	−54.336	6.675	−1.117

[a] The N–N separation in bohr. The equilibrium value of $R_{\mathrm{N-N}}$ is 2.068 bohr

[b] From Ref. [64]

[c] Based on the ECCSD formalism of Ref. [31]

[d] The zero-body moment or the CCSD-like energy expression, Eq. (31), calculated using the ECCSD rather than CCSD values of T_1 and T_2, obtained with the ECCSD theory of Ref. [31]

[e] Equivalent to the GMMCC(2,4) energy, Eq. (54), calculated with the CCSD values of T_1 and T_2 and $|\Psi_0\rangle$ defined by Eq. (59)

[f] The GMMCC(2,4) energy, Eq. (54), calculated with the ECCSD values of T_1 and T_2 and $|\Psi_0\rangle$ defined by Eq. (59). The T_1 and T_2 clusters were obtained with the ECCSD theory of Ref. [31]

[g] The GMMCC(2,4) energy, Eq. (54), calculated with the BECCSD values of T_1 and T_2 and $|\Psi_0\rangle$ defined by Eq. (59). The T_1 and T_2 clusters were obtained with the bilinear approximation to the ECCSD theory of Ref. [31], termed BECCSD, introduced in Ref. [64] (cf. Eq. (113))

the ECCSD method or one of its approximate variants based on the ECC theory [31, 145, 146, 147, 148, 149, 150, 151, 152, 153, 154]. Similar findings have been reported by Head-Gordon and coworkers [137, 138, 143, 144]. It is, therefore, interesting to examine if the low-order MMCC corrections of the CR-CCSD(TQ),b type can provide an accurate description of multiple bond breaking (e.g., triple bond breaking in N_2), when the CCSD values of T_1 and T_2 cluster amplitudes are replaced by the ECCSD values. As explained in Sects. 2.1 and 3, the MMCC formalism can be generalized to a situation where the cluster components that are used to calculate the MMCC energy corrections are not obtained by solving the standard CC equations (cf., e.g., Eqs. 30, 32, 51, and 54).

The detailed description of the ECC theory can be found in Refs. [31, 145, 146, 147, 148, 149, 150, 151, 152, 153, 154]. Additional information about the ECC methods, including the ECCSD approaches that can be used to study multiple bond breaking, can be found in Refs. [64, 65, 137, 138, 143, 144]. In the following, we restrict ourselves to the most essential information, focusing on the basic ECCSD method. Just like the standard CCSD theory, the ECCSD approach uses only one and two-body cluster components. The fundamental difference between the standard CCSD method or other CC approximations and the ECC formalism is the use of two independent sets of cluster amplitudes in the ECC calculations. Thus, in addition to the cluster operator T, used in the standard CC methods, we introduce the auxiliary cluster operator Σ. In the ECCSD case, T is approximated by singly and doubly excited components, T_1 and T_2, respectively (cf., e.g., Eqs. 4, 5, 6), and a similar truncation scheme is applied to Σ, i.e.,

$$\Sigma \approx \Sigma^{(\mathrm{CCSD})} = \Sigma_1 + \Sigma_2 \ , \tag{105}$$

where

$$\Sigma_1 = \sum_{\substack{i_1\\a_1}} \sigma^{i_1}_{a_1} E^{a_1}_{i_1} \tag{106}$$

and

$$\Sigma_2 = \sum_{\substack{i_1<i_2\\a_1<a_2}} \sigma^{i_1 i_2}_{a_1 a_2} E^{a_1 a_2}_{i_1 i_2} \ , \tag{107}$$

with $\sigma^{i_1}_{a_1}$ and $\sigma^{i_1 i_2}_{a_1 a_2}$ representing the corresponding amplitudes. The T and Σ operators, or the amplitudes that define them, are optimized by considering the asymmetric, doubly connected, energy functional [31, 145, 146, 147, 148, 149, 150, 151, 152, 153, 154]

$$\begin{aligned} E_0^{(\mathrm{ECC})}(\Sigma, T) &= \langle \Phi | \mathrm{e}^{\Sigma^\dagger} \mathrm{e}^{-T} H \mathrm{e}^{T} | \Phi \rangle = \langle \Phi | \mathrm{e}^{\Sigma^\dagger} \bar{H} \mathrm{e}^{-\Sigma^\dagger} | \Phi \rangle \\ &= \langle \Phi | [\mathrm{e}^{\Sigma^\dagger} (H \mathrm{e}^{T})_C]_C | \Phi \rangle \ , \end{aligned} \tag{108}$$

where $\bar{H}$ is the similarity-transformed Hamiltonian, Eq. (18). The major advantage of the ECC energy functional, Eq. (108), over the expectation value of the Hamiltonian with the CC wave function (cf. Eq. (104)) is the fact that $E_0^{(\mathrm{ECC})}(\Sigma, T)$, Eq. (108), can be represented by a computationally tractable finite series in T and $\Sigma^\dagger$.

There can be several different ways of calculating the T and Σ operators in the ECC methods. In the original formulation of the ECC theory by Arponen, Bishop and coworkers [145, 146, 147, 148, 149, 150, 151, 152, 153, 154], the T and Σ operators are determined by requiring that $E_0^{(\mathrm{ECC})}(\Sigma, T)$ is stationary with respect to T and $\Sigma^\dagger$. In an alternative formulation by Piecuch and Bartlett [31], the operators T and Σ are determined by considering the doubly transformed form of the electronic Schrödinger equation for the CC wave function, Eq. (3), i.e.,

$$\bar{\bar{H}}\,|\Phi\rangle = E_0|\Phi\rangle \ , \tag{109}$$

where

$$\begin{aligned}\bar{\bar{H}} &= \mathrm{e}^{\Sigma^\dagger}(\mathrm{e}^{-T}H\mathrm{e}^{T})\mathrm{e}^{-\Sigma^\dagger} = \mathrm{e}^{\Sigma^\dagger}\bar{H}\mathrm{e}^{-\Sigma^\dagger} \\ &= [\mathrm{e}^{\Sigma^\dagger}(H\mathrm{e}^{T})_{\mathrm{C}}]_{\mathrm{C}} \ ,\end{aligned} \tag{110}$$

and the left-hand analog of Eq. (109), i.e.,

$$\langle\tilde{\Phi}|\,\bar{\bar{H}} = E_0\langle\tilde{\Phi}| \ , \tag{111}$$

in which we require that the left-hand state $\langle\tilde{\Phi}|$ is identical to the right-hand reference state $|\Phi\rangle$. Both ECC approaches lead to nonlinear systems of equations for the cluster amplitudes defining T and Σ ($t_{a_1}^{i_1}$ and $t_{a_1a_2}^{i_1i_2}$ for T and $\sigma_{a_1}^{i_1}$ and $\sigma_{a_1a_2}^{i_1i_2}$ for Σ in the ECCSD case). We refer the reader to the original papers [31, 145, 146, 147, 148, 149, 150, 151, 152, 153, 154] and recent work [64, 65, 137, 138, 143, 144] for further details.

Although there are differences between the forms of the amplitude equations used to determine the cluster operators T and Σ in the ECC theories of Arponen, Bishop and coworkers [145, 146, 147, 148, 149, 150, 151, 152, 153, 154] and Piecuch and Bartlett [31], our experiences to date indicate that these differences are not essential in the context of improving the results in the bond breaking region. For example, the bi-stationary character of the ECC theory of Arponen, Bishop and coworkers, which is no longer preserved in the ECC theory of Piecuch and Bartlett and which is convenient in the calculations of energy derivatives and molecular properties [212, 213, 214, 215, 216, 217, 218, 219, 220], is of lesser significance in studies of bond breaking. As shown in Refs. [64, 65], the most important factor that contributes to significant improvements in the quality of the T_1 and T_2 cluster components in the bond breaking region is the flexibility of the ECC theories, which rely on two independent sets of cluster amplitudes. The standard CC theory, based on Eqs. (9) and (14), uses only one set of cluster amplitudes and this is not sufficient to obtain a correct description of multiple bond breaking by the standard CCSD method. Another feature of all ECC methods, which is particularly useful in the context of bond breaking, is the fact that in analogy to the so-called expectation value CC approaches [31, 221, 222], the ECC methods are capable of describing various higher-order effects, including the effect of T_4 clusters, even at the basic ECCD or ECCSD levels of theory. Those effects are brought into the ECC formalism as products of the low-order many-body components of $\Sigma^\dagger$ and T and their powers. For example, an important part of the fifth-order effect due to T_4 clusters, usually referred to as the $E_{\mathrm{QQ}}^{[5]}$ energy contribution [223, 224, 225], appears in the ECC theory in the form of the $\frac{1}{4}\langle\Phi|(\Sigma_2^\dagger)^2(V_{\mathrm{N}}T_2^2)_{\mathrm{C}}|\Phi\rangle$ term, where Σ_2 is a two-body component of Σ (see Refs. [31, 64, 65] for further details and analysis). This term is present in the ECC energy, Eq. (108), even at the lowest ECCD level, in which $T = T_2$ and $\Sigma = \Sigma_2$. As demonstrated in Ref. [64], this useful feature of the ECC formalism helps the description of bond breaking by the ECC theories, since the effects of high-order cluster components, such as T_4, are very important at larger internuclear separations.

The usefulness of the ECCSD theory in improving the results for multiple bond breaking becomes apparent when we examine the results shown in Table 3 and Fig. 7. As one can see, the ECCSD method, based on the ECC theory of Piecuch and Bartlett [31], employing the ground-state RHF orbitals, provides remarkable improvements in the very poor description of the potential energy curve of N_2 by the standard CCSD method. The huge negative errors in the CCSD results at larger N–N separations of about −200 millihartree reduce to much smaller positive errors, on the order of 30–38 millihartree, in the ECCSD case. Very similar findings were reported in Refs. [137, 138, 143, 144], where the authors used the ECCD method of Arponen, Bishop and coworkers [145, 146, 147, 148, 149, 150, 151, 152, 153, 154] and the full CI Brueckner orbitals. As shown in Fig. 7, the ECCSD approach eliminates the pathological behavior of the CCSD method at larger N–N distances, restoring the variational description of the potential-energy curve of N_2 at all internuclear separations. As demonstrated in Refs. [64, 65], the quality of the ECCSD wave function $\mathrm{e}^{T_1+T_2}|\Phi\rangle$, where T_1 and T_2 are obtained in the ECCSD calculations, and of the corresponding T_1 and T_2 cluster components, as measured by forming overlaps of the normalized ECCSD and full CI states at various internuclear separations in N_2, only slightly deteriorates with the increasing $R_{\mathrm{N-N}}$ values.

Although the ECCSD approach does not provide a perfect description of bond breaking in N_2, the ECCSD results are so much better than their CCSD analogs that it is worthwhile to examine the effect of replacing the CCSD values of the T_1 and T_2 cluster components in the MMCC calculations by the ECCSD values of these clusters. Since the ECCSD method is no longer a standard CC theory, so we can no longer assume that the singly and doubly excited moments, $\mathscr{M}_{a_1}^{i_1}(2)$ and $\mathscr{M}_{a_1a_2}^{i_1i_2}(2)$, Eqs. (33) and (34), respectively, vanish, we must use the GMMCC formalism, discussed in Sect. 2.1 and represented by Eqs. (30) and (32), to determine the final ground-state energies. In the ECCSD case that interests us here, we must use Eq. (32) (rather than the usual MMCC expression, Eq. 28). Thus, we first use the ECCSD values of the T_1 and T_2 clusters to calculate the zero-body moment $M_0(2)$, Eq. (31) (a CCSD-like energy expression, in which the CCSD values of T_1 and T_2 are replaced by their ECCSD counterparts), and then add various terms expressed in terms of all or some moments $\mathscr{M}_{a_1\ldots a_k}^{i_1\ldots i_k}(2)$, $k = 1-6$, Eqs. (33), (34), (24), (25), (26) and (27), respectively, calculated with the ECCSD values of

T_1 and T_2, to correct the $M_0(2)$ energy. In practice, we are interested in a truncated form of Eq. (32) that leads to relatively low costs of calculating the energy. Our tests indicate that the lowest-order GMMCC scheme, based on using Eq. (32) and the ECCSD values of T_1 and T_2, which provides excellent results for multiple bond breaking, is the GMMCC(2,4) approach defined by Eq. (54). In this approach, referred to as the GMMCC(2,4)/ECCSD method, we only consider the generalized moments $\mathscr{M}^{i_1 \ldots i_k}_{a_1 \ldots a_k}(2)$ with $k = 1 - 4$, i.e. moments corresponding to projections on singly, doubly, triply, and quadruply excited configurations. As in other approximate MMCC calculations, we had to decide what to do with the wave function $|\Psi_0\rangle$ that enters the GMMCC(2,4)/ECCSD energy formula, Eq. (54). Since we are mainly interested in the black-box MMCC approaches of the CR-CC type, in this preliminary study of the performance of the GMMCC(2,4)/ECCSD theory, we utilized exactly the same wave function $|\Psi_0\rangle$ in Eq. (54) as previously used in defining the CR-CCSD(TQ),b approach (the $|\Psi_0^{\mathrm{CCSD(TQ)},b}\rangle$ wave function, Eq. 59, where the required T_1 and T_2 clusters are taken from the ECCSD calculations). The GMMCC(2,4)/ECCSD theory discussed in this section reduces to the CR-CCSD(TQ),b approach described in Sect. 3.1 if the T_1 and T_2 clusters originating from the ECCSD calculations are replaced in Eq. (54) by their CCSD analogs. This straightforward relationship between the GMMCC(2,4)/ECCSD and CR-CCSD(TQ),b methods immediately implies that once the T_1 and T_2 clusters are determined by solving the ECCSD equations, the computer cost of calculating the GMMCC(2,4)/ECCSD energy is the same as the computer cost of the CR-CCSD(TQ),b calculations, which scale as $n_{\mathrm{o}}^2 n_{\mathrm{u}}^5$ with the numbers of occupied and unoccupied orbitals in a basis set.

The GMMCC(2,4)/ECCSD results for the STO-3G model of N_2 are shown in Fig. 7 and Table 3. As one can see, the GMMCC(2,4)/ECCSD method provides spectacular improvements in the description of triple bond breaking in N_2 reducing huge unsigned errors in the CCSD and CR-CCSD(TQ),b results in the $R_{\mathrm{N-N}} \geq 5.0$-bohr region, on the order of 200–210 and 40–50 millihartree, respectively, and the 30–38-millihartree errors in the ECCSD results to as little as 6–7 millihartree. The errors in the GMMCC(2,4)/ECCSD results in the entire $R_{\mathrm{N-N}} \leq 4.0$-bohr (approx $2R_{\mathrm{e}}$) region do not exceed 3 millihartree, being much smaller in the $R_{\mathrm{N-N}} \approx R_{\mathrm{e}}$ region. As shown in Fig. 7 and Table 3, the GMMCC(2,4)/ECCSD potential energy curve is located only slightly above the full CI curve and there is no hump on it. Interestingly enough, the zero-body moment $M_0(2)$, Eq. (31), calculated with the ECCSD values of T_1 and T_2, which is corrected in the GMMCC(2,4) energy formula, Eq. (54), by adding terms expressed in terms of singly, doubly, triply, and quadruply excited moments $\mathscr{M}^{i_1 \ldots i_k}_{a_1 \ldots a_k}(2)$ with $k = 1 - 4$, is a poor approximation to the exact, full CI, energy in the region of large N–N separations (Table 3). This shows once again the remarkable ability of the MMCC formalism to restore high accuracies in the bond breaking region even when the CC energy that we are trying to correct (in this case, the $M_0(2)$/ECCSD energy) is itself very poor.

We have already mentioned that the most expensive steps of the GMMCC(2,4)/ECCSD energy calculations scale as $n_{\mathrm{o}}^2 n_{\mathrm{u}}^5$. There is, however, an additional cost associated with the underlying ECCSD calculations. Independent of the formulation of the ECC theory (that of Arponen, Bishop and coworkers or that of Piecuch and Bartlett), the ECCSD calculations are considerably more expensive than the standard CCSD calculations. The ECCSD method uses only singly and doubly excited cluster components, but they are used in a rather complicated fashion. This is a problem that must be properly addressed before the GMMCC(2,4)/ECCSD method becomes practical. So far, we have tried to address this issue by considering various approximate ECCSD algorithms, which scale as $\mathscr{N}^6$ with the system size. These include the quadratic and bilinear ECCSD methods (QECCSD and BECCSD, respectively), described in Refs. [64, 65]. Similar methods were considered by Head-Gordon and coworkers (the so-called QCCD approach [138, 143]) and Pal, Vaval and coworkers [216, 217, 218, 219, 220] (the quadratic and cubic ECCSD schemes). For example, in the BECCSD method, we replace the doubly transformed Hamiltonian

$$\begin{aligned}\bar{\bar{H}}^{(\mathrm{ECCSD})} &= \mathrm{e}^{\Sigma_1^\dagger + \Sigma_2^\dagger}(\mathrm{e}^{-T_1 - T_2} H \mathrm{e}^{T_1 + T_2})\mathrm{e}^{-\Sigma_1^\dagger - \Sigma_2^\dagger} \\ &= \mathrm{e}^{(\Sigma^{(\mathrm{CCSD})})^\dagger} \bar{H}^{(\mathrm{CCSD})} \mathrm{e}^{-(\Sigma^{(\mathrm{CCSD})})^\dagger} \qquad (112)\end{aligned}$$

of the full ECCSD theory, where $\bar{H}^{(\mathrm{CCSD})}$ and $\Sigma^{(\mathrm{CCSD})}$ are defined by Eqs. (13) and (105), respectively, by its simplified form in which we only retain terms that are linear and bilinear in $\Sigma^{(\mathrm{CCSD})}$, i.e.,

$$\begin{aligned}\bar{\bar{H}}^{(\mathrm{BECCSD})} = {} & [1 + (\Sigma^{(\mathrm{CCSD})})^\dagger] \bar{H}^{(\mathrm{CCSD})} [1 - (\Sigma^{(\mathrm{CCSD})})^\dagger] \\ & + \frac{1}{2} [(\Sigma^{(\mathrm{CCSD})})^\dagger]^2 \bar{H}^{(\mathrm{CCSD})} \\ & + \frac{1}{2} \bar{H}^{(\mathrm{CCSD})} [(\Sigma^{(\mathrm{CCSD})})^\dagger]^2 \ . \qquad (113)\end{aligned}$$

The QECCSD equations are similar to the BECCSD equations [64, 65]. As shown in Table 3, the GMMCC(2,4) calculations employing the BECCSD values of T_1 and T_2 lead to an excellent description of triple bond breaking in N_2. Although it is quite likely that this is a fortuitous cancellation of errors, the results of the GMMCC(2,4)/BECCSD calculations are even better than their GMMCC(2,4)/ECCSD analogs. There is a tiny hump on the GMMCC(2,4)/BECCSD potential energy curve for N_2, but the 0–3-millihartree errors in the GMMCC(2,4)/BECCSD results in the entire $R_{\mathrm{N-N}} = 1.0 - 8.0$-bohr region are better than other MMCC results for N_2 discussed in this article. The tiny hump on the GMMCC(2,4)/BECCSD potential energy curve can be eliminated if we use the QECCSD approximation [64, 65] instead of the BECCSD method to generate T_1 and T_2. The GMMCC(2,4) results employing the QECCSD values of the T_1 and T_2 clusters are virtually identical to the GMMCC(2,4)/ECCSD results shown in Table 3.

The detailed study of the performance of the GMMCC(2,4) method, employing various ECCSD approximations to generate the T_1 and T_2 cluster components and the ECC theories of Arponen, Bishop and coworkers and Piecuch and Bartlett, will be described elsewhere. The preliminary results discussed in this section are very encouraging, since the calculation of the GMMCC(2,4) energy is as easy as the calculations of the CR-CCSD(TQ),b or QMMCC(2,4) energies [and these have the same cost as the standard CCSD(TQ$_\mathrm{f}$) method] and, at the same time, the ECCSD-based GMMCC(2,4) approach removes the failing of the related CCSD-based CR-CCSD(TQ),b and QMMCC(2,4) methods (and other single-reference CC approximations) in a very complicated case of triple bond breaking in N_2. The excellent performance of the relatively inexpensive GMMCC(2,4) approach in describing the large nondynamic correlation effects characterizing N_2 clearly demonstrates that the MMCC theory is a very flexible formalism, in which we can continue improving the accuracy in the bond breaking region without substantially increasing the computer costs. This is a consequence of a good understanding of the nature and many-body structure of the remanent errors that occur in the standard CC calculations offered by the fundamental MMCC and GMMCC formulas, Eqs. (21) and (30).

4 Approximate MMCC approaches to excited states

As explained in Sect. 2.2, the MMCC formalism can be extended to excited states. In this case, the noniterative corrections $\delta_K^{(\mathrm{A})}$, Eq. (39), expressed in terms of the generalized moments of the EOMCC equations, Eq. (41) or (42), are added, in a state-selective manner, to the excited-state energies $E_K^{(\mathrm{A})}$ obtained in the standard EOMCC calculations. If the excited-state energies that we want to correct are obtained in the EOMCCSD calculations, we use Eq. (47) and the generalized moments of the EOMCCSD equations, Eq. (44), such as $\mathscr{M}_{K,a_1a_2a_3}^{i_1i_2i_3}(2)$, Eq. (46), to calculate the relevant corrections $\delta_K^{(\mathrm{EOMCCSD})}$.

As in the ground-state case, the exact excited-state corrections $\delta_K^{(\mathrm{A})}$ or $\delta_K^{(\mathrm{EOMCCSD})}$, which recover the exact, full CI, energies, are also expressed in terms of the full CI wave functions $|\Psi_K\rangle$ (cf. Eqs. 39 and 47). Thus, in order to develop practical computational schemes, based on Eq. (39) or (47), we must rely on some approximate forms of wave functions $|\Psi_K\rangle$ in constructing the noniterative corrections $\delta_K^{(\mathrm{A})}$ or $\delta_K^{(\mathrm{EOMCCSD})}$. Essentially all approximate MMCC methods for excited states proposed to date are based on employing the wave functions $|\Psi_K\rangle$ that are either designed using the MBPT-like arguments [12, 74] or obtained in inexpensive limited CI calculations [12, 72, 73]. Typically, the CI expansions of the wave functions $|\Psi_K\rangle$ used in the MMCC calculations for excited states are relatively short and do not contain higher–than–m_B-tuply excited components relative to the reference configuration $|\Phi\rangle$, where the excitation level m_B is not much higher than the excitation level m_A defining the EOMCC approximation that we are trying to improve. The condition that the wave functions $|\Psi_K\rangle$ used in Eq. (39) or Eq. (47) do not contain higher–than–m_B-tuply excited components relative to $|\Phi\rangle$ defines the excited-state analogs of the ground-state MMCC($m_\mathrm{A}, m_\mathrm{B}$) schemes, in which the energies are calculated as follows [12, 72, 73, 74]:

$$E_K^{(\mathrm{MMCC})}(m_\mathrm{A}, m_\mathrm{B}) = E_K^{(\mathrm{A})} + \delta_K(m_\mathrm{A}, m_\mathrm{B}), \tag{114}$$

where $E_K^{(\mathrm{A})}$ is the energy of the Kth electronic state, obtained with some standard EOMCC method A, and

$$\begin{aligned}\delta_K(m_\mathrm{A}, m_\mathrm{B}) = \sum_{n=m_\mathrm{A}+1}^{m_\mathrm{B}} \sum_{k=m_\mathrm{A}+1}^{n} &\langle\Psi_K|C_{n-k}(m_\mathrm{A}) \\ &\times M_{K,k}(m_\mathrm{A})|\Phi\rangle / \langle\Psi_K|R_K^{(\mathrm{A})} \mathrm{e}^{T^{(\mathrm{A})}}|\Phi\rangle\end{aligned} \tag{115}$$

is the relevant MMCC correction to $E_K^{(\mathrm{A})}$. In analogy to the ground-state MMCC($m_\mathrm{A}, m_\mathrm{B}$) calculations, the generalized moments of the EOMCC equations, $\mathscr{M}_{K,a_1\ldots a_k}^{i_1\ldots i_k}(m_\mathrm{A})$, Eqs. (41) and (42), enter Eqs. (114) and (115) through quantities $M_{K,k}(m_\mathrm{A})|\Phi\rangle$, Eq. (40), and $C_{n-k}(m_\mathrm{A})$ are the many-body components of $\mathrm{e}^{T^{(\mathrm{A})}}$, defined by Eq. (22), where $T^{(\mathrm{A})}$ is the cluster operator defining (along with the excitation operator $R_K^{(\mathrm{A})}$) the EOMCC calculations A, whose results we want to correct.

As in the case of the ground-state methods discussed in Sect. 3, we limit our discussion of the MMCC methods for excited states to the low-order MMCC($m_\mathrm{A}, m_\mathrm{B}$) schemes with $m_\mathrm{A} = 2$, which can be used to correct the results of the EOMCCSD calculations. In this category, two schemes are particularly useful, namely, MMCC(2,3) and MMCC(2,4), although, in analogy to the ground-state methods, we can always contemplate higher-order MMCC(2,5) and MMCC(2,6) approaches. The MMCC(2,3) and MMCC(2,4) energy expressions for the excited-state energies E_K, which one can easily obtain by setting $m_\mathrm{A} = 2$ and $m_\mathrm{B} = 3$ or 4 in Eqs. (114) and (115), are as follows [12, 61, 72, 73, 74]:

$$\begin{aligned}E_K^{(\mathrm{MMCC})}(2,3) = E_K^{(\mathrm{EOMCCSD})} &+ \langle\Psi_K|M_{K,3}(2)|\Phi\rangle / \\ &\langle\Psi_K|R_K^{(\mathrm{CCSD})} \mathrm{e}^{T_1+T_2}|\Phi\rangle\end{aligned} \tag{116}$$

and

$$\begin{aligned}E_K^{(\mathrm{MMCC})}(2,4) = E_K^{(\mathrm{EOMCCSD})} &+ \langle\Psi_K|\{M_{K,3}(2) \\ &+ [M_{K,4}(2) + T_1 M_{K,3}(2)]\}|\Phi\rangle / \\ &\langle\Psi_K|R_K^{(\mathrm{CCSD})} \mathrm{e}^{T_1+T_2}|\Phi\rangle,\end{aligned} \tag{117}$$

where $E_K^{(\mathrm{EOMCCSD})}$ is the EOMCCSD energy for the Kth electronic state, $R_K^{(\mathrm{CCSD})}$ is the corresponding excitation operator (cf. Eq. 45), T_1 and T_2 are the singly and doubly excited clusters obtained in the CCSD calculations, and $M_{K,3}(2)|\Phi\rangle$ and $M_{K,4}(2)|\Phi\rangle$ are the quantities that are expressed in terms of the triply and quadruply excited moments of the EOMCCSD equations, $\mathscr{M}_{K,a_1a_2a_3}^{i_1i_2i_3}(2)$ and $\mathscr{M}_{K,a_1a_2a_3a_4}^{i_1i_2i_3i_4}(2)$, respectively, using Eq. (48), where $k = 3$ and 4. As in the ground-state case, these moments are easy to calculate. For example, as implied by Eq. (46), the triexcited moments $\mathscr{M}^{i_1 i_2 i_3}_{K,a_1 a_2 a_3}(2)$ are expressed in terms of the triples–reference, triples–singles, and triples–doubles blocks of the matrix representing the EOMCCSD similarity transformed Hamiltonian $\bar{H}^{\mathrm{CCSD}}$, Eq. (13). An analogous expression for the quadruply excited moments $\mathscr{M}^{i_1 i_2 i_3 i_4}_{K,a_1 a_2 a_3 a_4}(2)$, based on Eq. (42), implies that the only blocks of the matrix representing $\bar{H}^{\mathrm{CCSD}}$ that are involved in computing moments $\mathscr{M}^{i_1 i_2 i_3 i_4}_{K,a_1 a_2 a_3 a_4}(2)$ are the quadruples–reference, quadruples–singles, and quadruples–doubles blocks [73]. The expensive triples–triples, triples–quadruples, quadruples–triples, and quadruples–quadruples blocks do not enter the expressions for $\mathscr{M}^{i_1 i_2 i_3}_{K,a_1 a_2 a_3}(2)$ and $\mathscr{M}^{i_1 i_2 i_3 i_4}_{K,a_1 a_2 a_3 a_4}(2)$. In consequence, the most expensive steps of the excited-state calculations using the MMCC(2,3) and MMCC(2,4) methods are essentially identical to the $n_{\mathrm{o}}^3 n_{\mathrm{u}}^4$ and $n_{\mathrm{o}}^2 n_{\mathrm{u}}^5$ noniterative steps of the ground-state CCSD(T) and CCSD(TQ$_{\mathrm{f}}$) calculations, respectively. Similar remarks apply to the memory and disk-space requirements. Clearly, those are great simplifications in the computer effort, compared with the higher-level EOMCC approaches, such as EOMCCSDT [70, 71, 121], particularly if we realize that we only have to use the T_1 and T_2 clusters, obtained in the CCSD calculations, to construct matrix elements of $\bar{H}^{(\mathrm{CCSD})}$ that enter $\mathscr{M}^{i_1 i_2 i_3}_{K,a_1 a_2 a_3}(2)$ and $\mathscr{M}^{i_1 i_2 i_3 i_4}_{K,a_1 a_2 a_3 a_4}(2)$. In practical implementations of the MMCC(2,3), MMCC(2,4), and related CR-EOMCCSD(T) approaches, we do not construct matrix elements of $\bar{H}^{(\mathrm{CCSD})}$ to calculate $\mathscr{M}^{i_1 i_2 i_3}_{K,a_1 a_2 a_3}(2)$ and $\mathscr{M}^{i_1 i_2 i_3 i_4}_{K,a_1 a_2 a_3 a_4}(2)$; we rather evaluate $\mathscr{M}^{i_1 i_2 i_3}_{K,a_1 a_2 a_3}(2)$ and $\mathscr{M}^{i_1 i_2 i_3 i_4}_{K,a_1 a_2 a_3 a_4}(2)$ using the recursively generated intermediates [226]. Another nice feature of the MMCC(2,3) and MMCC(2,4) approximations for excited states [which applies to all excited-state MMCC($m_{\mathrm{A}}, m_{\mathrm{B}}$) schemes] is the fact that Eqs. (116) and (117) reduce to the ground-state MMCC(2,3) and MMCC(2,4) methods defined by Eqs. (52) and (53), respectively, when $K = 0$ (cf. Sect. 2.2), offering us the possibility of obtaining a balanced description of ground and excited states in a single formalism.

Depending on the form of the wave function $|\Psi_K\rangle$ in Eqs. (116) and (117), we distinguish between the perturbative MMCC approaches for excited states, such as CR-EOMCCSD(T) [12, 74], which might be viewed as the excited-state extensions of the ground-state CR-CCSD(T) method discussed in Sect. 3.1, and the CI-corrected MMCC approaches [12, 72, 73], which represent a natural extension of the idea of the ground-state MMCC/CI method overviewed in Sect. 3.3. A few examples of the performance of these two classes of the excited-state MMCC methods are examined in Sects. 4.1 and 4.2.

4.1 The CR-EOMCCSD(T) methods

The ground-state CR-CCSD[T] and CR-CCSD(T) approaches, described in Sect. 3.1, are obtained by replacing the wave function $|\Psi_0\rangle$ in the MMCC(2,3) energy formula, Eq. (52), with the perturbative expressions, Eqs. (55) and (56), which contain the lowest-order information about triply excited clusters. Similar expressions can be proposed for excited states, if we perform the perturbative analysis of the EOMCCSDT or CISDT eigenvalue problems [74]. By replacing the wave functions $|\Psi_K\rangle$ that enter the excited-state MMCC(2,3) formula, Eq. (116), with the expressions that result from analyzing the EOMCCSDT or CISDT equations, we obtain the noniterative approximations for excited states, termed the CR-EOMCCSD(T) methods. Several CR-EOMCCSD(T) schemes, which can be regarded as the renormalized extensions of the existing EOM-CCSD(T) [37], EOMCCSD($\tilde{\mathrm{T}}$) [38], EOMCCSD(T′) [38], and CCSDR(3) [42, 43] approaches, have recently been developed [12, 74] and tested [12, 74, 227]. They are all obtained by replacing the wave functions $|\Psi_K\rangle$ in the excited-state MMCC(2,3) formula, Eq. (116), by the perturbative expressions of one of the following three types [74]:

$$\begin{aligned}|\Psi_K^{\mathrm{I}}\rangle &= (P + Q_1 + Q_2 + Q_3)(R_{K,0} + R_{K,1} + R_{K,2} \\ &\quad + \tilde{R}_{K,3})\mathrm{e}^{T_1 + T_2}|\Phi\rangle \\ &= \{R_{K,0} + (R_{K,1} + R_{K,0}T_1) + [R_{K,2} + R_{K,1}T_1 \\ &\quad + R_{K,0}(T_2 + \frac{1}{2}T_1^2)] + [\tilde{R}_{K,3} + R_{K,2}T_1 \\ &\quad + R_{K,1}(T_2 + \frac{1}{2}T_1^2) \\ &\quad + R_{K,0}(T_1 T_2 + \frac{1}{6}T_1^3)]\}|\Phi\rangle, \end{aligned} \tag{118}$$

$$\begin{aligned}|\Psi_K^{\mathrm{II}}\rangle &= (P + Q_1 + Q_2)(R_{K,0} + R_{K,1} + R_{K,2})\mathrm{e}^{T_1 + T_2}|\Phi\rangle \\ &\quad + \tilde{R}_{K,3}|\Phi\rangle \\ &= \{R_{K,0} + (R_{K,1} + R_{K,0}T_1) + [R_{K,2} + R_{K,1}T_1 \\ &\quad + R_{K,0}(T_2 + \frac{1}{2}T_1^2)] + \tilde{R}_{K,3}\}|\Phi\rangle, \end{aligned} \tag{119}$$

or

$$|\Psi_K^{\mathrm{III}}\rangle = (C_{K,0} + C_{K,1} + C_{K,2} + \tilde{C}_{K,3})|\Phi\rangle, \tag{120}$$

where T_1 and T_2 are the singly and doubly excited clusters obtained in the CCSD calculations, $R_{K,0}$, $R_{K,1}$, and $R_{K,2}$ are the reference, singly excited, and doubly excited components of the EOMCCSD excitation operator $R_K^{(\mathrm{CCSD})}$, and $C_{K,0}|\Phi\rangle$, $C_{K,1}|\Phi\rangle$, and $C_{K,2}|\Phi\rangle$ are the reference, singly excited, and doubly excited components of the CI singles and doubles (CISD) wave function for the Kth electronic state. The operator $P = |\Phi\rangle\langle\Phi|$ is the projection operator onto the one-dimensional manifold spanned by the reference $|\Phi\rangle$ and $Q_k = \sum_{\substack{i_1 < \cdots < i_k \\ a_1 < \cdots < a_k}} |\Phi^{a_1 \ldots a_k}_{i_1 \ldots i_k}\rangle\langle\Phi^{a_1 \ldots a_k}_{i_1 \ldots i_k}|$ is the projection operator onto the subspace of all k-tuply excited configurations relative to $|\Phi\rangle$. The triply excited components of the EOMCC excitation operator R_K, which enter the wave functions $|\Psi_K^{\mathrm{I}}\rangle$ and $|\Psi_K^{\mathrm{II}}\rangle$, Eqs. (118) and (119), respectively, and which can be determined through perturbative analysis of the EOMCCSDT equations, are defined as follows [74]:

$$\tilde{R}_{K,3} = \sum_{\substack{i_1<i_2<i_3\\ a_1<a_2<a_3}} \tilde{R}^{i_1i_2i_3}_{K,a_1a_2a_3} E^{a_1a_2a_3}_{i_1i_2i_3}, \tag{121}$$

where

$$\tilde{R}^{i_1i_2i_3}_{K,a_1a_2a_3} = \mathscr{M}^{i_1i_2i_3}_{K,a_1a_2a_3}(2)/D^{i_1i_2i_3}_{K,a_1a_2a_3}, \tag{122}$$

with moments $\mathscr{M}^{i_1i_2i_3}_{K,a_1a_2a_3}(2)$ given by Eq. (46) and the perturbative denominator $D^{i_1i_2i_3}_{K,a_1a_2a_3}$ given by

$$\begin{aligned} D^{i_1i_2i_3}_{K,a_1a_2a_3} &= E_K^{(\mathrm{EOMCCSD})} - \langle \Phi^{a_1a_2a_3}_{i_1i_2i_3} | \bar{H}^{(\mathrm{CCSD})} | \Phi^{a_1a_2a_3}_{i_1i_2i_3} \rangle \\ &= \omega_K^{(\mathrm{EOMCCSD})} - \langle \Phi^{a_1a_2a_3}_{i_1i_2i_3} | \bar{H}^{(\mathrm{CCSD})}_{\mathrm{open}} | \Phi^{a_1a_2a_3}_{i_1i_2i_3} \rangle \\ &= \omega_K^{(\mathrm{EOMCCSD})} - \langle \Phi^{a_1a_2a_3}_{i_1i_2i_3} | \bar{H}^{(\mathrm{CCSD})}_1 | \Phi^{a_1a_2a_3}_{i_1i_2i_3} \rangle \\ &\quad - \langle \Phi^{a_1a_2a_3}_{i_1i_2i_3} | \bar{H}^{(\mathrm{CCSD})}_2 | \Phi^{a_1a_2a_3}_{i_1i_2i_3} \rangle \\ &\quad - \langle \Phi^{a_1a_2a_3}_{i_1i_2i_3} | \bar{H}^{(\mathrm{CCSD})}_3 | \Phi^{a_1a_2a_3}_{i_1i_2i_3} \rangle. \end{aligned} \tag{123}$$

Here, $\omega_K^{(\mathrm{EOMCCSD})}$ represents the EOMCCSD excitation energy,

$$\omega_K^{(\mathrm{EOMCCSD})} = E_K^{(\mathrm{EOMCCSD})} - E_0^{(\mathrm{CCSD})}, \tag{124}$$

$\bar{H}^{(\mathrm{CCSD})}_{\mathrm{open}}$ is the open part of $\bar{H}^{(\mathrm{CCSD})}$ (all diagrams of $\bar{H}^{(\mathrm{CCSD})}$ that have external lines), and $\bar{H}^{(\mathrm{CCSD})}_k$ is a k-body component of $\bar{H}^{(\mathrm{CCSD})}$. The triply excited components of the CI-like wave function $|\Psi_K^{\mathrm{III}}\rangle$, Eq. (120), which are estimated using the singly and doubly excited components of $|\Psi_K^{\mathrm{III}}\rangle$ obtained in the single-reference CISD calculations (i.e. the $C_{K,1}|\Phi\rangle$ and $C_{K,2}|\Phi\rangle$ terms), are defined as follows [74]:

$$\tilde{C}_{K,3}|\Phi\rangle = \sum_{\substack{i_1<i_2<i_3\\ a_1<a_2<a_3}} \tilde{C}^{i_1i_2i_3}_{K,a_1a_2a_3} |\Phi^{a_1a_2a_3}_{i_1i_2i_3}\rangle, \tag{125}$$

where

$$\begin{aligned} \tilde{C}^{i_1i_2i_3}_{K,a_1a_2a_3} =& \langle \Phi^{a_1a_2a_3}_{i_1i_2i_3} | H(C_{K,1} + C_{K,2}) | \Phi \rangle / \\ & \Delta^{i_1i_2i_3}_{K,a_1a_2a_3}, \end{aligned} \tag{126}$$

with the denominator $\Delta^{i_1i_2i_3}_{K,a_1a_2a_3}$ given by

$$\Delta^{i_1i_2i_3}_{K,a_1a_2a_3} = E_K^{(\mathrm{EOMCCSD})} - \langle \Phi^{a_1a_2a_3}_{i_1i_2i_3} | H | \Phi^{a_1a_2a_3}_{i_1i_2i_3} \rangle. \tag{127}$$

These expressions apply to the ground and excited states. For the wave function $|\Psi_K^{\mathrm{III}}\rangle$, Eq. (120), we simply use the ground-state CISD solution to construct the $K = 0$ form of $|\Psi_K^{\mathrm{III}}\rangle$. In the case of wave functions $|\Psi_K^{\mathrm{I}}\rangle$ and $|\Psi_K^{\mathrm{II}}\rangle$, Eqs. (118) and (119), respectively, we obtain the ground-state ($K = 0$) formulas by replacing $R_{K,0}$ by 1, $R_{K,1}$ and $R_{K,2}$ by 0, and $\tilde{R}_{K,3}$ by

$$\tilde{R}_{0,3} = \sum_{\substack{i_1<i_2<i_3\\ a_1<a_2<a_3}} \tilde{R}^{i_1i_2i_3}_{0,a_1a_2a_3} E^{a_1a_2a_3}_{i_1i_2i_3}, \tag{128}$$

where

$$\tilde{R}^{i_1i_2i_3}_{0,a_1a_2a_3} = \mathscr{M}^{i_1i_2i_3}_{a_1a_2a_3}(2)/D^{i_1i_2i_3}_{0,a_1a_2a_3}, \tag{129}$$

with moments $\mathscr{M}^{i_1i_2i_3}_{a_1a_2a_3}(2)$ given by Eq. (24) and the denominator $D^{i_1i_2i_3}_{0,a_1a_2a_3}$ given by

$$\begin{aligned} D^{i_1i_2i_3}_{0,a_1a_2a_3} =& - \langle \Phi^{a_1a_2a_3}_{i_1i_2i_3} | \bar{H}^{(\mathrm{CCSD})}_1 | \Phi^{a_1a_2a_3}_{i_1i_2i_3} \rangle \\ & - \langle \Phi^{a_1a_2a_3}_{i_1i_2i_3} | \bar{H}^{(\mathrm{CCSD})}_2 | \Phi^{a_1a_2a_3}_{i_1i_2i_3} \rangle \\ & - \langle \Phi^{a_1a_2a_3}_{i_1i_2i_3} | \bar{H}^{(\mathrm{CCSD})}_3 | \Phi^{a_1a_2a_3}_{i_1i_2i_3} \rangle. \end{aligned} \tag{130}$$

The three types of wave functions $|\Psi_K\rangle$, Eqs. (118), (119), (120), that are used to replace $|\Psi_K\rangle$ in the excited-state MMCC(2,3) formula, Eq. (116), lead to three different classes of the CR-EOMCCSD(T) approximations, referred to as the CR-EOMCCSD(T),I, CR-EOMCCSD(T),II, and CR-EOMCCSD(T),III methods [74]. Additional variants of the CR-EOMCCSD(T),I and CR-EOMCCSD(T),II approaches are obtained by simplifying the formulas for the perturbative denominators $D^{i_1i_2i_3}_{K,a_1a_2a_3}$, Eq. (123), defining the triexcited components $\tilde{R}^{i_1i_2i_3}_{K,a_1a_2a_3}$, Eq. (122). We can, for example, ignore the last two terms involving two- and three-body components of $\bar{H}^{(\mathrm{CCSD})}$ and replace the complete many-body expansion for $D^{i_1i_2i_3}_{K,a_1a_2a_3}$, Eq. (123), by

$$\begin{aligned} \tilde{D}^{i_1i_2i_3}_{K,a_1a_2a_3} =& \ \omega_K^{(\mathrm{EOMCCSD})} \\ & - \langle \Phi^{a_1a_2a_3}_{i_1i_2i_3} | \bar{H}^{(\mathrm{CCSD})}_1 | \Phi^{a_1a_2a_3}_{i_1i_2i_3} \rangle. \end{aligned} \tag{131}$$

We can go even further and replace $\tilde{D}^{i_1i_2i_3}_{K,a_1a_2a_3}$, Eq. (131), by the usual MBPT-like denominators $\omega_K^{(\mathrm{EOMCCSD})} + \epsilon_{i_1} + \epsilon_{i_2} + \epsilon_{i_3} - \epsilon_{a_1} - \epsilon_{a_2} - \epsilon_{a_3}$, where ϵ's are the Hartree–Fock orbital energies. If we do this, we obtain the CR-EOMCCSD(T) method, which becomes virtually identical to the CR-CCSD(T) and QMMCC(2,3) ground-state approaches when $K = 0$. All these different variants of the CR-EOMCCSD(T) approach have been carefully analyzed and tested in Ref. [74]. In this article, we focus on the mixed CR-EOMCCSD(T),I approach, based on the wave function $|\Psi_K^{\mathrm{I}}\rangle$, Eq. (118), in which we use the full perturbative denominator $D^{i_1i_2i_3}_{K,a_1a_2a_3}$, Eq. (123), to calculate the excited-state energies (the $K > 0$ case) and the simplified form of this denominator, Eq. (131), to calculate the ground-state ($K = 0$) energies. A few results of the CR-EOMCCSD(T),III calculations, based in Eq. (120), are shown too. Our experience to date indicates that mixed CR-EOMCCSD(T) approaches and the CR-EOMCCSD(T),III approach provide the best overall results for ground- and excited-state PESs along bond breaking coordinates and the very good balance between ground- and excited-state energies in calculations of excitation energies corresponding to two-electron transitions. We refer the reader to the original work [74] for further details.

Before discussing a few examples illustrating the performance of the CR-EOMCCSD(T) approach, we would like to compare the CR-EOMCCSD(T) methods discussed in this section and the noniterative triples EOMCC or response CC approaches developed by Bartlett's and Jørgensen's groups [37, 38, 42, 43]. There are two fundamental differences between the CR-EOMCCSD(T) methods that originate from the MMCC theory and the previously proposed EOMCCSD(T) [37], EOMCCSD($\tilde{\mathrm{T}}$) [38], EOMCCSD(T′) [38], and CCSDR(3) [42, 43] approaches that originate from the standard (sometimes quite complicated) MBPT analysis of the EOMCC or response CC equations. First of all, the CR-EOMCCSD(T) methods allow us to describe the entire excited-state PESs or, at least, their large fragments, whereas the applicability of the EOMCCSD(T), EOMCCSD($\tilde{T}$), EOMCCSD(T′), and CCSDR(3) approaches is usually limited to vertical excitation energies at or near the ground-state equilibrium geometry. The standard noniterative methods of the EOMCCSD(T) or CCSDR(3) type and their iterative extensions, such as EOMCCSDT-*n* [37, 38] and CC3 [40, 41, 42, 43], have problems with providing a balanced description of excited states having large contributions due to doubly excited configurations, particularly if the ground state has a quasidegenerate character. Second, the EOMCCSD(T), EOMCCSD($\tilde{T}$), EOMCCSD(T′), and CCSDR(3) methods are based on the idea of adding noniterative corrections to the EOMCCSD excitation energies $\omega_K^{(\mathrm{EOMCCSD})}$, not to the individual energies of the electronic states of interest. As all other MMCC approaches, the CR-EOMCCSD(T) methods provide us with a well-defined and systematic procedure of correcting the EOMCCSD energies of individual electronic states in a state selective fashion, which is very important for the applications involving the calculations of molecular PESs. At the same time, the CR-EOMCCSD(T) approaches, which will soon be available in the GAMESS package [226], are characterized by the relatively low computer costs and ease of use of the standard ground-state CCSD(T) method.

A few examples of applications of the CR-EOMCCSD(T) methods to excited-state PESs of CH^+ and HF, vertical excitation energies of C_2, and adiabatic excitation energies of ozone, taken from Refs. [74, 227], are shown in Tables 4, 5 and 6 and Fig. 8. For CH^+, we used the [5s3p1d/3s1p] basis set of Olsen et al. [228], for which the exact, full CI, results at the equilibrium geometry, $R_{\mathrm{C-H}} = R_{\mathrm{e}} = 2.13713$ bohr, and several stretched geometries can be found in Refs. [75, 228]. For HF, we used the DZ basis set [164], for which we could perform the full CI calculations ourselves. For the C_2 molecule, we used the modified aug-cc-pVDZ basis set [165, 181] described by Christiansen et al. [43], since these authors used this basis set to perform the full CI calculations for the low-lying excited states of C_2. Finally, for ozone, we used the polarized basis set of Sadlej [229], which is often used in calculations of excited states. Additional calculations for ozone, employing Sadlej's and other larger basis sets, and including the calculations for several electronic states of each symmetry, can be found in Ref. [227].

Table 4. A comparison of the CR-EOMCCSD(T), MMCC(2,3)/CI, and MMCC(2,4)/CI vertical excitation energies of the CH^+ ion, as described by the [5s3p1d/3s1p] basis set of Olsen et al. [228], at the equilibrium geometry $R_{\mathrm{C-H}} = R_{\mathrm{e}}$ and two stretched geometries, $R_{\mathrm{C-H}} = 1.5R_{\mathrm{e}}$ and $R_{\mathrm{C-H}} = 2R_{\mathrm{e}}$, with the exact, full CI, data and other CC results. The full CI values are the excitation energies. All other values are the deviations from the full CI results. The $n\ ^1X$ energy is the vertical excitation energy from the ground state ($1\ ^1\Sigma^+$) to the *n*th singlet state of symmetry *X*. All energies are in electronvolts

State	Full CI[a]	EOMCCSD[b]	CC3[c]	EOMCCSDt[b,d]	EOMCCSDT[b]	MMCC(2,3)/CI[d,e]	MMCC(2,4)/CI[d,e]	CR-EOMCCSD(T)[f]
$R_{\mathrm{C-H}} = R_{\mathrm{e}}$[g]								
$2\ ^1\Sigma^+$	8.549	0.560	0.230	0.092	0.074	0.084	0.023	0.105
$3\ ^1\Sigma^+$	13.525	0.055	0.016	0.000	0.001	0.000	−0.001	−0.001
$4\ ^1\Sigma^+$	17.217	0.099	0.026	0.012	−0.002	0.015	0.008	0.014
$1\ ^1\Pi$	3.230	0.031	0.012	0.003	−0.003	0.007	0.010	−0.005
$2\ ^1\Pi$	14.127	0.327	0.219	0.094	0.060	0.105	0.037	0.101
$1\ ^1\Delta$	6.964	0.924	0.318	0.057	0.040	0.051	0.031	0.016
$2\ ^1\Delta$	16.833	0.856	0.261	0.016	−0.038	0.006	0.061	−0.014
$R_{\mathrm{C-H}} = 1.5R_{\mathrm{e}}$								
$2\ ^1\Sigma^+$	6.954	0.668		0.064	0.055	0.072	0.020	0.087
$3\ ^1\Sigma^+$	9.344	0.124		0.025	0.023	0.005	0.004	−0.007
$4\ ^1\Sigma^+$	13.988	0.256		0.057	0.037	0.025	−0.046	0.134
$1\ ^1\Pi$	1.718	0.109		0.003	0.001	0.024	0.018	0.013
$2\ ^1\Pi$	8.202	0.564		0.067	0.059	0.059	−0.006	0.046
$1\ ^1\Delta$	5.847	1.114		0.076	0.069	0.065	0.025	−0.015
$2\ ^1\Delta$	13.949	2.095		0.038	0.017	−0.086	0.034	0.473
$R_{\mathrm{C-H}} = 2R_{\mathrm{e}}$								
$2\ ^1\Sigma^+$	5.353	0.299		−0.024	−0.032	0.074	0.013	0.059
$3\ ^1\Sigma^+$	6.681	0.532		0.135	0.126	0.048	0.016	0.050
$4\ ^1\Sigma^+$	11.005	0.771		0.021	0.019	−0.046	−0.001	0.327
$1\ ^1\Pi$	0.566	0.234		0.002	0.002	0.045	0.021	0.027
$2\ ^1\Pi$	5.363	0.467		0.031	0.026	−0.007	−0.004	−0.016
$1\ ^1\Delta$	4.964	1.178		0.112	0.103	0.079	0.027	−0.043
$2\ ^1\Delta$	10.901	3.950		0.167	0.157	0.029	0.029	−0.769

[a] The full CI results for $R_{\mathrm{C-H}} = R_{\mathrm{e}}$ taken from Ref. [228]. The full CI results for $R_{\mathrm{C-H}} = 1.5R_{\mathrm{e}}$ and $R_{\mathrm{C-H}} = 2R_{\mathrm{e}}$ taken from Ref. [75]

[b] From Ref. [71]

[c] From Ref. [41]

[d] The active space consisted of the 3σ, $1\pi_x \equiv 1\pi$, $1\pi_y \equiv 2\pi$, and 4σ orbitals

[e] From Ref. [73] (see, also, Ref. [72])

[f] From Ref. [74]. The results of the calculations with the mixed variant of the CR-EOMCCSD(T),I approach described in the text

[g] The equilibrium C–H bond length, R_{e}, equals 2.13713 bohr

Table 5. A comparison of the CR-EOMCCSD(T), MMCC(2,3)/CI, and MMCC(2,4)/CI vertical excitation energies of the C_2 molecule, as described by the modified augmented correlation-consistent polarized valence double zeta basis set [165, 181] described in Ref. [43], with the exact, full CI, data and other CC results. The full CI values, taken from Ref. [43], represent the vertical excitation energies. All other values are the deviations from the full CI results. The $n\ ^1X$ energy is the vertical excitation energy from the ground state ($1\ ^1\Sigma_g^+$) to the nth singlet state of symmetry X calculated at the equilibrium geometry $R_{C-C} = 2.348$ bohr. All energies are in electronvolts. The two lowest-energy core orbitals were kept frozen

State	Full CI[a]	EOMCCSD[b]	CC3[a]	EOMCCSDt[c,d]	EOMCCSDT[c]	MMCC(2,3)/CI[b,d]	MMCC(2,4)/CI[b,d]	CR-EOMCCSD(T)[e]
$1\ ^1\Pi_u$	1.385	0.089	−0.068	−0.047	0.034	−0.078	−0.044	−0.191
$1\ ^1\Delta_g$	2.293	2.054	0.859	0.285	0.407	0.130	0.011	0.094
$1\ ^1\Sigma_u^+$	5.602	0.197	−0.047	0.088	0.113	−0.032	−0.039	−0.143
$1\ ^1\Pi_g$	4.494	1.708	0.496	0.075	0.088	−0.026	0.057	−0.135

[a] From Ref. [43]

[b] From Ref. [73]

[c] From Ref. [12]

[d] The active space consisted of the $1\pi_u$, $2\pi_u$, $3\sigma_g$, $3\sigma_u$, $1\pi_g$, and $2\pi_g$ orbitals

[e] From Ref. [74]. The results of the calculations with the mixed variant of the CR-EOMCCSD(T),I approach described in the text

Table 6. A comparison of the CR-EOMCCSD(T) adiabatic excitation energies of ozone with other theoretical and experimental data. The theoretical energy values corresponding to the electronic state $n\ ^1X$ represent the adiabatic excitation energies T_e from the minimum on the ground-state potentialenergy surface (PES) ($1\ ^1A_1$) to the minimum on the PES for the nth singlet state of symmetry X. *Numbers* in *parentheses* represent the adiabatic excitation energies T_0, i.e., the T_e values corrected for the zero-point vibrations. All energies are in electronvolt. In all ab initio calculations, the three lowest-energy core orbitals were kept frozen

State[a]	EOMCCSD[b]	CR-EOMCCSD(T)[b]	MRDCI[c]	CASPT2[d]	Expt.
$2\ ^1A_1^\alpha$	10.017[e] (9.950)	3.648 (3.581)	2.50		3.45–4.02[f] Huggins band
$2\ ^1A_1^\beta$	9.499[e]	4.437	3.61		
$1\ ^1B_2$	4.870	4.519	4.34	3.87 (3.84)	4.13–6.20[g] Hartley band
$1\ ^1B_1$	2.287	2.173	1.82	1.67 (1.65)	1.46–2.82[g], 2.05[h] Chappuis band
$1\ ^1A_2$	1.667 (1.597)	1.616 (1.546)	1.44	1.20 (1.19)	1.46—2.82[g], 1.58[i] Chappuis band

[a] The global and secondary minima on the $2\ ^1A_1$ PES, discussed in Ref. [230], are designated as $2\ ^1A_1^\alpha$ and $2\ ^1A_1^\beta$, respectively

[b] From Refs. [74, 227]. The CR-EOMCCSD(T) calculations were performed with the mixed variant of the CR-EOMCCSD(T),I approach described in the text and Sadlej's basis set [229]. The geometry of the minimum on the ground-state PES ($R_{O-O} = 2.4052$ bohr and $\angle(O-O-O) = 116.75°$) was taken from Refs. [241, 242]. The geometries of the minima on excited-state PESs were taken from Ref. [230]. The zero-point energy of the ground state, required to estimate the T_0 values, was calculated using the harmonic vibrational frequencies reported in Ref. [243]. The zero-point energies of the $2\ ^1A_1$ and $1\ ^1A_2$ states were calculated using the vibrational constants listed in Table III of Ref. [231] (the $2\ ^1A_1$ state) and fundamental frequencies given in Ref. [249] (the $1\ ^1A_2$ state)

[c] The calculations performed with the MRDCI variant [233, 234] of the MRCI approach. The results were taken from Ref. [230] (for more results and further analysis, see Ref. [232])

[d] The CASPT2 results taken from Ref. [246]

[e] The EOMCCSD method provides an incorrect ordering of excited states [74,227]. In particular, the EOMCCSD state characterized by the adiabatic excitation energies to the global and secondary minima on the $2\ ^1A_1$ PES of 10.017 and 9.499 eV, respectively, corresponds to the third-excited $^1A_1$ eigenvalue of $\bar{H}^{(CCSD)}$. After adding the CR-EOMCCSD(T) corrections due to triples, this EOMCCSD state becomes the first-excited $^1A_1$ state (see Refs. [74,227] for further details)

[f] Information about the energy range corresponding to the Huggins absorption band taken from Ref. [231]

[g] Information about the energy range corresponding to the Hartley and Chappuis absorption bands taken from Ref. [245]. The Hartley band has a maximum at 4.86 eV [245]

[h] The experimental adiabatic excitation energy taken from Ref. [247] (also reported in Ref. [246])

[i] The experimental adiabatic excitation energy taken from Ref. [248] (also reported in Ref. [246])

We begin our discussion of the performance of the CR-EOMCCSD(T) method with the results for CH^+ at $R_{C-H} = R_e$. In this case, three of the seven excited states listed in Table 4, namely, the first-excited $^1\Sigma^+$ state ($2\ ^1\Sigma^+$) and the lowest two $^1\Delta$ states ($1\ ^1\Delta$ and $2\ ^1\Delta$, respectively), are dominated by double excitations, and the second $^1\Pi$ state ($2\ ^1\Pi$) has a significant biexcited component. The remaining three states ($3\ ^1\Sigma^+$, $4\ ^1\Sigma^+$, and $1\ ^1\Pi$) are dominated by singles. As shown in Table 4, for transitions to the four states that have a predominantly biexcited character or significant doubly excited components (the $2\ ^1\Sigma^+$, $1\ ^1\Delta$, $2\ ^1\Delta$, and $2\ ^1\Pi$ states), the errors in the vertical excitation energies at the equilibrium geometry, relative to full CI, obtained with the CR-EOMCCSD(T) approach, are only 0.01–0.10 eV. This should be compared to the much larger, 0.33–0.92-eV, errors obtained with the EOMCCSD approach and the 0.2–0.3-eV errors obtained [41] with the standard CC3 approach [40, 41, 42, 43], which is an iterative perturbative triples response CC method, similar to the EOMCCSDT-n approaches of Watts and Bartlett [37, 38]. For the three states dominated by singles, the errors

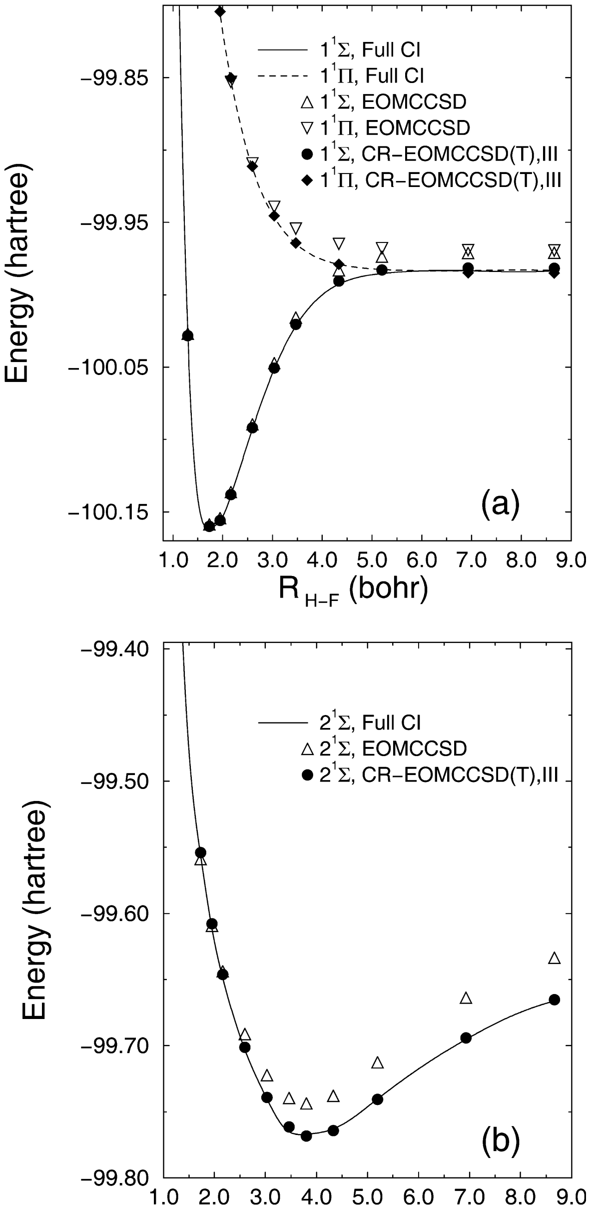

Fig. 8. Ground- and excited-state potential energy curves of the HF molecule, as described by the DZ basis set, obtained in the EOMCCSD, CR-EOMCCSD(T),III, and full CI calculations: **a** the ground state ($1\,^1\Sigma^+$) and the lowest $^1\Pi$ ($1\,^1\Pi$) state; **b** the second $^1\Sigma^+$ state ($2\,^1\Sigma^+$) (see Ref. [74] for the original data)

in the CR-EOMCCSD(T) results are on the order of 0.00–0.01 eV, which is a considerable improvement compared with the EOMCCSD approach, which gives errors of 0.03–0.10 eV.

This great performance of the CR-EOMCCSD(T) approach is not limited to vertical excitation energies at $R_{\mathrm{C-H}} = R_{\mathrm{e}}$. As shown in Table 4, the CR-EOMCCSD(T) approach provides an excellent description of excited states at stretched nuclear geometries, including $R_{\mathrm{C-H}} = 1.5R_{\mathrm{e}}$ and $R_{\mathrm{C-H}} = 2R_{\mathrm{e}}$, for which all seven states listed in Table 4 and the ground state gain a significant multi-reference character and large doubly and, in some cases, even triply excited components [70, 72]. Typically, the huge (often greater than 1-eV) errors in the EOMCCSD results at stretched nuclear geometries of CH^+ reduce in the CR-EOMCCSD(T) calculations to 0.01–0.10 eV. The only exceptions are the CR-EOMCCSD(T) results for the high-lying $4\,^1\Sigma^+$ and $2\,^1\Delta$ states at $R_{\mathrm{C-H}} = 2R_{\mathrm{e}}$ and the $2\,^1\Delta$ state at $R_{\mathrm{C-H}} = 1.5R_{\mathrm{e}}$, but even in these three cases we observe a great reduction of errors in the poor EOMCCSD results (e.g., from 2.10 to 0.47 eV for the $2\,^1\Delta$ state at $R_{\mathrm{C-H}} = 1.5R_{\mathrm{e}}$). Further improvements in the CR-EOMCCSD(T) results for the $4\,^1\Sigma^+$ and $2\,^1\Delta$ states at $R_{\mathrm{C-H}} = 2R_{\mathrm{e}}$ and the $2\,^1\Delta$ state at $R_{\mathrm{C-H}} = 1.5R_{\mathrm{e}}$ can be obtained by employing the CI-corrected MMCC(2,3) and MMCC(2,4) methods (Table 4, Sect. 4.2). As shown in Table 4, with the very few exceptions mentioned earlier, the excellent performance of the noniterative CR-EOMCCSD(T) method is comparable to that of the expensive full EOMCCSDT approach or its active-space EOMCCSDt variant [69, 70, 71], in which the most important triple excitations of the iterative EOMCCSDT method are selected through active orbitals.

Great improvements in the EOMCCSD results in calculations of excited-state PESs are also shown in Fig. 8, where we examine the ground- and excited-state potential energy curves of the HF molecule. As one can see, the CR-EOMCCSD(T) method provides spectacular improvements in the poor description of the entire excited-state potential energy curves of HF by the EOMCCSD approach. The CR-EOMCCSD(T) results are so accurate that it is hard to distinguish between the CR-EOMCCSD(T) and exact, full CI, results shown in Fig. 8. The 0.28–0.40-eV errors in the EOMCCSD results for the lowest $^1\Pi$ state (Fig. 8a) in the $R_{\mathrm{H-F}} = 2R_{\mathrm{e}} - 5R_{\mathrm{e}}$ region are reduced to 0.00–0.05 eV, when the CR-EOMCCSD(T) method is employed [74]. The 0.59–0.89-eV errors in the EOMCCSD results for the second $^1\Sigma^+$ state (Fig. 8b) in the $R_{\mathrm{H-F}} = 2R_{\mathrm{e}} - 5R_{\mathrm{e}}$ region are reduced in the CR-EOMCCSD(T) calculations to 0.01–0.04 eV [74]. Similar or even bigger improvements are observed for other excited states of HF [74]. As shown in Fig. 8a, the results of the CR-EOMCCSD(T) calculations for the ground-state PES of HF are virtually identical to the CR-CCSD(T) results discussed in Sect. 3.1. This is a consequence of the similarities between the CR-EOMCCSD(T) energy expressions written for the ground states and their CR-CCSD(T) analog. The CR-EOMCCSD(T) method is capable of numerically (i.e., approximately) restoring the asymptotic degeneracy of the ground electronic state and the lowest state of the $^1\Pi$ symmetry [both states should dissociate into $\mathrm{H}(1s\,^2\mathrm{S}) + \mathrm{F}(2p^5\,^2\mathrm{P})$], broken by the EOMCCSD approach (see Fig. 8a). The ability of the MMCC methods to restore asymptotic degeneracies of electronic states, which are often broken by the RHF-based EOMCCSD approach, was discussed earlier in Ref. [72] (see, also, Ref. [12]). Other examples of this type can be found in Ref. [74]. We can also see the numerical restoration of the asymptotic degeneracies by the CR-EOMCCSD(T) and CI-corrected MMCC methods (discussed in Sect. 4.2) in Table 4 for CH^+. For example, the full CI energies of the $2\,^1\Sigma^+$ and $2\,^1\Pi$ states of CH^+ differ by only 0.01 eV at $R_{\mathrm{C-H}} = 2R_{\mathrm{e}}$, since these two states, along with the $1\,^1\Delta$ state, dissociate into $\mathrm{C}(2p^2\,^1D) + \mathrm{H}^+$. The CR-EOMCCSD(T) energies of the $2\,^1\Sigma^+$ and $2\,^1\Pi$ states at $R_{\mathrm{C-H}} = 2R_{\mathrm{e}}$ differ by 0.06 eV, which is a considerably better result than the 0.18-eV difference between the energies of these two states obtained with the EOMCCSD approach.

The CR-EOMCCSD(T) method is equally effective in providing great improvements in the description of excited states for the challenging cases of the C_2 and O_3 molecules. Both molecules provide us with examples of different types of excited states, including complicated excited states dominated by doubles, in a situation where the T_3 and T_4 clusters are large and the CCSD approach provides a poor description of the ground state. Those kinds of states are particularly difficult to describe by the EOMCCSD and perturbative triples methods, such as CC3 or EOMCCSDT-*n* and their various noniterative analogs mentioned earlier [EOMCCSD(T) etc.]. This is clearly shown in Table 5, where we compare the CR-EOMCCSD(T) and other MMCC results for the vertical excitation energies of C_2 with the corresponding full CI, EOMCCSD, CC3, EOMCCSDt, and EOMCCSDT results. For example, for the lowest $^1\Delta_g$ state of C_2, which is dominated by the double excitations, the EOMCCSD and CC3 methods give errors of 2.054 and 0.859 eV, respectively. This state is so complex that even the full EOMCCSDT approach gives an error of 0.407 eV. With the judicious choice of active orbitals, the active-space analog of the full EOMCCSDT approach, termed EOMCCSDt, gives a smaller, 0.285-eV, error, but this is probably a coincidence due to the fortuitous cancellation of errors in the ground- and excited-state calculations. Remarkably enough, the CR-EOMCCSD(T) approach, which is capable of providing an accurate and well-balanced description of ground and excited states, reduces the 2.054-, 0.859-, and 0.407-eV errors in the EOMCCSD, CC3, and EOMCCSDT results for the lowest $^1\Delta_g$ state of C_2 to as little as 0.094 eV. Similar remarks apply to the lowest $^1\Pi_g$ state, which is also characterized by significant contributions from double excitations. In this case, the 1.708- and 0.496-eV errors in the results of the EOMCCSD and CC3 calculations reduce to 0.135 eV, when the CR-EOMCCSD(T) approach is employed. The EOMCCSDT method provides a slightly better result, but one has to remember that the EOMCCSDT approach is orders of magnitude more expensive than the noniterative CR-EOMCCSD(T) approximation. For the remaining two states of C_2 listed in Table 5 (the $1\,^1\Pi_{\mathrm{u}}$ and $1\,^1\Sigma_{\mathrm{u}}^+$ states), which are dominated by singles, the CR-EOMCCSD(T) method provides results of the EOMCCSD quality, which are very good in this case.

The first-excited $^1\mathrm{A}_1$ state of ozone (the $2\,^1\mathrm{A}_1$ state in Table 6; as in Ref. [230], we limit our discussion to the C_{2v} symmetry), which is associated with the Huggins band in the UV part of the absorption spectrum [231], provides us with another example of an electronic state dominated by doubly excited contributions. As shown, for example, in Ref. [230] (see, also, Ref. [232]), where the authors used the MRDCI variant [233, 234] of the MRCI approach, this state has two minima, the global minimum designated as $2\,^1\mathrm{A}_1^{\alpha}$ and the secondary minimum designated as $2\,^1\mathrm{A}_1^{\beta}$. Other interesting features of the $2\,^1\mathrm{A}_1$ state include the well-known conical intersection with the ground state ($1\,^1\mathrm{A}_1$) identified by Ruedenberg et al. [235] (see, also, Refs. [236, 237, 238, 239, 240]). As shown in Table 6, the significantly doubly excited character of the $2\,^1\mathrm{A}_1$ state of ozone, combined with the significant role of higher–than–doubly excited clusters in describing the ground state, lead to huge, 5–6-eV, errors in the EOMCCSD results relative to the position of the Huggins absorption band described by Katayama [231]. The purely electronic adiabatic excitation energy, T_{e}, obtained by calculating the difference of the EOMCCSD energy at the geometry of the global minimum on the $2\,^1\mathrm{A}_1$ PES, determined in Ref. [230], and the ground-state CCSD energy at the experimental equilibrium geometry, taken from Refs. [241, 242], and its T_0 counterpart corrected for the zero-point vibrations (using the vibrational constants for the $2\,^1\mathrm{A}_1$ state reported in Ref. [231] and the harmonic vibrational frequencies for the ground state taken from Ref. [243]), are approximately 6.5 eV larger than the position of the low-energy end of the Huggins band reported in Ref. [231]. If we used the secondary minimum on the $2\,^1\mathrm{A}_1$ PES (the $2\,^1\mathrm{A}_1^{\beta}$ minimum) instead of the global minimum, we would obtain an equally large discrepancy between the energy range of the Huggins band and the EOMCCSD values of T_{e} or T_0 (Table 6). These results and other results described in our more detailed studies of the excited states of ozone [74, 227], including vertical excitation energies at the equilibrium geometry (also calculated in Ref. [244]), show that the EOMCCSD PES of the $2\,^1\mathrm{A}_1$ state is completely unphysical and located a few electronvolts above the true PES. As a matter of fact, the EOMCCSD method provides an incorrect ordering of the $^1\mathrm{A}_1$ states, so we must use the third-excited EOMCCSD state of the $^1\mathrm{A}_1$ symmetry (i.e., the fourth $^1\mathrm{A}_1$ state, using the CCSD/EOMCCSD energy ordering of ground and excited states) to calculate the noniterative CR-EOMCCSD(T) triples correction that describes the $2\,^1\mathrm{A}_1$ state (see footnote e in Table 6 and Refs. [74, 227] for further details). Without calculating several states of each symmetry at the EOMCCSD level prior to CR-EOMCCSD(T) calculations, we would risk losing information about some low-lying doubly excited states. Because of the limitations of the EOMCCSD approximation, some doubly excited states resulting from the EOMCCSD calculations are shifted to high energies, mixing with the singly excited states that are accurately described by the EOMCCSD method. After correcting the EOMCCSD energies for the effects of triples, these doubly excited states may become low-lying states. This is what we observe in the case of the $2\,^1\mathrm{A}_1$ state, which shows up as the higher-energy $4\,^1\mathrm{A}_1$ state in the CCSD/EOMCCSD calculations and the $2\,^1\mathrm{A}_1$ state in the CR-EOMCCSD(T) calculations.

As shown in Table 6, the CR-EOMCCSD(T) approach is capable of providing spectacular improvements in the poor results for the $2\,^1\mathrm{A}_1$ state obtained with the EOMCCSD approach. The adiabatic excitation energy T_{e}, obtained by calculating the difference of the CR-EOMCCSD(T) energies at the global minima on the $2\,^1\mathrm{A}_1$ and $1\,^1\mathrm{A}_1$ PESs, is in very good agreement with the position of the low-energy end of the Huggins band. After correcting the CR-EOMCCSD(T) value of T_e by the zero-point energies, we obtain the adiabatic excitation energy T_0, which agrees with the position of the low-energy end of the Huggins band to within 0.13 eV. The truly multireference MRDCI approach gives the adiabatic excitation energy, corresponding to the $2\,^1A_1^{\alpha}$ minimum, which is smaller than the position of the low-energy end of the Huggins band by almost 1 eV. This result seems to be worse than our adiabatic excitation energy obtained with the much simpler single-reference and noniterative CR-EOMCCSD(T) approximation. Considerable improvements in the EOMCCSD results are also observed when the CR-EOMCCSD(T) approach is applied to the remaining three excited states of ozone listed in Table 6 (the $1\,^1B_2$, $1\,^1B_1$, and $1\,^1A_2$ states). These three states, which are associated with the Hartley and Chappuis bands [245], are dominated by single excitations, so the EOMCCSD method describes them reasonably well, but it is good to see that even in this case the CR-EOMCCSD(T) method offers nontrivial improvements in the calculated adiabatic excitation energies, which lead to very good agreements between the CR-EOMCCSD(T) and MRDCI values of T_e and the location of the Hartley and Chappuis bands. The CR-EOMCCSD(T) adiabatic excitation energies for the $1\,^1B_2$, $1\,^1B_1$, and $1\,^1A_2$ states seem to be better than the T_e or T_0 values obtained with the multireference CASPT2 approach [246], which provides energies that are somewhat too low. Remarkably enough, our CR-EOMCCSD(T) values of T_e or T_0 differ by as little as 0.04–0.12 eV from the experimentally derived values of the adiabatic excitation energies for the $1\,^1B_1$ [247] and $1\,^1A_2$ [248] states. In calculating the EOMCCSD and CR-EOMCCSD(T) values of T_0 for the $1\,^1A_1 \rightarrow 1\,^1A_2$ transition, we used the harmonic vibrational frequencies of the ground-state ozone molecule reported in Ref. [243] and the fundamental frequencies characterizing the $1\,^1A_2$ state of ozone given in Ref. [249].

The previous examples clearly indicate that the MMCC-based CR-EOMCCSD(T) approaches represent powerful new techniques that can offer a remarkably accurate description of excited-state PESs with the ease of use of the ground-state CCSD(T) approach. However, there may always be some cases where the black-box CR-EOMCCSD(T) methods are too simple to provide highly accurate results. Alternative MMCC approaches for excited states that may help in those situations are described in the next section.

4.2 The CI-corrected MMCC(2,3) and MMCC(2,4) methods

The CR-EOMCCSD(T) approaches discussed in the previous section are, in our view, the preferred methods for routine applications, because of the excellent compromise between the ease of use and high accuracy that these methods offer, but there may be situations where the CR-EOMCCSD(T) methods do not provide the desired improvements. An example of the failure of the CR-EOMCCSD(T) approach is provided by the second $^1\Delta$ state of CH^+ at the stretched geometries $R_{C-H} = 1.5R_e$ and $R_{C-H} = 2R_e$ (see Table 4). In this case, the errors in the CR-EOMCCSD(T) results of 0.47 and 0.77 eV, respectively, although considerably smaller than the 2.10–3.95-eV errors in the EOMCCSD results, are too big to be considered as acceptable in many applications. In cases like that, it is useful to switch to the CI-corrected MMCC(2,3) and MMCC(2,4) approaches (the MMCC(2,3)/CI and MMCC(2,4)/CI methods, respectively), which are the analogs of the MMCC/CI ground-state methods discussed in Sect. 3.3.

In the excited-state MMCC(2,3)/CI and MMCC(2,4)/CI approaches, introduced in Refs. [72, 73], we replace the wave functions $|\Psi_K\rangle$ in Eqs. (116) and (117) by the multi-reference-like CISDt and CISDtq wave functions defined by the excited-state analogs of Eqs. (95) and (96). Thus, the final formulas for the MMCC(2,3)/CI and MMCC(2,4)/CI energies are very similar to the formulas for the ground-state energies discussed in Sect. 3.3. For example, the MMCC(2,3)/CI energy expression, obtained by inserting the CISDt wave function for state $|\Psi_K\rangle$, i.e.,

$$|\Psi_K^{\text{CISDt}}\rangle = (C_{K,0} + C_{K,1} + C_{K,2} + c_{K,3})|\Phi\rangle, \tag{132}$$

where $C_{K,0}|\Phi\rangle$, $C_{K,1}|\Phi\rangle$, and $C_{K,2}|\Phi\rangle$ are the reference, singly excited, and doubly excited contributions to $|\Psi_K^{\text{CISDt}}\rangle$ and where

$$c_{K,3}|\Phi\rangle = \sum_{\substack{i_1<i_2<\mathbf{I}_3\\ a_1>a_2>\mathbf{A}_3}} c_{K,a_1a_2\mathbf{A}_3}^{i_1i_2\mathbf{I}_3} E_{i_1i_2\mathbf{I}_3}^{a_1a_2\mathbf{A}_3} \tag{133}$$

are the internal and semiinternal triples containing at least one active occupied and one active unoccupied spin-orbital indices included in $|\Psi_K^{\text{CISDt}}\rangle$, into Eq. (116), has the following form:

$$\begin{aligned} E_K^{(\text{MMCC/CI})}(2,3) = & E_K^{(\text{EOMCCSD})} + \sum_{\substack{i_1<i_2<\mathbf{I}_3\\ a_1>a_2>\mathbf{A}_3}} c_{K,a_1a_2\mathbf{A}_3}^{i_1i_2\mathbf{I}_3} \\ & \times \mathscr{M}_{K,a_1a_2\mathbf{A}_3}^{i_1i_2\mathbf{I}_3}(2) / \\ & \langle\Psi_K^{\text{CISDt}}|R_K^{(\text{CCSD})} e^{T_1+T_2}|\Phi\rangle, \end{aligned} \tag{134}$$

where $c_{K,a_1a_2\mathbf{A}_3}^{i_1i_2\mathbf{I}_3}$ are the CI coefficients obtained in the CISDt calculations for the Kth electronic state, $\mathscr{M}_{K,a_1a_2\mathbf{A}_3}^{i_1i_2\mathbf{I}_3}(2)$ are the subset of all triexcited moments of the EOMCCSD equations defined by Eq. (46), T_1 and T_2 are the singly and doubly excited cluster components obtained in the CCSD calculations, and $R_K^{(\text{CCSD})}$ is the EOMCCSD excitation operator for the Kth electronic state. A very similar expression, based on inserting the CISDtq wave function into Eq. (117), can be written for the MMCC(2,4)/CI energy. All remaining details of the MMCC(2,3)/CI and MMCC(2,4)/CI calculations, including the related computer costs and selection of active occupied and active unoccupied spin-orbitals that define the triply and quadruply excited components of the CISDt and CISDtq wave functions, Eqs. (99) and (100), respectively, are exactly the same as in the ground-state case discussed in Sect. 3.3. We choose active spin-orbitals in a usual way by using information about the dominant orbital excitations defining the excited states of interest. Examples of the good choices of active orbitals for the calculations of the valence excited states of CH^+ and C_2 can be found in Tables 4 and 5 (see footnotes d in Tables 4, 5). As one can see, it is often sufficient to use a very small number of active orbitals in the MMCC(2,3)/CI and MMCC(2,4)/CI calculations to obtain excellent results for excited states. In analogy to the ground-state MMCC/CI calculations discussed in Sect. 3.3, the active orbital spaces used in the MMCC/CI calculations for excited states reported in Tables 4 and 5 are so small that the numbers of all triples used in the CISDt-based MMCC(2,3) calculations represent no more than 30 % of all triples. The numbers of quadruples used in the CISDtq-based MMCC(2,4) calculations reported in Tables 4 and 5 represent less than 6 % of all quadruples (see Refs. [72, 73] for further details).

As shown in Tables 4 and 5, the CI-corrected MMCC(2,3) and MMCC(2,4) approaches provide an excellent description of the electronic excitations in CH^+ and C_2. The MMCC(2,3)/CI results for CH^+ at $R_{C-H} = R_e$ are as good as the highly accurate CR-EOMCCSD(T) results discussed in Sect. 4.1 and comparable to the results of the expensive full EOMCCSDT calculations. The MMCC(2,4)/CI method offers additional improvements. For example, the 0.023- and 0.037-eV errors in the MMCC(2,4)/CI results for the $2\,^1\Sigma^+$ and $2\,^1\Pi$ states, respectively, are 2–3 times smaller than the errors obtained with the MMCC(2,3)/CI and full EOMCCSDT approximations. The MMCC(2,3)/CI results for CH^+ at $R_{C-H} = 1.5R_e$ and $2R_e$, where all electronic states listed in Table 4 gain multireference character, causing significant troubles for the EOMCCSD method, are excellent too. The mean errors in the excitation energies corresponding to all seven states included in Table 4, obtained in the MMCC(2,3)/CI and MMCC(2,4)/CI calculations, are 0.048 and 0.022 eV, respectively, at $R_{C-H} = 1.5R_e$ and 0.047 and 0.016 eV, respectively, at $R_{C-H} = 2R_e$. This should be compared with the very large 1.114- and 2.095-eV errors in the EOMCCSD results for the lowest two $^1\Delta$ states at $R_{C-H} = 1.5R_e$ and to the 1.178- and 3.950-eV errors in the EOMCCSD results for the same two states at $R_{C-H} = 2R_e$. In particular, the MMCC(2,3)/CI approach improves the relatively poor CR-EOMCCSD(T) results for the second $^1\Delta$ state at $R_{C-H} = 1.5R_e$ and $2R_e$, reducing the unsigned errors of 0.473 and 0.769 eV to 0.086 and 0.029 eV, respectively. As in the case of the equilibrium geometry, the MMCC(2,4)/CI method reduces the small errors in the MMCC(2,3)/CI results at $R_{C-H} = 1.5R_e$ and $2R_e$ even further, providing us with the final reduction of mean absolute errors in the EOMCCSD results at these two nuclear geometries by impressive factors of 32 and 66, respectively.

The MMCC(2,3)/CI and MMCC(2,4)/CI results for the excited states of C_2 shown in Table 5 are equally remarkable. In particular, the MMCC(2,3)/CI method reduces the 2.054- and 1.708-eV errors in the EOMCCSD results for the lowest $^1\Delta_g$ and $^1\Pi_g$ states of C_2 that are dominated by doubles to 0.130 and 0.026 eV, respectively, which is a level of improvement comparable to that offered by the CR-EOMCCSD(T) approach. The MMCC(2,4)/CI method reduces the small, 0.130-eV, error in the MMCC(2,3)/CI results for the complicated $1\,^1\Delta_g$ state of C_2 even further (to 0.011 eV). The overall performance of the MMCC(2,3)/CI and MMCC(2,4)/CI methods in describing the valence excited states of C_2 is better than that of the EOMCCSDT approach or its active-space EOMCCSDt variant and much better than the performance of the perturbative triples CC3 method. The MMCC(2,4)/CI approach, which provides a mean absolute error in describing excited states of C_2 of 0.038 eV, is also more accurate than the CR-EOMCCSD(T) method discussed in Sect. 4.1 [the mean absolute error in describing excited states of C_2 characterizing the CR-EOMCCSD(T) approach is 0.141 eV; the MMCC(2,3)/CI method gives an average error of 0.067 eV]. We must remember, however, that the CR-EOMCCSD(T) approach is less expensive and easier to use than the MMCC(2,4)/CI method, while providing reasonable results for C_2.

The analysis of the MMCC/CI results for CH^+ and C_2 indicates that the MMCC theory for excited states is as robust as the ground-state MMCC formalism. Since we can always increase the active orbital space in the MMCC/CI calculations or switch to higher-level MMCC(2,5) or MMCC(2,6) approximations or, if none of this works, change the form of the wave functions $|\Psi_K\rangle$ used in the excited-state MMCC calculations, we can conclude that one can always improve the CR-EOMCCSD(T) and CI-corrected MMCC results based on the general MMCC formulas for the excited-state energies discussed in Sect. 2.2 by working on the relevant elements of the MMCC calculations. The MMCC theory seems to be flexible enough to enable such improvements.

5 Summary and concluding remarks

In this article, we have described the MMCC formalism, which provides a systematic way of improving the results of the standard CC and EOMCC calculations for the ground- and excited-state energies of atomic and molecular systems. The MMCC theory is based on a few rigorous relationships that define the many-body structure of the differences between the full CI and CC or EOMCC energies in a given basis set. These relationships, which employ the concept of the generalized moments of the CC/EOMCC equations, provide us with precise information about how to estimate the remanent errors that occur in the standard CC or EOMCC calculations and how to design suitable noniterative corrections to the CC/EOMCC energies that are close to the exact, full CI, energies. The MMCC theory is particularly valuable in designing the noniterative CC/EOMCC approximations for PESs involving bond breaking, quasidegenerate electronic states characterized by a large degree of nondynamic correlation, and PESs of excited states, including excited states dominated by two-electron and other many-electron transitions. In all those situations, the standard CC/EOMCC methods, such as CCSD or EOMCCSD, and their various noniterative extensions, such as CCSD(T) or EOMCCSD(T), fail because of inadequate information about higher–than–doubly excited clusters and divergent behavior of the MBPT expansions on which the standard noniterative methods of the CCSD(T) type are based.

We have discussed several approximate variants of the MMCC theory, including the renormalized and completely renormalized CC/EOMCC methods, the QMMCC approaches, the CI-corrected MMCC methods, and the GMMCC approaches. We have focused on approaches that use the spin- and symmetry-adapted references of the RHF or ROHF type and approaches that employ only one- and two-body cluster components resulting from CCSD/EOMCCSD or other CCSD-like calculations in designing the noniterative MMCC energy corrections. The MMCC theory can be used to correct the results of the higher-level CC/EOMCC calculations, such as CCSDT, CCSDTQ, or EOMCCSDT, but we have not discussed the MMCC approaches of this type in this article, since our focus has been on relatively inexpensive and yet accurate methods that are based on one- and two-body clusters. Along with previously published results, we have reviewed several of the most recent developments, including the open-shell extensions of the CR-CC methods, the MMCC approaches employing the ECCSD theory, and the CR-EOMCC methods for excited states (for a complete list of acronyms representing quantum-chemical approaches discussed or referred to in this article, see Table 7 in appendix).

The renormalized and completely renormalized CC methods, including the CR-CCSD(T) and CR-CCSD(TQ) approaches, in which simple and relatively inexpensive noniterative corrections of the CCSD(T) type are added to the CCSD energies, are useful in improving the results of the standard CCSD(T) and CCSD(TQ$_{\mathrm{f}}$) calculations for the ground-state PESs involving single and double bond stretching or breaking. The CR-CCSD(T) and CR-CCSD(TQ) methods can be regarded as computational black boxes, which are as easy to use as the popular CCSD(T) approach or its CCSD(TQ$_{\mathrm{f}}$) extension. The CR-EOMCCSD(T) approach, which is an analog of the ground-state CR-CCSD(T) approximation, enables us to obtain a highly accurate description of excited states dominated by doubles and large fragments of excited-state PESs with the ease of the ground-state CCSD(T) calculation. The QMMCC approaches allow us to improve the CR-CC results for multiple bond breaking by considering the carefully selected higher-order terms in the expressions defining the MMCC corrections to the CCSD energies. The CI-corrected MMCC methods, in which the approximate information about the ground- and excited-state wave functions $|\Psi_0\rangle$ and $|\Psi_K\rangle$ that enter the MMCC energy expressions is obtained with the multireference-like CI approaches, provide us with alternative ways of improving the results of CC/EOMCC calculations for single and multiple bond breaking and excited-state PESs, even when the CR-CC and CR-EOMCC methods do not work well. Finally, the GMMCC theory enables us to use the cluster amplitudes obtained in non-CC calculations. This option is very useful for obtaining considerable improvements in the description of multiple bond breaking. As it turns out, much better MMCC results are obtained if the singly and doubly excited clusters, T_1 and T_2, respectively, obtained in the standard CCSD calculations, are replaced by the T_1 and T_2 clusters resulting from the ECCSD calculations. Our results in the area of combining the MMCC and ECC formalisms are still preliminary in nature, but they are very promising too, so we plan to pursue this new method of improving the results for multiple bond breaking and other cases involving large nondynamic correlation effects in the future.

We have demonstrated that the MMCC and GMMCC formalisms offer many advantages, which can help to design new classes of noniterative CC/EOMCC approximations. Interestingly enough, the MMCC and GMMCC theories are so robust that we can obtain an accurate description of bond breaking and excited-state PESs with the ease of single-reference calculations. They allow us to use the CC and non-CC cluster amplitudes and work equally well for ground and excited states. One of the unexplored ideas is the applicability of the MMCC theory in MRCC calculations. The general theory of improving the results of MRCC calculations using the noniterative MMCC corrections to eigenvalues of the effective Hamiltonians used in MRCC theories has been described in Ref. [133] (see, also, Ref. [76]). It may be worth testing this genuine multireference extension of the MMCC formalism. This and other ideas of improving the results of standard CC/EOMCC and MRCC calculations via the MMCC formalism will be explored in the future.

6 About the authors

This article has several authors, who have contributed to various aspects of the research described in this article. K. Kowalski is a codiscoverer of the MMCC and GMMCC formalisms (with P. Piecuch) and a major contributor to all aspects of the MMCC/GMMCC theory, including the formulation of various approximate methods and their implementation and testing discussed in this article. I.S.O. Pimienta has been responsible for the development of the QMMCC and CI-corrected MMCC methods for the ground-state problem. P.-D. Fan and M. Lodriguito have contributed to the development and testing of the GMMCC methods employing the ECC cluster amplitudes. M.J. McGuire has played a vital role in testing the R-CC and CR-CC methods and comparing the results with those obtained with multireference methods. T. Kuś and S.A. Kucharski have helped us to develop efficient computer codes for the open-shell R-CCSD[T], R-CCSD(T), CR-CCSD[T], and CR-CCSD(T) methods. S.A. Kucharski and M. Musiał have worked with K. Kowalski and P. Piecuch on writing efficient computer codes for the R-CCSD[T], R-CCSD(T), CR-CCSD[T], and CR-CCSD(T) methods, which are currently available in GAMESS, and their CR-EOMCCSD(T) extensions which will be included in the official GAMESS distribution in the near future.

Acknowledgements. P.P. would like to express his most sincere thanks to Donald G. Truhlar and Christopher J. Cramer for inviting him to write this feature article. We would like to thank Martin Schütz for providing us with the CASPT2 and MRCI(Q) data for ethane and methyl fluoride that were used to prepare Figs. 1b and 1c. We would also like to thank Michael W. Schmidt and Mark S. Gordon for helping us to interface our CR-CC and CR-EOMCC codes with GAMESS and for several useful discussions. This work was supported by the Department of Energy, Office of Basic Energy Sciences, SciDAC Computational Chemistry Program (grant no. DE-FG02-01ER15228) and by the Alfred P. Sloan Foundation (awards provided to P.P.). Additional support by the National Science Foundation under grant no. CHE-0309517 (P.P) is gratefully appreciated.

Appendix

Table 7. Acronyms representing quantum-chemical approaches discussed or referred to in this article

Acronym	*Meaning*
Coupled-cluster (CC) methods	
CCSD	Coupled-cluster method with singly and doubly excited clusters
CCSDT	Coupled-cluster method with singly, doubly, and triply excited clusters
CCSDTQ	Coupled-cluster method with singly, doubly, triply, and quadruply excited clusters
CCSDTQP	Coupled-cluster method with singly, doubly, triply, quadruply, and pentuply excited clusters
CCSD[T], CCSD(T)	Two standard coupled-cluster methods with singles, doubles, and noniterative corrections due to triples
CCSD(TQ$_f$)	Coupled-cluster method with singles, doubles, and noniterative corrections due to triples and quadruples
CCSDT(Q$_f$)	Coupled-cluster method with singles, doubles, triples, and noniterative corrections due to quadruples
MRCC	Multireference coupled-cluster theories
Equation-of-motion coupled-cluster (EOMCC) and related methods for excited states	
EOMCCSD	Equation-of-motion coupled-cluster method with singles and doubles
EOMCCSDT	Equation-of-motion coupled-cluster method with singles, doubles, and triples
EOMCCSDt	Equation-of-motion coupled-cluster method with all singles and doubles, and triples selected via active orbitals
EOMCCSD($\underset{\sim}{T}$)	Equation-of-motion coupled-cluster method with singles, doubles, and noniterative corrections due to triples
EOMCCSD($\tilde{T}$)	One of the modifications of the EOMCCSD(T) approach
EOMCCSD(T$'$)	One of the modifications of the EOMCCSD(T) approach
EOMCCSDT-*n*	Equation-of-motion coupled-cluster methods with singles, doubles, and iterative perturbative triples
CC3	Response coupled-cluster method with singles, doubles, and iterative perturbative triples
CCSDR(3)	Response coupled-cluster method with singles, doubles, and noniterative corrections due to triples
Extended coupled-cluster (ECC) methods	
ECCD, QCCD	Extended coupled-cluster method with doubles, quadratic approximation to ECCD
ECCSD	Extended coupled-cluster method with singles and doubles
BECCSD, QECCSD	Bilinear and quadratic approximations to ECCSD
Many-body perturbation theory (MBPT) methods	
MBPT(2)	Second-order many-body perturbation theory
MRMBPT	Multireference many-body perturbation theories
CASPT2	Second-order multireference many-body perturbation theory using CASSCF reference
Configuration interaction (CI) methods	
CISD	Single-reference configuration interaction approach with singles and doubles
CISDT	Single-reference configuration interaction approach with singles, doubles, and triples
CISDt	Configuration interaction approach with all singles and doubles, and triples selected using active orbitals
CISDtq	An extension of the CISDt approach, where triples and quadruples are selected using active orbitals
CISDtqp	An extension of the CISDt approach, where triples to pentuples are selected using active orbitals
CISDtqph	An extension of the CISDt approach, where triples to hextuples are selected using active orbitals
MRCI	Multireference configuration interaction methods
MRCI(Q)	Internally contracted interaction approach with the Davidson correction
Method of moments of coupled-cluster equations (MMCC) ($\|\Psi_K >$ and $\|\Psi_0 >$ are the wave functions entering the MMCC formulas)	
MMCC(2,3)	MMCC correction to the CCSD/EOMCCSD energy in which $\|\Psi_K\rangle$ is truncated at triples
MMCC(2,4)	MMCC correction to the CCSD/EOMCCSD energy in which $\|\Psi_K\rangle$ is truncated at quadruples
MMCC(2,5)	MMCC correction to the CCSD/EOMCCSD energy in which $\|\Psi_K\rangle$ is truncated at pentuples
MMCC(2,6)	MMCC correction to the CCSD/EOMCCSD energy in which $\|\Psi_K\rangle$ is truncated at hextuples
CR-CC, R-CC	Completely renormalized and renormalized coupled-cluster approaches ($\|\Psi_K\rangle$ from the MBPT analysis)
CR-CCSD[T]	Completely renormalized CCSD[T] approach [based on the MMCC(2,3) approximation]
CR-CCSD(T)	Completely renormalized CCSD(T) approach [based on the MMCC(2,3) approximation]
CR-CCSD(TQ)	Completely renormalized CCSD(TQ) approach [based on the MMCC(2,4) approximation]
CR-EOMCCSD(T)	Completely renormalized EOMCCSD(T) approach for excited states [based on the MMCC(2,3) approximation]
R-CCSD[T]	Renormalized CCSD[T] approach [based on the MMCC(2,3) method; approximation to CR-CCSD[T]]
R-CCSD(T)	Renormalized CCSD(T) approach [based on the MMCC(2,3) method; approximation to CR-CCSD(T)]
R-CCSD(TQ)	Renormalized CCSD(TQ) approach [based on the MMCC(2,4) method; approximation to CR-CCSD(TQ)]
QMMCC	Quadratic MMCC approaches (the exponential wave function $\|\Psi_0\rangle$ truncated at quadratic terms)
QMMCC(2,3)	Quadratic MMCC method based on the MMCC(2,3) approximation
QMMCC(2,4)	Quadratic MMCC method based on the MMCC(2,4) approximation
QMMCC(2,5)	Quadratic MMCC method based on the MMCC(2,5) approximation
QMMCC(2,6)	Quadratic MMCC method based on the MMCC(2,6) approximation
MMCC/CI	CI-corrected MMCC approaches ($\|\Psi_K\rangle$ obtained in limited single-reference or multireference CI calculations)

Table 7. (continued)

Acronym	*Meaning*
MMCC(2,3)/CI	CI-corrected MMCC(2,3) method ($\lvert\Psi_K\rangle$ obtained in the CISDt calculations)
MMCC(2,4)/CI	CI-corrected MMCC(2,4) method ($\lvert\Psi_K\rangle$ obtained in the CISDtq calculations)
MMCC(2,5)/CI	CI-corrected MMCC(2,5) method ($\lvert\Psi_K\rangle$ obtained in the CISDtqp calculations)
MMCC(2,6)/CI	CI-corrected MMCC(2,6) method ($\lvert\Psi_K\rangle$ obtained in the CISDtqph calculations)
GMMCC	Generalized MMCC approaches allowing for the use of non-CC values of the cluster operator T
GMMCC(2,3)	Generalized MMCC(2,3) approximation allowing for the use of non-CCSD values of T_1 and T_2 clusters
GMMCC(2,4)	Generalized MMCC(2,4) approximation allowing for the use of non-CCSD values of T_1 and T_2 clusters
GMMCC(2,5)	Generalized MMCC(2,5) approximation allowing for the use of non-CCSD values of T_1 and T_2 clusters
GMMCC(2,6)	Generalized MMCC(2,6) approximation allowing for the use of non-CCSD values of T_1 and T_2 clusters
GMMCC(2,4)/ECCSD	Generalized MMCC(2,4) approximation employing the ECCSD values of T_1 and T_2 clusters
Self-consistent-field methods	
RHF, ROHF, UHF	Restricted, restricted open-shell, and unrestricted Hartree–Fock methods
CASSCF	Complete-active-space self-consistent-field method

References

1. Coester F (1958) Nucl Phys 7: 421
2. Coester F, Kümmel H (1960) Nucl Phys 17: 477
3. Čížek J (1966) J Chem Phys 45: 4256
4. Čížek J (1969) Adv Chem Phys 14: 35
5. Čížek J, Paldus J (1971) Int J Quantum Chem 5: 359
6. Paldus J (1992) In: Wilson S, Diercksen GHF (eds) Methods in computational molecular physics. NATO ASI series B: physics, vol 293. Plenum, New York, p 99
7. Bartlett RJ (1995) In: Yarkony DR (ed) Advanced series in physical chemistry. Modern electronic structure theory, part I. World Scientific, Singapore, p 1047
8. Lee TJ, Scuseria GE (1995) In: Langhoff SR (ed) Quantum mechanical electronic structure calculations with chemical accuracy. Kluwer, Dordrecht, The Netherlands, p 47
9. Paldus J, Li X (1999) Adv Chem Phys 110: 1
10. Crawford TD, Schaefer HF III (2000) Rev Comput Chem 14: 33
11. Gauss J (1998) In: Schleyer PvR, Allinger NL, Clark T, Gasteiger J, Kollman PA, Schaefer HF III, Schreiner PR (eds) Encyclopedia of computational chemistry, vol 1. Wiley, Chichester, UK, p 615
12. Piecuch P, Kowalski K, Pimienta ISO, McGuire, MJ (2002) Int Rev Phys Chem 21: 527
13. Purvis GD III, Bartlett RJ (1982) J Chem Phys 76: 1910
14. Urban M, Noga J, Cole SJ, Bartlett RJ (1985) J Chem Phys 83: 4041
15. Raghavachari K, Trucks GW, Pople JA, Head-Gordon M (1989) Chem Phys Lett 157: 479
16. Scuseria GE, Scheiner AC, Lee TJ, Rice JE, Schaefer HF III (1987) J Chem Phys 86: 2881
17. Scuseria GE, Janssen CL, Schaefer HF III (1988) J Chem Phys 89: 7382
18. Lee TJ, Rice JE (1988) Chem Phys Lett 150: 406
19. Piecuch P, Paldus J (1989) Int J Quantum Chem 36: 429
20. Piecuch P, Paldus J (1990) Theor Chim Acta 78: 65
21. Piecuch P, Toboła R, Paldus J (1995) Int J Quantum Chem 55: 133
22. Monkhorst H (1977) Int J Quantum Chem Symp 11: 421
23. Sekino H, Bartlett RJ (1984) Int J Quantum Chem Symp 18: 255
24. Daalgard E, Monkhorst H (1983) Phys Rev A 28: 1217
25. Takahashi M, Paldus J (1986) J Chem Phys 85: 1486
26. Koch H, Jørgensen P (1990) J Chem Phys 93: 3333
27. Koch H, Jensen HJA, Jørgensen P, Helgaker T (1990) J Chem Phys 93: 3345
28. Geertsen J, Rittby M, Bartlett RJ (1989) Chem Phys Lett 164: 57
29. Comeau DC, Bartlett RJ (1993) Chem Phys Lett 207: 414
30. Stanton JF, Bartlett RJ (1993) J Chem Phys 98: 7029
31. Piecuch P, Bartlett RJ (1999) Adv Quantum Chem 34: 295
32. Nakatsuji H, Hirao K (1977) Chem Phys Lett 47: 569
33. Nakatsuji H, Hirao K (1978) J Chem Phys 68: 2053, 4279
34. Nakatsuji H (1978) Chem Phys Lett 59: 362
35. Nakatsuji H (1979) Chem Phys Lett 67: 329, 334
36. Nakatsuji H (1997) In: Leszczyński J (ed) Computational chemistry: reviews of current trends, vol 2. World Scientific, Singapore, p 62
37. Watts JD, Bartlett RJ (1995) Chem Phys Lett 233: 81
38. Watts JD, Bartlett RJ (1996) Chem Phys Lett 258: 581
39. Watts JD, Bartlett RJ (1994) J Chem Phys 101: 3073
40. Koch H, Christiansen O, Jørgensen P, Olsen J (1995) Chem Phys Lett 244: 75
41. Christiansen O, Koch H, Jørgensen P (1995) J Chem Phys 103: 7429
42. Christiansen O, Koch H, Jørgensen P (1996) J Chem Phys 105: 1451
43. Christiansen O, Koch H, Jørgensen P, Olsen J (1996) Chem Phys Lett 256: 185
44. Kucharski SA, Bartlett RJ (1998) J Chem Phys 108: 9221
45. Lee YS, Bartlett RJ (1984) J Chem Phys 80: 4371
46. Lee YS, Kucharski SA, Bartlett RJ (1984) J Chem Phys 81: 5906; Lee YS, Kucharski SA, Bartlett RJ (1985) J Chem Phys 82: 5761 (E)
47. Noga J, Bartlett RJ, Urban M (1987) Chem Phys Lett 134: 126
48. Trucks GW, Noga J, Bartlett RJ (1988) Chem Phys Lett 145: 548
49. Kucharski SA, Bartlett RJ (1989) Chem Phys Lett 158: 550
50. Laidig WD, Saxe P, Bartlett RJ (1987) J Chem Phys 86: 887
51. Ghose KB, Piecuch P, Adamowicz L (1995) J Chem Phys 103: 9331
52. Piecuch P, Špírko V, Kondo AE, Paldus J (1996) J Chem Phys 104: 4699
53. Piecuch P, Kucharski SA, Bartlett RJ (1999) J Chem Phys 110: 6103
54. Piecuch P, Kucharski SA, Špirko V (1999) J Chem Phys 111: 6679
55. Piecuch P, Kowalski K (2000) In: Leszczyński J (ed) Computational chemistry: reviews of current trends, vol 5. World Scientific, Singapore, p 1
56. Kowalski K, Piecuch P (2000) J Chem Phys 113: 18
57. Kowalski K, Piecuch P (2000) J Chem Phys 113: 5644
58. Kowalski K, Piecuch P (2001) Chem Phys Lett 344: 165
59. Piecuch P, Kucharski SA, Kowalski K (2001) Chem Phys Lett 344: 176
60. Piecuch P, Kucharski SA, Špirko V, Kowalski K (2001) J Chem Phys 115: 5796
61. Piecuch P, Kowalski K, Pimienta ISO, Kucharski SA (2002) In: Hoffmann MR, Dyall KG (eds) Low-lying potential energy surfaces. ACS symposium series, vol 828. American Chemican Society, Washington, DC, p 31

62. Piecuch P, Kowalski K, Pimienta ISO (2002) Int J Mol Sci 3: 475
63. McGuire MJ, Kowalski K, Piecuch P (2002) J Chem Phys 117: 3617
64. Piecuch P, Kowalski K, Fan PD, Pimienta ISO (2003) In: Maruani J, Lefebvre R, Brändas E (eds) Advanced topics in theoretical chemical physics. Progress in theoretical chemistry and physics, vol 12. Kluwer, Dordrecht, p 119
65. Piecuch P, Pimienta ISO, Fan PD, Kowalski K (2004) In: Wilson AK (ed) Recent progress in electron correlation methodology. ACS symposium series, American Chemican Society, Washington, DC (in press)
66. Pimienta ISO, Kowalski K, Piecuch P (2003) J Chem Phys 119: 2951
67. Larsen H, Olsen J, Jørgensen P, Christiansen O (2000) J Chem Phys 113: 6677; Larsen H, Olsen J, Jørgensen P, Christiansen O (2001) J Chem Phys 114: 10985 (E)
68. Hald K, Jørgensen P, Olsen J, Jaszuński M (2001) J Chem Phys 115: 671
69. Kowalski K, Piecuch P (2000) J Chem Phys 113: 8490
70. Kowalski K, Piecuch P (2001) J Chem Phys 115: 643
71. Kowalski K, Piecuch P (2001) Chem Phys Lett 347: 237
72. Kowalski K, Piecuch P (2001) J Chem Phys 115: 2966
73. Kowalski K, Piecuch P (2002) J Chem Phys 116: 7411
74. Kowalski K, Piecuch P (2004) J Chem Phys 120: 1715
75. Krylov AI, Sherrill CD, Head-Gordon M (2000) J Chem Phys 113: 6509
76. Piecuch P, Kowalski K (2002) Int J Mol Sci 3: 676
77. Paldus J, Pylypow L, Jeziorski B (1989) In: Kaldor U (ed) Many-body methods in quantum chemistry. Lecture notes in chemistry, vol 52. Springer, Berlin Heidelberg New York, p 151
78. Paldus J, Piecuch P, Jeziorski B, Pylypow L (1992) In: Ainsworthy TL, Campbell CE, Clements BE, Krotschek E (eds) Recent progress in many-body theories, vol 3. Plenum, New York, p 287
79. Paldus J, Piecuch P, Pylypow L, Jeziorski B (1993) Phys Rev A 47: 2738
80. Piecuch P, Paldus J (1994) Phys Rev A 49: 3479
81. Piecuch P, Paldus J (1994) J Chem Phys 101: 5875
82. Kowalski K, Piecuch P (2000) Phys Rev A 61: 052506
83. Jankowski K, Paldus J, Grabowski I, Kowalski K (1992) J Chem Phys 97: 7600; Jankowski K, Paldus J, Grabowski I, Kowalski K (1994) J Chem Phys 101: 1759 (E)
84. Jankowski K, Paldus J, Grabowski I, Kowalski K (1994) J Chem Phys 101: 3085
85. Mahapatra US, Datta B, Mukherjee D (1998) Mol Phys 94: 157
86. Mahapatra US, Datta B, Mukherjee D (1999) J Chem Phys 110: 6171
87. Mach P, Mášik J, Urban J, Hubač I (1998) Mol Phys 94: 173
88. Mášik J, Hubač I (1999) Adv Quantum Chem 31: 75
89. Pittner J, Nachtigall P, Čársky P, Mášik J, Hubač I (1999) J Chem Phys 110: 10275
90. Hubač I, Pittner J, Čársky P (2000) J Chem Phys 112: 8779
91. Sancho-Garcia JC, Pittner J, Čársky P, Hubač I (2000) J Chem Phys 112: 8785
92. Pittner J, Nachtigall P, Čársky P, Hubač I (2001) J Phys Chem A 105: 1354
93. Nooijen M, Lotrich V (2001) J Mol Struct (THEOCHEM) 547: 253
94. Nooijen M, Lotrich V (2000) J Chem Phys 113: 4549
95. Oliphant N, Adamowicz L (1991) J Chem Phys 94: 1229
96. Oliphant N, Adamowicz L (1992) J Chem Phys 96: 3739
97. Oliphant N, Adamowicz L (1993) Int Rev Phys Chem 12: 339
98. Piecuch P, Oliphant N, Adamowicz L (1993) J Chem Phys 99: 1875
99. Piecuch P, Adamowicz L (1994) J Chem Phys 100: 5792
100. Piecuch P, Adamowicz L (1994) Chem Phys Lett 221: 121
101. Piecuch P, Adamowicz L (1995) J Chem Phys 102: 898
102. Ghose KB, Adamowicz L (1995) J Chem Phys 103: 9324
103. Ghose KB, Piecuch P, Pal S, Adamowicz L (1996) J Chem Phys 104: 6582
104. Adamowicz L, Piecuch P, Ghose KB (1998) Mol Phys 94: 225
105. Olsen J (2000) J Chem Phys 113: 7140
106. Krogh JW, Olsen J (2001) Chem Phys Lett 344: 578
107. Kállay M, Surján PR, Szalay P (2002) J Chem Phys 117: 980
108. Li X, Paldus J (1997) J Chem Phys 107: 6257
109. Li X, Paldus J (1998) J Chem Phys 108: 637
110. Li X, Paldus J (1998) Chem Phys Lett 286: 145
111. Li X, Paldus J (1999) J Chem Phys 110: 2844
112. Li X, Paldus J (2000) Mol Phys 98: 1185
113. Li X, Paldus J (2000) J Chem Phys 113: 9966
114. Kowalski K, Piecuch P (2001) Chem Phys Lett 334: 89
115. Noga J, Bartlett RJ (1987) J Chem Phys 86: 7041; Noga J, Bartlett RJ (1988) J Chem Phys 89: 3401 (E)
116. Scuseria GE, Schaefer HF III (1988) Chem Phys Lett 152: 382
117. Kucharski SA, Bartlett RJ (1991) Theor Chim Acta 80: 387
118. Kucharski SA, Bartlett RJ (1992) J Chem Phys 97: 4282
119. Oliphant N, Adamowicz L (1991) J Chem Phys 95: 6645
120. Musiał M, Kucharski SA, Bartlett RJ (2002) J Chem Phys 116: 4382
121. Kucharski SA, Włoch M, Musiał M, Bartlett RJ (2001) J Chem Phys 115: 8263
122. Pulay P (1983) Chem Phys Lett 100: 151
123. Saebø S, Pulay P (1985) Chem Phys Lett 113: 13
124. Saebø S, Pulay P (1993) Annu Rev Phys Chem 44: 213
125. Schütz M (2000) J Chem Phys 113: 9986
126. Schütz M, Werner HJ (2000) Chem Phys Lett 318: 370
127. Schütz M (2002) J Chem Phys 116: 8772
128. Nooijen M, Bartlett RJ (1997) J Chem Phys 106: 6441, 6449
129. Nooijen M, Bartlett RJ (1997) J Chem Phys 107: 6812
130. Gwaltney SR, Bartlett RJ (1998) J Chem Phys 108: 6790
131. Korona T, Werner HJ (2003) J Chem Phys 118: 3006
132. Crawford TD, King RA (2002) Chem Phys Lett 366: 611
133. Kowalski K, Piecuch P (2001) J Mol Struct (THEOCHEM) 547: 191
134. Gwaltney SR, Head-Gordon M (2000) Chem Phys Lett 323: 21
135. Gwaltney SR, Sherrill CD, Head-Gordon M, Krylov AI (2000) J Chem Phys 113: 3548
136. Gwaltney SR, Head-Gordon M (2001) J Chem Phys 115: 2014
137. Gwaltney SR, Byrd EFC, Van Voorhis T, Head-Gordon M (2002) Chem Phys Lett 353: 359
138. Head-Gordon M, Van Voorhis T, Gwaltney SR, Byrd EFC (2002) In: Hoffmann MR, Dyall KG (eds) Low-lying potential energy surfaces. ACS symposium series, vol 828. American Chemican Society, Washington, DC, p 93
139. Stanton JF (1997) Chem Phys Lett 281: 130
140. Krylov AI (2001) Chem Phys Lett 338: 375
141. Krylov AI, Sherrill CD (2002) J Chem Phys 116: 3194
142. Slipchenko LV, Krylov AI (2002) J Chem Phys 117: 4694
143. Van Voorhis T, Head-Gordon M (2000) Chem Phys Lett 330: 585
144. Byrd EFC, Van Voorhis T, Head-Gordon M (2002) J Phys Chem B 106: 8070
145. Arponen JS (1983) Ann Phys 151: 311
146. Arponen JS, Bishop RF, Pajanne E (1987) Phys Rev A 36: 2519
147. Arponen JS, Bishop RF, Pajanne E (1987) Condens Matter Theor 2: 357
148. Bishop RF, Arponen JS, Pajanne E (1989) In: Mukherjee D (ed) Aspects of many-body effects in molecules and extended systems. Lecture notes in chemistry, vol 50. Springer, Berlin Heidelberg New York, p 79
149. Bishop RF, Arponen JS (1990) Int J Quantum Chem Symp 24: 197
150. Arponen JS, Bishop RF (1991) Ann Phys 207: 171
151. Bishop RF, Robinson NI, Arponen J (1990) Condens Matter Theor 5: 37
152. Bishop RF (1991) Theor Chim Acta 80: 95

153. Arponen J (1997) Phys Rev A 55: 2686
154. Arponen JS, Bishop RF, Pajanne E (1987) Phys Rev A 36: 2539
155. Kowalski K, Dean DJ, Hjorth-Jensen M, Papenbrock T, Piecuch P (2004) Phys Rev Lett, 92: 132501
156. Li X, Paldus J (2001) J Chem Phys 115: 5759
157. Li X, Paldus J (2001) J Chem Phys 115: 5774
158. Li X, Paldus J (2002) J Chem Phys 117: 1941
159. Kantorovich LV, Krylov VI (1958) Approximate methods of higher analysis. Interscience, New York, p 150
160. Jankowski K, Paldus J, Piecuch P (1991) Theor Chim Acta 80: 223
161. Meissner L, Bartlett RJ (2001) J Chem Phys 115: 50
162. Piecuch P, Kucharski SA, Kowalski K, Musiał M (2002) Comp Phys Commun 149: 71
163. Schmidt MW, Baldridge KK, Boatz JA, Elbert ST, Gordon MS, Jensen JH, Koseki S, Matsunaga N, Nguyen KA, Su SJ, Windus TL, Dupuis M, Montgomery JA (1993) J Comput Chem 14: 1347
164. Dunning TH (1970) J Chem Phys 53: 2823
165. Dunning TH Jr (1989) J Chem Phys 90: 1007
166. Werner HJ, Knowles PJ (1988) J Chem Phys 89: 5803
167. Knowles PJ, Werner HJ (1988) Chem Phys Lett 145: 514
168. Roos BO, Linse P, Siegbahn PEM, Blomberg MRA (1982) Chem Phys 66: 197
169. Andersson K, Malmqvist PÅ, Roos BO, Sadlej AJ, Woliński K (1990) J Phys Chem 94: 5483
170. Andersson K, Malmqvist PÅ, Roos BO (1992) J Chem Phys 96: 1218
171. Woliński K, Sellers HL, Pulay P (1987) Chem Phys Lett 140: 225
172. Woliński K, Pulay P (1989) J Chem Phys 90: 3647
173. Hirao K (1992) Int J Quantum Chem Symp 26: 517
174. Hirao K (1992) Chem Phys Lett 190: 374
175. Nakano H (1993) J Chem Phys 99: 7983
176. Kozłowski PM, Davidson ER (1994) J Chem Phys 100: 3672
177. Kozłowski PM, Davidson ER (1994) Chem Phys Lett 222: 615
178. Schmidt MW, Gordon MS (1998) Annu Rev Phys Chem 49: 233
179. Werner HJ (1996) Mol Phys 89: 645
180. Werner HJ and Knowles PJ, MOLPRO, a package of ab initio programs, version 2002.1, with contributions from Amos RD, Bernhardsson A, Berning A, Celani P, Cooper DL, Deegan MJO, Dobbyn AJ, Eckert F, Hampel C, Hetzer G, Knowles PJ, Korona T, Lindh R, Lloyd AW, McNicholas SJ, Manby FR, Meyer W, Mura ME, Nicklass A, Palmieri P, Pitzer R, Rauhut G, Schütz M, Schumann U, Stoll H, Stone AJ, Tarroni R, Thorsteinsson T, Werner HJ
181. Kendall RA, Dunning Jr TH, Harrison RJ (1992) J Chem Phys 96: 6769
182. Huber KP, Herzberg G (1979) Molecular spectra and molecular structure, vol. 4. Constants of diatomic molecules. Van Nostrand, New York
183. Coxon JA, Hajigeorgiou PG (1990) J Mol Spectrosc 142: 254
184. Rydberg R (1931) Z Phys 73: 376
185. Rydberg R (1933) Z Phys 80: 514
186. Klein O (1932) Z Phys 76: 226
187. Rees ALG (1947) Proc Phys Soc 59: 998
188. Zemke WT, Stwalley WC, Coxon JA, Hajigeorgiou PG (1991) Chem Phys Lett 177: 412
189. Zemke WT, Stwalley WC, Langhoff SR, Valderrama GL, Berry MJ (1991) J Chem Phys 95: 7846
190. Schor H, Chapman S, Green S, Zare RN (1978) J Chem Phys 69: 3790
191. Chapman S, Dupuis M, Green S (1983) Chem Phys 78: 93
192. Aguado A, Sanz V, Paniagua M (1997) Int J Quantum Chem 61: 491
193. Kuntz PJ, Roach AC (1981) J Chem Phys 74: 3420
194. Roach AC, Kuntz PJ (1981) J Chem Phys 74: 3435
195. Kuntz PJ, Schreiber JL (1982) J Chem Phys 76: 4120
196. Garcia E, Lagana A (1985) Mol Phys 56: 629
197. Liu X, Murrell JN (1991) J Chem Soc Faraday Trans 87: 435
198. Aguado A, Sieiro C, Paniagua M (1992) J Mol Struct (THEOCHEM) 260: 179
199. Huzinaga S, Andzelm J, Kłobukowski M, Radzio-Andzelm E, Sakai Y, Tatewaki H (1984) Gaussian basis sets for molecular calculations. Elsevier, Amsterdam
200. Farnell L, Pople JA, Radom L (1983) J Phys Chem 87: 79
201. Murphy R, Schaefer HF III, Nobes RH, Radom L, Pitzer RS (1986) Int Rev Phys Chem 5: 229
202. Watts JD, Bartlett RJ (1991) J Chem Phys 95: 6652
203. Cartwright DC, Hay PJ (1987) Chem Phys 114: 305
204. Tuckett RP, Dale AR, Jaffey DM, Jarrett PS, Kelly T (1983) Mol Phys 49: 475
205. Paldus J, Čížek J, Takahashi M (1984) Phys Rev A 30: 2193
206. Piecuch P, Toboła R, Paldus J (1996) Phys Rev A 54: 1210
207. Paldus J, Planelles J (1994) Theor Chim Acta 89: 13
208. Peris G, Planelles J, Paldus J (1997) Int J Quantum Chem 62: 137
209. Stolarczyk L (1994) Chem Phys Lett 217: 1
210. Hehre WJ, Stewart RF, Pople JA (1969) J Chem Phys 51: 2657
211. Van Voorhis T, Head-Gordon M (2000) J Chem Phys 113: 8873
212. Pal S (1984) Theor Chim Acta 66: 151
213. Pal S (1986) Phys Rev A 33: 2240
214. Pal S (1986) Phys Rev A 34: 2682
215. Ghose KB, Pal S (1987) Phys Rev A 36: 1539
216. Vaval N, Ghose KB, Pal S (1994) J Chem Phys 101: 4914
217. Vaval N, Pal S (1996) Phys Rev A 54: 250
218. Kumar AB, Vaval N, Pal S (1998) Chem Phys Lett 295: 189
219. Vaval N, Kumar AB, Pal S (2001) Int J Mol Sci 2: 89
220. Vaval N (2000) Chem Phys Lett 318: 168
221. Bartlett RJ, Noga J (1988) Chem Phys Lett 150: 29
222. Bartlett RJ, Kucharski SA, Noga J, Watts JD, Trucks GW (1989) In: Kaldor U (ed) Many-body methods in quantum chemistry. Lecture notes in chemistry, vol 52. Springer, Berlin Heidelberg New York, p 124
223. Bartlett RJ, Watts JD, Kucharski SA, Noga J (1990) Chem Phys Lett 165: 513
224. Kucharski SA, Bartlett RJ (1986) Adv Quantum Chem 18: 281
225. Raghavachari K, Pople JA, Replogle ES, Head-Gordon M (1990) J Phys Chem 94: 5579
226. Kowalski K, Piecuch P, Kucharski SA, Musiał M, Schmidt MW, Comput Phys Commun
227. Kowalski K, Piecuch P, Chem Phys Lett
228. Olsen J, Sánchez de Merás AM, Jensen HJA, Jørgensen P (1989) Chem Phys Lett 154: 380
229. Sadlej AJ (1988) Collect Czech Chem Commun 53: 1995
230. Banichevich A, Peyerimhoff SD (1993) Chem Phys 174: 93
231. Katayama DH (1979) J Chem Phys 71: 815
232. Banichevich A, Peyerimhoff SD, Grein F (1993) Chem Phys 178: 155
233. Buenker RJ, Peyerimhoff SD (1974) Theor Chim Acta 35: 33
234. Buenker RJ, Peyerimhoff SD (1975) Theor Chim Acta 39: 217
235. Ruedenberg K, Xantheas S, Elbert ST (1990) J Chem Phys 93: 7519
236. Xantheas S, Atchity GJ, Elbert ST, Ruedenberg K (1991) J Chem Phys 94: 8054
237. Atchity GJ, Ruedenberg K (1993) J Chem Phys 99: 3790
238. Atchity GJ, Ruedenberg K (1997) Theor Chem Acc 96: 176
239. Atchity GJ, Ruedenberg K (1997) Theor Chem Acc 96: 195
240. Atchity GJ, Ruedenberg K (1997) Theor Chem Acc 96: 205
241. Tyuterev VG, Tashkun S, Jensen P, Barbe A, Cours T (1999) J Mol Spectrosc 198: 57
242. Tyuterev VG, Tashkun S, Schwenke DW, Jensen P, Cours T, Barbe A, Jacon M (2000) Chem Phys Lett 316: 271
243. Steinfeld JI, Adler-Golden SM, Gallagher JW (1987) J Phys Chem Ref Data 16: 911
244. Watts JD, Bartlett RJ (1999) Spectrochim Acta A 55: 495
245. Griggs M (1968) J Chem Phys 49: 857

246. Borowski P, Fülscher M, Malmqvist PÅ, Roos BO (1995) Chem Phys Lett 237: 195
247. Anderson SM, Maeder J, Mauersberger K (1991) J Chem Phys 94: 6351
248. Arnold DW, Xu C, Kim EH, Neumark DM (1994) J Chem Phys 101: 912
249. Anderson SM, Morton J, Mauersberger K (1990) J Chem Phys 93: 3826